

https://dspace.org/

Development of self and mutual impedance theory to analyse arrays comprising half wave dipole and folded dipole elements.

Clark, Alan, Robert

1993
http://hdl.handle.net/10539/22822

Downloaded from a DSpace repository. https://dspace.org/

Development of Self and Mutual Impedance Theory to Analyse Arrays Comprising Halfwave Dipole and Folded Dipole Elements

Alan Robert Clark

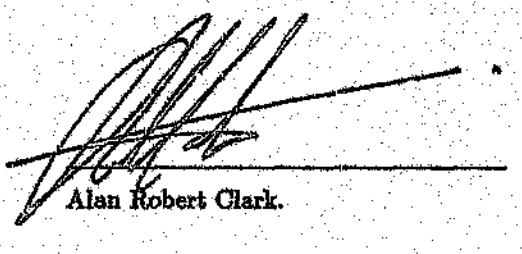
A thesis submitted to the Faculty of Engineering, University of the Witwatersrand, Johannesburg, in fulfilment of the requirements for the degree of Doctor of Philosophy.

Johannesburg, November 1993

Declaration

I declare that this thesis is my own, unaided work, except where otherwise acknowledged. It is being submitted for the degree of Doctor of Philosophy in the University of the Witwatersrand, Johannesburg. It has not been submitted before for any degree or examination in any other university.

Signed this Sixth day of November, 1993



Alan Robert Clark.

Abstract

The aim of the thesis is to develop techniques for the analysis of antennas composed of dipoles and folded dipoles that are efficient relative to the method-of-moments. The techniques developed are based on circuit network theory, where the antenna is characterised by the self and mutual impedances of its elements. Dipole self impedances are approximated by free space impedances, giving rise to a limitation of the method at full wavelength. Folded dipole self impedances are found by applying the well known transmission line model. This model is inadequate for folded dipoles with an element separation of greater than one hundredth of a wavelength. The model is extended to allow the inter-element separation to be as large as one-sixth of a wavelength, which covers most folded dipoles of interest. The mutual impedance for a folded dipole has been derived from a combination of the induced-emf method, and a consideration of the transmission line model of the folded dipole. The mutual impedance between a folded dipole and a dipole is found to be twice that of two dipoles; and the mutual impedance between two folded dipoles is four times that of two dipoles. A thickness sensitivity analysis has shown that the mutual impedance expressions used are only applicable to element radii of less than one hundredth of a wavelength. The analysis method in this thesis has been coded in a computer package called SCAT. Results of this package are compared to those of the Numerical Electromagnetics Code, Version 2 for several simple antenna arrays. For thin dipoles, the impedance and radiation pattern results compare favourably, with mixed dipoles and folded dipoles, but not for thicker radius elements. It is recommended that mutual impedance expressions are found which take thickness of the dipoles into account. Two problems which prevent integer wavelength long elements from being analyzed also need further attention.

Acknowledgements

I wish to gratefully acknowledge:

My wife, Lesley, for her patience, endurance and above all, encouragement and ability to get me working when all else failed!.

My supervisor, Dr. André Fourie, who was always available for discussion and able to see the wood for the trees.

José Faria, a 4th year student I supervised, who performed the Z-parameter measurements presented in the thesis.

Eberhard Mattes for providing a superbly written Public Domain TEX.

My External Examiners, Dr B. Austin and Dr H.C. Reader, who provided many useful comments and suggestions.

In memory of my mother

Kathleen Clark

1924—1966

and my step-mother

Ans van Tienhoven

1927—1992

Contents

Declaration i

Abstract ii

Acknowledgements iii

Contents v

List of Figures ix

List of Tables xii

List of Symbols xiii

1 INTRODUCTION 1

1.1 Aim 1

1.2 Importance of the Problem 1

1.3 Limitations 2

1.4 Overview of the Thesis 3

2 BACKGROUND 5

2.1 Method-of-Moments 5

2.1.1 General Theory 6

2.1.2 The NEC2 implementation of MOM 9

2.1.3 NEC2 Limitations 13

2.2 n–Port Circuit Network Theory 14

2.3 Folded Dipole Input Impedance 15

2.4 Mutual Impedance – a Literature Survey 17

2.5 Radiation Pattern Theory 20

3 DEVELOPMENT OF THEORY 24

3.1 Dipole Self-Impedance 24

3.2 Folded Dipole Self-Impedance 29

3.3 Mutual impedance involving a folded dipole 31

3.3.1 Combining the transmission line model of the folded dipole and the induced-emf method 31

3.3.2 Folded dipole to folded dipole 33

3.3.3 Using NEC2 to obtain mutual impedance 34

4 RESULTS 36

4.1 Folded Dipole Self Impedance 36

4.1.1 Deterioration of accuracy of Thiele's transmission line model with increasing inter-element spacing. 36

4.1.2 The deterioration of accuracy of the first-order modification to the transmission line model with increasing radius. 40

4.1.3 The final correction to the transmission line model 43

4.2 Measurement Procedure 47

4.3 Mutual Impedance 49

4.3.1 Verification of the NEC2 method of obtaining mutual impedance . . . 49

4.3.2 Mutual impedance – folded dipole to dipole 51

4.3.3 Mutual impedance between two folded dipoles 53

4.3.4 An investigation of the effect of thickness on mutual impedance 55

4.4 Array Analysis 57
4.4.1 Case 1 – 2 Element Yagi-Uda, dipole feed 57
4.4.2 Case2 – 2 element Yagi-Uda, folded dipole feed 59
4.4.3 Case 3 – 5 element Yagi-Uda, dipole feed 61
4.4.4 Case 4 – 5 element Yagi-Uda, folded dipole feed 65
4.4.5 Case 5 – 5 element Yagi-Uda, folded dipole feed, 19mm diameter . . . 67
4.4.6 Array Analysis timing results 69

5 CONCLUSIONS 71

5.1 Document Summary 71
5.2 Original Contribution 72
5.3 Recommendations for further investigation 73

A SCAT MANUAL 74

A.1 Overview 74
A.2 User Interface 75
A.2.1 Description of the parts of the screen 75
A.2.2 Environment Variables 76
A.2.3 The Configuration File 76
A.2.4 Description of the menus 77
A.3 Unit Hierarchy 84
A.3.1 Unit Description 85
A.3.2 Unit Dependency 85
A.3.3 Unit Interface Listing 86

B Extension factor derivation for Folded Dipole transmission line model 99

C Tables of Input Impedance of the Cylindrical Dipole 106

D Feed geometry sensitivity of the measured results 117

References 121

Bibliography 124

List of Figures

2.1 General radiating body 6

2.2 Definition of currents in a two port network 14

2.3 The decomposition of the folded dipole current into an antenna mode and a transmission line mode 15

2.4 Geometry of two parallel dipoles in echelon 16

2.5 The far-field radiation geometry 21

3.1 The current distribution on half and full wavelength dipoles 25

3.2 The self-impedance/free space impedance experimental geometry 26

3.3 Comparison of Free space vs Self impedance of a dipole 27

3.4 Percentage error in the use of $Z_{11\text{Free}}$ instead of Z_{11} 28

3.5 Resonant length of a bent wire 30

3.6 Coupling geometry with a folded dipole as the second antenna 32

4.1 Compared folded dipole input impedance for $s = 3\lambda_c/200$. Thiele vs. NEC2 vs. SCAT $\alpha = 0.39$ 37

4.2 Compared folded dipole input impedance for $s = \lambda_c/20$. Thiele vs. NEC2 vs. SCAT $\alpha = 0.39$ 38

4.3 Compared folded dipole input impedance for $s = \lambda_c/10$. Thiele vs. NEC2 vs. SCAT $\alpha = 0.39$ 39

4.4 Compared folded dipole input impedance for $r = \lambda_c/400$ (e=22.4Ω) 41

4.5 Compared folded dipole input impedance for $r = 2\lambda_c/400$ (e=53.5Ω) 42

4.6 Compared folded dipole input impedance for $s = 3\lambda_c/400$ (e=56Ω) 43

4.7 Compared FDZin using the full correction. $r = \lambda_c/400$ (e=32.3Ω) 44

4.8 Compared FDZin using the full correction. $r = 2\lambda_c/400$ (e=33.0Ω) 45

4.9 Compared FDZin using the full correction. $r = 3\lambda_c/400$ (e=28.68Ω) 46

4.10 The Measurement Geometry 48

4.11 Geometry used for the NEC2 Z12 verification 49

4.12 Comparison of mutual impedances obtained from NEC2, theoretical (labelled SCAT) and measurement. 50

4.13 Folded Dipole to Dipole mutual impedance geometry 51

4.14 Folded dipole to dipole mutual impedance 52

4.15 Geometry for the mutual impedance of two folded dipoles 53

4.16 Folded dipole to folded dipole mutual impedance 54

4.17 The effect of dipole thickness on mutual impedance – curves are obtained from NEC2 and measurement. 56

4.18 Geometry of two element Yagi-Uda array 57

4.19 NEC vs SCAT input impedance – 2 element Yagi-Uda, dipole feed replacing the folded dipole; (error norm = 2.43Ω) 58

4.20 NEC vs SCAT radiation pattern – 2 element Yagi-Uda, dipole feed replacing the folded dipole 59

4.21 NEC vs SCAT input impedance – 2 element Yagi-Uda with a folded dipole feed; (error norm = 36.37Ω) 60

4.22 NEC vs SCAT radiation pattern – 2 element Yagi-Uda, folded dipole feed . . 61

4.23 Geometry for the 5 element Yagi-Uda 62

4.24 NEC vs SCAT impedance – 5 element Yagi-Uda, dipole feed replacing the folded dipole; (error norm = 6.12Ω) 63

4.25 NEC vs SCAT radiation pattern – 5 element Yagi-Uda, dipole feed replacing the folded dipole 64

4.26 NEC vs SCAT impedance – 5 element Yagi-Uda folded dipole feed; (error norm = 278.85Ω) 65

4.27 NEC vs SCAT radiation pattern – 5 element Yagi-Uda, folded dipole feed . . 66

4.28 NEC vs SCAT impedance – 5 element Yagi-Uda folded dipole feed, 19mm diameter tubing. (error norm = 382.53Ω) 67

4.29 NEC vs SCAT radiation pattern – 5 element Yagi-Uda, folded dipole feed, 19mm diameter tubing. 68

A.1 Main menu 77

A.2 Array analysis menu 78

A.3 Impedance manipulation menu 79

A.4 Mutual impedance menu 80

A.5 Automated NEC mutual impedance menu 81

A.6 Get NEC Zin vals...menu 82

A.7 Wire Geometry Data Entry menu 83

A.8 Radiation Pattern Specification 84

B.1 Compared fd zin $r = 10$mm $s = 120$mm 102

B.2 Compared fd zin $r = 10$mm $s = 100$mm 103

B.3 Compared fd zin $r = 10$mm $s = 80$mm 104

B.4 Compared fd zin $r = 10$mm $s = 50$mm 105

D.1 Real and imaginary impedance 118

D.2 Magnitude and phase impedance 119

List of Tables

4.1 Runtimes for case studies presented on 386SX-25 69

B.1 Optimized α values 100

B.2 Equivalent lengths 100

B.3 Linear regression in the s plane 100

B.4 Linearized equivalent lengths 101

List of Symbols

$\mathbf{E}^s_{tan}$	the scattered tangential electric field caused by the current density J on the body
$\mathbf{E}^i_{tan}$	the incident tangential field due to a source
$\mathbf{J}$	current density vector
I_n	complex coefficients
$\mathbf{J}_n$	basis functions describing the current distribution on the general radiating body.
S	the surface of the radiating body
$[Z]$	a generalized impedance matrix
$[I]$	a generalized current vector
$[V]$	a generalized voltage excitation vector
k	the wavenumber $(= \frac{2\pi}{\lambda})$
$\mathbf{K}$	magnetic current density
μ	permeability
ϵ	permittivity
$\mathbf{F}$	retarded vector electric potential
$\mathbf{A}$	retarded vector magnetic potential
V	retarded scalar electric potential
U	retarded scalar magnetic potential
r	linear distance between source point and observation point
$G(x, x')$	$\frac{e^{-jkr}}{4\pi r}$

I_T	transmission line mode current
I_A	antenna mode current
l	tip-to-tip length of the folded dipole
Z_0	characteristic impedance
s	separation of the folded dipole sides
l_n	total length of dipole n
$I_{m,n}$	the current maximum on dipole n
βr_n	the *Spacial* phase component of dipole n
ϕ_n	the phase component due to the *Current Phase* on dipole n
α	length extension factor, to be found
Ω	$2\ln\left(\frac{2h}{a}\right)$, the Thickness Factor
$k_0 h$	$\frac{2\pi h}{\lambda}$
a	dipole radius
h	dipole half-length

Chapter 1

INTRODUCTION

1.1 Aim

> The aim of the research is to provide an efficient method of analysing antenna arrays composed specifically of resonant dipoles and folded dipoles. n-Port coupling theory and mutual impedance expressions that are based on a sinusoidal current distribution are used in preference to the more general Method-of-Moments. The main areas addressed in attaining this aim are defining the mutual impedance and the self impedance of the folded dipole.

The coupling theory used in this thesis requires that the self and mutual impedances of the antenna elements be found. Extensions to the transmission line analysis method for folded dipoles are developed to define the self impedance of the folded dipole. New expressions are developed for mutual impedance involving a folded dipole, ie dipole to folded dipole and folded dipole to folded dipole coupling, by combining the transmission line model of the folded dipole and aspects of the induced-emf method.

The existing theory and the new developments were combined in the computer program SCAT, whose sole purpose is to evaluate the proposed theory.

1.2 Importance of the Problem

Although it may appear counter-productive to develop an analysis method only for antennas composed of dipole and folded dipoles, antennas consisting of these simple elements (or their duals[1]) are sufficiently important and common to warrant special treatment. The antenna elements may be driven, or parasitic; some examples of this class of antenna include:

- Yagi-Uda arrays.

[1] eg The small loop antenna is a magnetic dipole

- Log-Periodic Dipole Arrays.
- Stacked Dipoles
- Phased Arrays
- Direction Finding (DF) antennas
- Loops, and arrays of loops (small loops)
- Slot arrays.

A Method-of-Moments program such as NEC2 (Burke & Poggio 1981) is often used in the analysis of these antennas. However, since NEC2 is a general program that can analyze any radiating structure, it does not take advantage of the simplifications that may be made when analyzing dipole elements. As a result, NEC2 will be far slower and use more resources than a simplified method for this class of antenna.

Another benefit of a faster, simplified method is that it allows more continuity of thought in an iterative design process. In the initial stages of an iterative design, it is important to establish cause-and-effect relationships with the various antenna parameters. A simplified, faster method would thus be used for the establishment of the trends, and a slower, more accurate method for final optimization and inclusion of ground effects.

A strong emphasis of the method proposed in this thesis is the ability to analyze folded dipoles. The folded dipole often used because of its ability to provide a solidly bonded DC earth which is important for lightning protection. The folded dipole also provides a wider bandwidth and a higher mechanical strength than the dipole. Most other simplified methods of analysis ignore folded dipoles.

As an example of recent interest in simplified analysis, Mahony (1989) presents some approximate theory to aid in the design of microwave slot planar array design; and (Lawson 1986) presents some analysis aids for Amateur Band Yagi-Uda arrays.

1.3 Limitations

The current distribution on the antenna is found by multiport network theory, using the self and mutual impedances of the antenna elements. All antenna parameters of interest can be calculated from these currents. The research in this thesis is therefore limited to the determination of the self and mutual impedances of these elements, particularly with regard to the folded dipole.

The input impedances of the dipole elements are obtained from look-up tables generated by NEC2, taking the dipole thickness into account. However the tables are for the free-space dipole impedance, which is different from the self-impedance of an element within an array.

The difference between these two impedances is acceptable over most of the range of interest, but not when the dipole lengths are around a full wavelength long.

The mutual impedance expression is based on a sinusoidal current distribution, which produces a numerical singularity when the dipoles are a full wavelength long. As a result, the theory cannot analyse antennas whose elements are a full wavelength long.

The combination of the previous two problems at a full wavelength leads to the limitation of the scope of the thesis to dipoles at or relatively near half-wave resonance, although some suggestions are presented to circumvent them.

The mutual impedance derivation also assumes z-directed currents, ie that the dipole are parallel to a common axis (not necessarily collinear or coplanar) since this is the most common configuration. However, this is easily extended to coplanar-skew and even non-coplanar-skew systems, which are outside the scope of the thesis.

1.4 Overview of the Thesis

Chapter 2 on page 5 provides the theoretical background for the thesis:

- An overview of the Method-of-Moments is presented since it is used as a standard against which the theory in this thesis is measured. The Method-of-Moments implementation in the Numerical Electromagnetic Code is discussed with some of the practical implications.
- Circuit network theory is briefly reviewed as it applies to antenna systems.
- The transmission line model of the folded dipole is presented, which is used to determine its self impedance, and also used in the development of the mutual impedance expression.
- A literature survey of the development of mutual impedance expressions for dipoles is presented, and the induced-emf method is used to develop the usual mutual impedance expression.
- The theory linking the current distribution on an antenna to the far-field radiation pattern is reviewed as this is used in the SCAT package.

In Chapter 3 on page 24 the theory necessary for antenna analysis by the simplified method presented in chapter 2 is developed:

- A distinction between the free space input impedance and the self impedance of a dipole is made, and the conditions where they may be made to be equivalent are defined.

- The transmission line model of the folded dipole is inadequate for folded dipoles of practical interest. The model is extended by defining an equivalent length which takes the inter-element spacing of the folded dipole into account.
- The combination of the usual induced-emf method to derive mutual impedance, and the transmission line model of the folded dipole allows an expression to be derived for the mutual impedance between folded dipoles, and between dipoles and folded dipoles.
- A method of obtaining mutual impedance for any two antennas directly from the NEC2 package is presented.

Chapter 4 on page 36 presents the results of the theory:

- The folded dipole self impedance values derived from NEC2 and SCAT.
- Mutual impedance results are shown. The NEC method of obtaining the mutual impedance is validated, and the mutual impedance involving a folded dipole is thus shown to conform to the theory developed in Chapter 3.

Chapter 5 on page 71 summarises the findings and presents conclusions. Recommendations for further work are also presented.

Appendix A on page 74 is a manual for the SCAT computer package developed in this thesis. An overview of the package is given, followed by a brief discussion of its user interface, and a interface listing of all public procedures.

Appendix B on page 99 describes the empirical technique used to determine the extension factor for the transmission line model of the folded dipole.

Appendix C on page 106 is a tabulation of the dipole self impedance values derived from NEC that are used in SCAT.

The Bibliography lists references that were used in the background reading for the thesis, but were not specifically cited.

Chapter 2

BACKGROUND

The Method-of-Moments is used extensively to validate the accuracy of the simplified theory presented in this thesis (as embodied in the computer program SCAT). Section 2.1 gives the background to the theory of the Method-of-Moments and discusses some practical aspects of its implementation.

Circuit network theory is used to determine the coupling between dipole elements of the antennas. The relevant background theory is in section 2.2 which highlights some of the difficulties in applying it in an antenna environment (Clark & Fourie 1993). Essentially, antenna analysis with this method involves finding the self and mutual impedances of the antenna array elements.

Section 2.3 gives the background to the transmission line model of the folded dipole, which gives a computationally efficient method of calculating the input impedance.

This thesis presents the mutual impedance between folded dipoles, which is later shown to be an extension of the theory of the mutual impedance between cylindrical dipoles. Section 2.4 is a literature survey of the pertinent aspects of the development of the dipole mutual impedance theory.

Finally, section 2.5 reviews the theory to obtain the far field radiation pattern from currents on the antenna.

2.1 Method-of-Moments

The Method of Moments is used as an accuracy benchmark to validate the theory developed in the thesis, hence an overview of the method is given.

2.1.1 General Theory

The integral equations associated with a general electromagnetic system are reduced to a set of linear algebraic equations by the Method-of-Moments (MOM) (Harrington 1968). The unknowns in the method are the coefficients of the current distribution of the system, due to some excitation. A brief overview of the important aspects of MOM is given in this section.

Consider the conducting and radiating body shown in figure 2.1

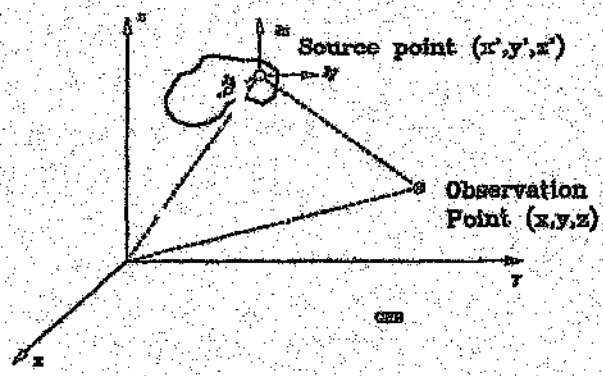


Figure 2.1: General radiating body

Maxwell's electric field boundary condition states that the total tangential electric field on the surface is zero, since it is a perfectly conducting body, ie:

$$0 = \mathbb{E}^s_{tan} + \mathbb{E}^i_{tan} \tag{2.1}$$

where

$\mathbb{E}^s_{tan}$ = the scattered tangential electric field caused by the current density $\mathbb{J}$ on the body

$\mathbb{E}^i_{tan}$ = the incident tangential field due to a source

The relationship between the scattered field $\mathbb{E}^s_{tan}$ and the current density $\mathbb{J}$ which causes it, is given in general by a linear operator L_{op}, often in the form of an integro-differential equation. Thus (the subscript $_{tan}$ being omitted, but understood) we define:

$$L_{op}(\mathbb{J}) \equiv -\mathbb{E}^s = \mathbb{E}^i \tag{2.2}$$

The unknown current distribution J can be obtained in terms of the known excitation, $\mathbb{E}^i$, by rearranging equation (2.2):

$$\mathbb{J} = L_{op}^{-1}(\mathbb{E}^i) \tag{2.3}$$

Note that the Linear Operator L_{op} must therefore perform a *conformal* mapping from the subset containing J to a subset containing $\mathbb{E}^i$ in the operator domain.

Equation (2.3) obtains the solution for J by inverting the linear operator. As the operator is usually an integral operator, it is never explicitly inverted in this manner. Instead, a method-of-moments technique is developed which has the advantage of greater numerical stability and is generally easier to implement.

In the method-of-moments technique, the current density J is is broken up into a series of current densities distributed over the body, which describe the *form* of the current distribution, ie it is expressed as a linear combination of basis functions $\mathbb{J}_n$:

$$\mathbb{J} = \sum_n I_n \mathbb{J}_n \tag{2.4}$$

where

I_n = complex coefficients

$\mathbb{J}_n$ = basis functions describing the current distribution on the general radiating body.

Substituting equation (2.4) into equation (2.2) gives:

$$L_{op}\left(\sum_n I_n \mathbb{J}_n\right) = \mathbb{E}^i \tag{2.5}$$

Since L_{op} is a linear operator, we can re-arrange the integral and the summation as:

$$\sum_n I_n L_{op}(\mathbb{J}_n) = \mathbb{E}^i \tag{2.6}$$

The form shown in the above equation gives rise to the formation of the (scalar) inner product, $< \mathbb{J}, \mathbb{E} >$, defined as the surface integral:

$$< \mathbb{J}, \mathbb{E} > = \oint \mathbb{J} \circ \mathbb{E} dS \tag{2.7}$$

where

S = the surface of the radiating body

The inner product is called Reaction as this is a physically observable quantity of the antenna. The reactions are weighted over the body by a set of weighting functions $\mathbb{W}_m$, thus forming the matrix equation:

$$\begin{bmatrix} <\mathbb{W}_1, L_{op}(\mathbb{J}_1)> & <\mathbb{W}_1, L_{op}(\mathbb{J}_2)> & \cdots \\ <\mathbb{W}_2, L_{op}(\mathbb{J}_1)> & \cdots & \cdot \\ \vdots & \ddots & \vdots \\ \cdot & \cdots & <\mathbb{W}_n, L_{op}(\mathbb{J}_n)> \end{bmatrix} \begin{bmatrix} I_1 \\ I_2 \\ \vdots \\ I_n \end{bmatrix} = \begin{bmatrix} <\mathbb{J}_1, \mathbb{E}^i> \\ <\mathbb{J}_2, \mathbb{E}^i> \\ \vdots \\ <\mathbb{J}_n, \mathbb{E}^i> \end{bmatrix} \tag{2.8}$$

The matrix equation is usually written in condensed form as

$$[Z][I] = [V] \tag{2.9}$$

where

$[Z]$ = a generalized impedance matrix
$[I]$ = a generalized current vector
$[V]$ = a generalized voltage excitation vector

whose solution takes the form:

$$[I] = [Z]^{-1}[V] \tag{2.10}$$

which defines the general method of moments applicable to any radiating, conducting body. In order to solve this system of equations, the following still needs to be defined:

- the set of weighting functions, $\mathbb{W}_m$
- the set of basis functions, $\mathbb{J}_n$, and
- the form of the linear operator, L_{op}

The choice of these three items distinguish the various implementations of the method of moments. The different choices also introduce different restrictions to the method.

After they have been defined, the impedance matrix $[Z]$ can be filled, the excitations $[V]$ specified, and the currents $[I]$ found. All antenna parameters of interest can be calculated from these currents, ie

- radiation pattern
- input impedance
- scattering cross section

- current distribution
- amount of coupling to other bodies

2.1.2 The NEC2 implementation of MOM

The Numerical Electromagnetic Code, Version 2 (NEC2) (Burke & Poggio 1981) is a well known implementation of the Method-of-Moments. NEC2 simulation results compare well with measured results provided that the program is used correctly. As the program can easily be mis-applied, various heuristical rules have been developed to avoid the more common pitfalls (Clark & Fourie 1980, Kubina 1983, Ludwig 1987)

NEC2 has been the primary antenna analysis tool for several years, and its validity has been verified against measured results by numerous researchers (eg (Chiodini 1989)). A new analysis method, such as the one proposed in this thesis can thus be validated against NEC2's results with confidence.

The weighting and basis functions, and the linear operator used by the NEC2 program will now be discussed. Only the Electric Field Integral Equation (EFIE) form will be discussed, as surface patch modelling using the Magnetic field Integral Equation (MFIE) form is beyond the scope of the thesis.

The choice of weighting functions

Since the linear operator is usually an integral operator, there are *two* integrations to be performed to evaluate each matrix element in the impedance matrix $[Z]$ (Equation 2.8) – one for the linear operator and one to determine the inner product (a surface integral). This is computationally expensive and it is desirable to reduce this load, if a judicious choice of weighting function can remove one integration. Consider using a Dirac Delta function as the weighting function:

Since the integral of an impulse weighted function is a sample of that function at the impulse point, or:

$$\int f(t)\delta(t-\tau)dt = f(\tau) \tag{2.11}$$

the inner product integration collapses to a sample of the dot product at the application point of the impulse. Thus, this technique is known as point matching (also known as the collocation method).

Physically, point matching implies that the boundary condition of zero tangential fields, as assumed in equation (2.1), holds only at the sampling points and may be non-zero at other

points. For the method to be accurate, enough samples must be used to ensure that the magnitude of the field at the non-sampled points is sufficiently small.

Note that in practice, it is not necessary to have equispaced sampling points on the numerical model of the structure, but it is usual in the more sensitive areas of the model, such as the feedpoint.

The choice of basis functions

Although the particular form of the basis function is not critical to the functioning of the method of moments, it has been shown that the closer the form of the basis function to the actual form of the current distribution on the radiating structure, the faster the method converges. (Thiele 1973, Pg 18) This implies that fewer samples need to be taken for a particular problem. Fewer samples are a definite advantage to a method since the order of the MOM impedance matrix, which needs inverting, is directly related to the number of sample points.

The basis functions used in NEC2 are known as sub-domain bases since they are valid for the sub-domain surrounding the point match and not over the entire radiating structure. Sub-domain bases ease the calculation of the inner product and help to ensure that the impedance matrix is well conditioned. (Burke & Poggio 1981, Pg I-10)

NEC2's basis functions consist of a linear combination of a sine, a cosine, and a constant term:

$$\mathbb{J}_i = a_i + b_i \sin(ks_i) + c_i \cos(ks_i) \tag{2.12}$$

where

$b_i \& c_i$ = constants, obtained from boundary conditions
a_i = constant, obtained by solving the impedance matrix.
k = the wavenumber $(= \frac{2\pi}{\lambda})$
s_i = the segment length (ie the sampling interval)

The form of the linear operator

Pocklington (1897) developed an integral equation describing the currents on a radiating body using Maxwell's equations for regions containing harmonic magnetic and electric sources. Pocklington's equation contains the linear operator required by the method of moments, as it is used by NEC2. We start with Maxwell's equations (harmonic electric and magnetic sources):

$$\nabla \times \mathbb{E} = -j\omega\mu\mathbb{H} - \mathbb{K}$$

$$\nabla \times \mathbb{H} = j\omega\epsilon\mathbb{E} + \mathbb{J} \tag{2.13}$$

where

$\mathbb{J}$ = electric current density
$\mathbb{K}$ = magnetic current density
μ = permeability
ϵ = permittivity

and reduce these in terms of the field quantities:

$$\begin{aligned} \mathbb{E} &= -j\omega\mathbf{A} - \nabla V - \frac{1}{\epsilon}\nabla \times \mathbf{F} \\ \mathbb{H} &= -j\omega\mathbf{F} - \nabla U + \frac{1}{\mu}\nabla \times \mathbf{A} \end{aligned} \tag{2.14}$$

where

$\mathbf{F}$ = retarded vector electric potential
$\mathbf{A}$ = retarded vector magnetic potential
V = retarded scalar electric potential
U = reterded scalar magnetic potential
r = linear distance between source point and observation point
$\rho; m$ = being the volume densities of electric and magnetic charge

defined as:

$$\begin{aligned} \mathbf{A} &= \mu \iiint \frac{\mathbb{J}e^{-jkr}}{4\pi r} dv' \\ \mathbf{F} &= \epsilon \iiint \frac{\mathbb{K}e^{-jkr}}{4\pi r} dv' \\ V &= \iiint \frac{\rho e^{-jkr}}{4\pi\epsilon r} dv' \\ U &= \iiint \frac{me^{-jkr}}{4\pi\mu r} dv' \end{aligned} \tag{2.15}$$

The relationship between the vector quantities $\mathbf{A}$ and $\mathbf{F}$ and the scalar quantities V and U are given by the Lorentz gauge equations:

$$\begin{aligned} \nabla \circ \mathbf{A} &= -j\omega\mu\epsilon V \\ \nabla \circ \mathbf{F} &= -j\omega\mu\epsilon U \end{aligned} \tag{2.16}$$

To simplify matters when dealing with typical radiating structures, we can assume:

- non-magnetic environments where the permeability is that of free space
- axially directed electric currents flowing only in the z-direction (ie this implies a limitation on the radiating body to be constructed of thin wires only

Then the two Lorentz equations simplify to one (more familiar) equation in one dimension:

$$\frac{\partial A_z}{\partial z} = -j\omega\mu\epsilon V \tag{2.17}$$

and thus equation (2.14) reduces to

$$E_z = -j\omega A_z - \frac{\partial V}{\partial z} \tag{2.18}$$

Differentiating equation (2.17) with respect to z and substituting for $\frac{\partial V}{\partial z}$ in the above equation yields:

$$E_z = \frac{1}{j\omega\mu\epsilon}\left(\frac{\partial^2 A_z}{\partial z^2} + k^2 A_z\right) \tag{2.19}$$

or, for an infinitesimal current element $\mathbf{J}dv'$:

$$dE_z = \frac{1}{j\omega\epsilon}\left[\frac{\partial^2 G(z,z')}{\partial z^2} + k^2 G(z,z')\right]\mathbf{J}dv' \tag{2.20}$$

From equation (2.15), $A_z = G(z,z')$ is defined as the free space Green's function.

where

$$G(z,z') = \frac{e^{-jkr}}{4\pi r}$$

Thus for a current density J parallel to the z axis:

$$E_z = \frac{1}{j\omega\epsilon}\iiint\left[\frac{\partial^2 G(z,z')}{\partial z^2} + k^2 G(z,z')\right]\mathbf{J}dv' \tag{2.21}$$

and finally, assuming that the current density J is restricted to the surface of the cylinder, and distributed uniformly (ie $a \ll \lambda$), then equation (2.21) reduces to a surface integral:

$$\int_{-L/2}^{L/2} I(z')\left[\frac{\partial^2 G(z,z')}{\partial z^2} + k^2 G(z,z')\right]dz' = -j\omega\epsilon E_z^i(z) \tag{2.22}$$

which is Pocklington's equation, and incorporates the necessary Linear Operator required for the Method of Moments.

2.1.3 NEC2 Limitations

NEC2 is a highly competent program, but its accuracy depends largely on the ability of the user to faithfully model the physical situation in numerical terms. As a result of the difficulty in modelling, there have been attempts to automate the heuristical approach to constructing NEC models (Givati, Clark & Fourie 1989), (Walker, Sorensen & Kenney 1989). Since NEC2 has been used extensively in obtaining results for this thesis, a brief list of the more important considerations is given:

- NEC2 converges when using ten or more segments per wavelength of straight wire (ie the sampling interval). A greater density, however, may be required in sensitive areas of the model (particularly at discontinuities) and a more relaxed density may be allowable on long sections relatively far from the feedpoint. (Burke & Poggio 1981)
- The length to thickness ratio of a wire segment may not be less than 8 – due to the assumption of filamentary current flow in the derivation of Pocklington's equation. If the Extended Green's function is specified for the kernel, however, the length to thickness ratio may go as low as 2. The implication of this limitation is that, for a particular wire thickness, the minimum length of the segment is restricted – effectively putting an upper frequency limit its evaluation. If higher frequency evaluation of the wire is necessary, wire cage modelling is the only option – which has limitations of its own, some of which are discussed in Clark & Fourie (1989)
- The thickness of abutting segments must be comparable. If they are sufficiently disparate, inaccuracies in the current flow across the junction will occur.
- The ratio of the segment lengths at a junction should be comparable to within a factor of five (Kubina 1983). This is a typical heuristical rule which cannot be substantiated by derivation, but only shown by experimentation. The accuracy degrades exponentially as this factor gets larger than five, and by a factor of six, the error is unacceptably large.
- The circumference of the wire must be much less than one wavelength, ie $\frac{2\pi a}{\lambda} \ll 1$ otherwise the basic assumption of axially directed current no longer holds.
- Segment match points may not overlap – or an indeterminate current will result. The implication is that wires with fairly short segments meeting at acute angles must be modelled with care.
- For acceptable results, wires should be several radii apart. If they are close, and parallel, then their segments should align.
- Modelling a solid surface with a wire grid is sometimes unpredictable, especially when near field quantities are being evaluated. Under these conditions the usual rule-of-thumb of ten wires per wavelength may not be a sufficient condition for convergence. The radius of the wires used for the grid also needs to be carefully chosen. (Ludwig 1987, Mayhan 1990)

- Choosing the feedpoint model can be difficult, the best one for the application can be the "wrong" model to use (Clark & Fourie 1989). The question of feedpoint models is receiving on-going investigation (Pages 1987, Cox 1993).

2.2 n-Port Circuit Network Theory

A two port circuit can be completely characterized in terms of the interaction between its two ports. The basic two port network theory can be extended to apply for two antenna radiators (Carter 1932, Balanis 1982). Defining the voltages and currents as in figure 2.2,

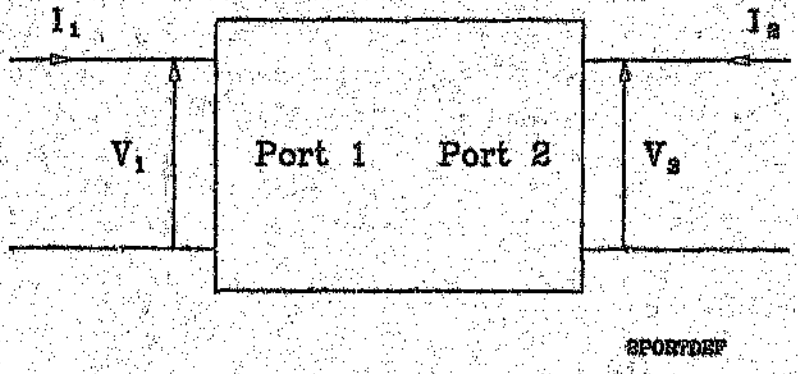


Figure 2.2: Definition of currents in a two port network

the interaction between the ports is given by the matrix equation:

$$\begin{bmatrix} V_1 \\ V_2 \end{bmatrix} = \begin{bmatrix} Z_{11} & Z_{12} \\ Z_{21} & Z_{22} \end{bmatrix} \begin{bmatrix} I_1 \\ I_2 \end{bmatrix} \tag{2.23}$$

where:

$$\begin{aligned} Z_{11} &= \left.\frac{V_1}{I_1}\right|_{I_2=0} \\ Z_{12} &= \left.\frac{V_1}{I_2}\right|_{I_1=0} \\ Z_{21} &= \left.\frac{V_2}{I_1}\right|_{I_2=0} \\ Z_{22} &= \left.\frac{V_2}{I_2}\right|_{I_1=0} \end{aligned} \tag{2.24}$$

For a general n-port network, the terms on the diagonal, Z_{nn} are called the self-impedances while the terms off the diagonal Z_{mn} are the mutual impedances. In a real passive system, $Z_{mn} = Z_{nm}$, so that the matrix is symmetrical about the diagonal.

It is usual to apply the network theory to a circuit, but it can be applied to two antennas in free space. However, there are problems with the definition of the self impedances as defined in equation (2.24). For example, the definition of the self impedance of the first antenna requires that the current I_2 in the second antenna be zero. In the circuits case, it is sufficient to open circuit the second port. Open circuiting the second antenna, however, does not remove its effects – as discussed in section 3.1 on page 24.

2.3 Folded Dipole Input Impedance

A folded dipole can be considered as an unbalanced transmission line which radiates as a result of its unbalanced condition (Tai 1948, Thiele, Tice & Henderson 1980). Thiele et al. (1980) showed that the current on the dipole can be considered to be composed of two modes: a transmission line mode and an antenna, or radiating mode, as shown in figure 2.3.

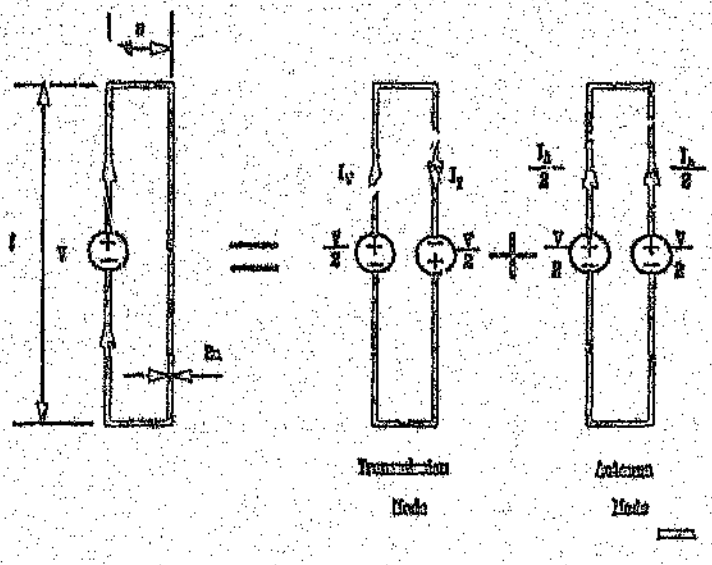


Figure 2.3: The decomposition of the folded dipole current into an antenna mode and a transmission line mode

By superposition of the two current modes in figure 2.3, the input impedance of the folded dipole is given by:

$$Z_{in} = \frac{V}{I_T + \frac{1}{2}I_A} \tag{2.25}$$

where

I_T = transmission line mode current

I_A = antenna mode current

The modal currents I_T and I_A are obtained by looking at the equivalent input impedances of the modes.

The impedance for the transmission line mode Z_T is that of a short-circuited lossless transmission line given by:

$$Z_T = -jZ_0 \tan\left(\frac{kl}{2}\right) \tag{2.26}$$

where

l = tip-to-tip length of the folded dipole

Z_0 = characteristic impedance

The characteristic impedance is that of a two-wire line and is given by:

$$Z_0 = 120 \ln\left[\frac{s + \sqrt{s^2 - 2a^2}}{2a}\right] \tag{2.27}$$

where

s = separation of the folded dipole sides

a = radius

The impedance for the antenna mode Z_D is that of a cylindrical dipole with an increased effective radius a_e which is a function of the spacing s and the wire radius a:

$$\begin{aligned} \ln(a_e) &= \ln(a) + \frac{1}{2}\ln\left(\frac{s}{a}\right) \\ \therefore a_e &= \sqrt{as} \end{aligned} \tag{2.28}$$

Z_D can be found using known methods such as the induced-EMF method (Balanis 1982), standard published impedance tables (King & Harrison 1969), or a Method-of-Moments code (Burke & Poggio 1981).

Thus the modal currents are given as:

$$I_T = \frac{V/2}{Z_T} = \frac{V}{2Z_T}$$

$$I_A = \frac{V}{2Z_D} \tag{2.29}$$

Substitution of the currents in equation (2.29) into equation (2.25) gives the input impedance as:

$$Z_{in} = \frac{4Z_T Z_D}{Z_T + 2Z_D} \tag{2.30}$$

The importance of equation (2.30) is that it gives a simple method of determining the folded dipole input impedance without resorting to complex methods like the method of moments. The transmission line method essentially presents a correction to tabulated cylindrical dipole impedances.

Unfortunately, the method is accurate only where the separation s is less than one hundredth of a wavelength, which is a severe restriction in practice. An extension to the transmission line method to overcome this restriction has been presented (Clark & Fourie 1991) which is discussed in section 3.2 on page 29.

2.4 Mutual Impedance – a Literature Survey

A brief history of the development of the standard expressions for mutual impedance is given here. Many of the references in the bibliography refer to work done in this regard, but these give the basic outline of the progression to the standard expression for mutual impedance between dipoles, derived by the induced-emf method (typically).

Carter (1932) introduces the circuits laws in relation to an antenna system. He showed that the circuit network theory can be applied to two dipole radiators of integral number of half wavelengths.

For wires that are an exact integral number of half waves long, he produces the standard field conditions at a point, from which the mutual impedance is derived. He solves these in closed form (Si and Ci integrals) for:

- parallel wires of equal length (Not Staggered),
- Parallel wires in Echelon,
- Collinear wires
- and (though not in closed form) for two wires forming a Vee (as in a rhombic)

In his classic treatise, Brown (1937) slightly extends the work of Carter, and uses the mutual impedances to produce graphical radiation patterns of an AM broadcast antenna.

Cox (1947) extends the theory to allow antennas of unequal lengths but as he was addressing the AM broadcast antennas of the day, his method does not allow the antennas to be staggered in echelon.

Tai (1948) was the first author to consider the effect of thickness on the calculation of the mutual impedance. Unfortuanately his method involves driving the antennas in a symmetric and anti-symmetric mode, his assumption of identical antennas is intrinsic to the method, which is also limited to non-staggered antennas. He produces curves of mutual impedance as it varies with thickness factor, which are of use.

King (1957) builds on Carter, Brown and Cox, to calculate the mutual impedance, in closed form, of unequal length antennas in echelon, for the cases of non-staggered, staggered, or collinear. He covers antennas of a half-wavelength long, or shorter. It is his non-closed form, integral equation that is of interest to the standard derivation of the mutual impedance.

Finally, the closed-form solutions are completed by Richmond & Geary (1970) who extend the work to the co-planar skew situation, followed by Richmond & Geary (1975) who treat non co-planar skew dipoles (ie arbitrary orientation)

No expressions have been given for the mutual impedance involving a folded dipole.

Most of the effort in the above references was expended in getting the integral equations into a closed, but non-general form (in most cases with the use of Ci and Si integrals, with as many as 40 such evaluations per point). However, it is now more useful to use the more general integral form and use an efficient integrating algorithm. (SCAT uses the Romberg Integration method, with a Trapezoidal starter, and Richardson Extrapolation).

The usual expression for the mutual impedance, evolved from the work outlined above, is now reviewed as a similar derivation is followed when deriving the folded dipole mutual impedance in Chapter 3. Using the the symbols identified in figure 2.4:

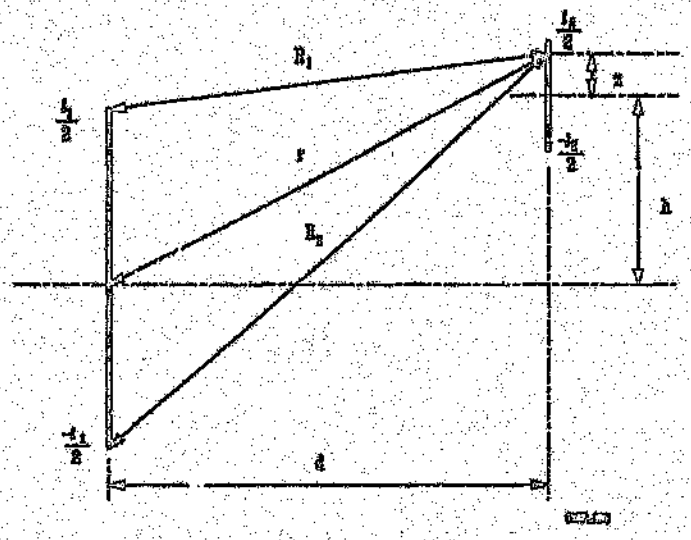


Figure 2.4: Geometry of two parallel dipoles in echelon

the open circuit voltage induced in antenna 2 due to the radiation from antenna 1 excited by a current I_1 can be expressed in the usual way as:

$$V_{21} = -\frac{1}{I_{2i}} \int_{-\frac{l_2}{2}}^{\frac{l_2}{2}} E_{z21}(z) I_2(z) dz \tag{2.31}$$

where

E_{z21} = E field component radiated by antenna 1 parallel to antenna 2

$I_2(z)$ = is the current distribution on antenna 2 as a function of z.

I_{2i} = is the current at the input to antenna 2.

Assume a sinusoidal current distribution for $I_2(z)$ of the form:

$$I_2(z) = I_m \sin\left[k\left(\frac{l}{2} - |z|\right)\right] \tag{2.32}$$

where

I_m = is the maximum current

l = is the dipole length.

The z-directed component of the electric field of a dipole given at a point P in space, assuming sinusoidal current distribution is of the standard form:

$$E_z = -j\frac{\eta I_m}{4\pi}\left[\frac{e^{-jkR_1}}{R_1} + \frac{e^{-jkR_2}}{R_2} - 2\cos\left(\frac{kl}{2}\right)\frac{e^{jkr}}{r}\right] \tag{2.33}$$

Substituting equation 2.33 and equation 2.32 into equation 2.31, and realizing that the mutual impedance (referred to the input terminals) is given by:

$$Z_{21i} = \frac{V_{21}}{I_{1i}} \tag{2.34}$$

$$\begin{aligned} Z_{21i} &= j\frac{\eta I_{1m} I_{2m}}{4\pi I_{1i} I_{2i}} \int_{\frac{-l_2}{2}}^{\frac{+l_2}{2}} \sin\left[k\left(\frac{l_2}{2} - |z|\right)\right] \\ &\times \left[\frac{e^{-jkR_1}}{R_1} + \frac{e^{-jkR_2}}{R_2} - 2\cos\left(\frac{kl_1}{2}\right)\frac{e^{jkr}}{r}\right] dz \end{aligned} \tag{2.35}$$

It is usual to refer the mutual impedance to the current maximum, and it is computationally useful to separate the real and imaginary parts:

$$\begin{aligned} Z_{21m} &= \frac{\eta}{4\pi}\int_{\frac{-l_2}{2}}^{\frac{l_2}{2}} \sin\left[k\left(\frac{l_2}{2} - |z|\right)\right] \times \left[\frac{\sin(kR_1)}{R_1} + \frac{\sin(kR_2)}{R_2} - \frac{2\cos\left(\frac{kl_1}{2}\right)\sin(kr)}{r}\right] dz \\ &+ j\frac{\eta}{4\pi}\int_{\frac{-l_2}{2}}^{\frac{l_2}{2}} \sin\left[k\left(\frac{l_2}{2} - |z|\right)\right] \times \left[\frac{\cos(kR_1)}{R_1} + \frac{\cos(kR_2)}{R_2} - \frac{2\cos\left(\frac{kl_1}{2}\right)\cos(kr)}{r}\right] dz \end{aligned} \tag{2.36}$$

To return to the required mutual impedance (referred to the input terminals) simply multiply equation 2.36 by the currents:

$$Z_{21i} = Z_{21m}\left(\frac{I_{1m}}{I_{1i}}\right)\left(\frac{I_{2m}}{I_{2i}}\right) = Z_{21m}\left[\frac{1}{\sin(kl_1/2)}\right]\left[\frac{1}{\sin(kl_2/2)}\right] \tag{2.37}$$

Note that the mutual impedance given by equation 2.37 will tend to infinity for full wavelength dipoles, due to the sinusoidal current assumption, which may be compensated for by a damping factor in the denominator, or by the inclusion of a quadrature current component, if desired.

2.5 Radiation Pattern Theory

The calculation of the far field radiation pattern from currents on radiators is a straightforward integration (summation) of the effects of the individual current elements at the evaluation point.

The theory developed in this thesis provides the magnitude and phase of the current in each z-directed dipole element, assumed to be sinusoidally distributed. There is no E_ϕ component of the radiated field, but only an E_θ component.

(Kraus 1988, Pg 221) shows from first principles that the radiated far fields from wire n are related to the sinusoidal currents flowing on it by:

$$E_{\theta,n} = \frac{j60\,[I_{0,n}]}{r}\left[\frac{\cos[(kl_n\cos\theta)/2] - \cos(kl_n/2)}{\sin\theta}\right] \tag{2.38}$$

where

l_n = total length of dipole n

$[I_{0,n}] = I_{m,n}e^{j(\omega t - \beta r_n + \phi_n)}$

$I_{m,n}$ = the current maximum on dipole n

βr_n = the *Spacial* phase component of dipole n

ϕ_n = the phase component due to the *Current Phase* on dipole n

r = distance from the current on the dipole to the field evaluation point.

θ = is the angle defined in figure 2.5.

The distance r to the evaluation point P is slightly different for each dipole in the antenna array. The difference in magnitude due to this slight change in r is negligible, especially for large r, but the path difference is crucial in the phase component. Thus the distance from the centre of each current element needs to be computed to obtain the spatial phase difference required for the vector summation of the fields at the evaluation point.

Figure 2.5 shows the necessary geometry. The current element is at point Q, and the vector from the origin to point Q is $\mathbf{r}' = (x', y', z')$. Assuming that the evaluation point P is very much further away from the origin as point Q, the required distance is the component of $\mathbf{r}'$ in the direction of the vector to P given by the vector $\mathbf{r} = (x, y, z)$ ie the dot-product of $\mathbf{r}'$ and a unit vector in the direction of $\mathbf{r}$.

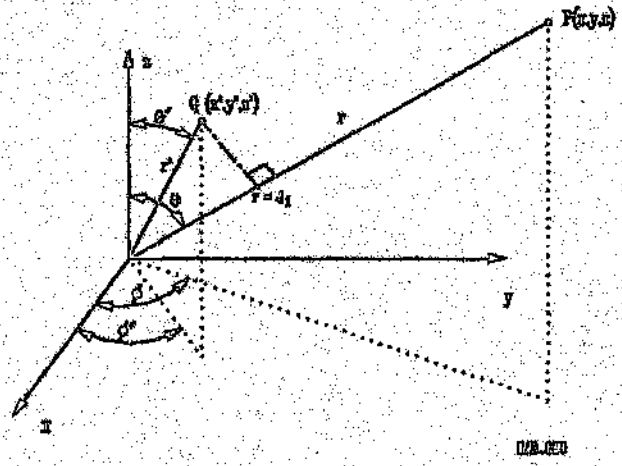


Figure 2.5: The far-field radiation geometry

$$\therefore d_1 = \mathbf{r}' \circ \frac{\mathbf{r}}{|\mathbf{r}|} \tag{2.39}$$

The required unit vector in the direction of the evaluation point is:

$$\frac{\mathbf{r}}{|\mathbf{r}|} = (\sin\theta\cos\phi, \sin\theta\sin\phi, \cos\phi) \tag{2.40}$$

the dot product of the two vectors yields a value for the point labelled d_1 in figure 2.5 and yields the spatial phase component $\angle e^{jkd_1}$ which is added to the phase due to the current on the element.

Fields due to all N dipole elements are vectorially summed to yield E_{Summed} at the evaluation point P and are divided by the field at that distance that would be generated by an isotropic source, $E_{\text{Isotropic}}$ to give the directivity in dBi.

$$E_{\text{Summed}} = \sum_{n=1}^{N} E_{\theta,n} \tag{2.41}$$

$$E_{\text{Isotropic}} = \sqrt{\frac{30P_{\text{in}}}{r}} \tag{2.42}$$

ie the directivity in the direction (θ, ϕ) is given by:

$$D(\theta,\phi) = 20\log_{10}\left(\frac{|E_{\text{Summed}}|}{|E_{\text{Isotropic}}|}\right)^2 \quad \text{(dBi)} \tag{2.43}$$

which is the value that SCAT produces when asked to generate a radiation pattern.

Chapter Summary

- NEC is the method of moments implementation used as a benchstick to measure the accuracy of the new methods developed in the thesis. A review of the method of moments has been given, as well as some implementation specific constraints of NEC2.
- Circuit network theory is used in the analysis of antenna arrays and has thus been reviewed, the conclusions being that the self and mutual impedances of the antenna elements need to be found.
- The transmission line model of the folded dipole has been reviewed, as it is an efficient means of finding the self-impedance of the folded dipole. Some limitations have been discussed.
- A review of the dipole mutual impedance derivation has been given, since a similar procedure is adopted in the mutual impedance derivation for folded dipoles.

- The far-field radiation pattern can be obtained from a knowledge of the currents on the antenna. The theory for this has been reviewed as it is instructive to compare patterns as well as input impedances when comparing analysis methods.

Chapter 3

DEVELOPMENT OF THEORY

Chapter 3 develops the theory reviewed in chapter 2. The primary concern is with the determination of self and mutual impedances of the antenna elements. The concept of self-impedance is looked at more fully, as compared to free-space (isolated) input impedance.

The folded dipole transmission line model, which due to certain restrictions cannot be applied to many folded dipoles of practical dimensions, is extended so that it applies to most folded dipoles. The model provides an efficient method of calculating the self impedance of the folded dipole.

The model also provides a convenient description of the folded dipole which is used in the induced-emf derivation of mutual impedance, providing an expression for the mutual impedance between a dipole and a folded dipole. An expression for the mutual impedance between two folded dipoles is provided by a logical extension.

3.1 Dipole Self-Impedance

In section 2.2 on page 14, network coupling theory was introduced, from which it is evident that antenna analysis depends on finding the self-impedance of each element and their mutual impedances.

The self impedance of a dipole, as defined in equation (2.24), requires zero current flow at the port of the other dipole. The free space input impedance, on the other hand, is evaluated in total isolation.

A distinction is thus made between the *free space dipole input impedance* $Z_{11\text{Free}}$ and the self-impedance Z_{11} as defined by equation (2.24). Figure 3.1 illustrates that an open circuit at the feed point of a second dipole in close proximity does not remove its effect on the first dipole.

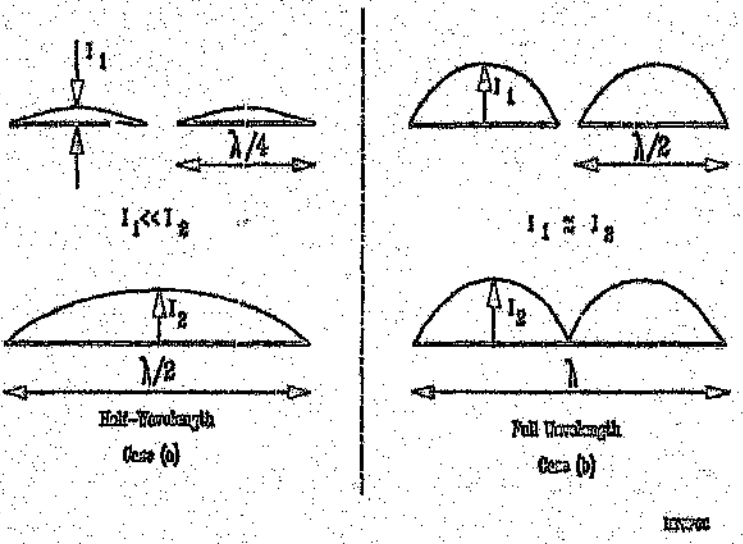


Figure 3.1: The current distribution on half and full wavelength dipoles

For the half-wavelength case (a) The magnitude of the induced currents on the two $\lambda/4$ sections of open circuited dipole is not particularly large since the sections are short in terms of wavelength, and the open circuit is forcing a current zero at the ends.

The coupling effects between the dipoles will be minimal and hence there will be no appreciable difference between the free-space input impedance $Z_{11\text{Free}}$ and the self impedance Z_{11}

For the Full wavelength case (b) The open circuited sections of one second dipole are resonant half wavelength long structures. Thus the magnitude of the induced currents on these sections will be of the same order as the current on the first dipole if they are close together.

Coupling effects will obviously be strong, and one would expect a marked difference in the values of the free space and self impedances.

The difference in the two impedances is of importance since the calculation of an input impedance Z_{11} in the presence of two open circuited sections of dipole is no longer trivial and is beyond the scope of a simplified analysis method. The advantage of using the free-space input impedance as an approximation to the self-impedance is that the free-space impedance is readily available in look-up table form (King & Harrison 1969), and other sources.

Many authors (Balanis 1982, Pg 297);(Jordan & Balmain 1968, Pg 537) and (Elliott 1981, Pg 327) state that in *most instances* the free-space dipole impedance $Z_{11\text{Free}}$ can be used in place of the self-impedance Z_{11}, *but they do not delimit the conditions under which this is true.* Collin (1985) does, however, demonstrate the case depicted in figure 3.1 and refers to

King (1969). King showed that for a two element array of full wavelength dipoles, the self admittance differs by "10-20" percent from that of an isolated dipole for spacings in the range 0.2λ—0.8λ.

A numerical experiment was performed to clarify the conditions on the use of the free-space impedance as a substitute for the self-impedance. Two equal length dipoles were placed adjacent to one another at a fixed spacing $d = \lambda/2$ as shown in figure 3.2.

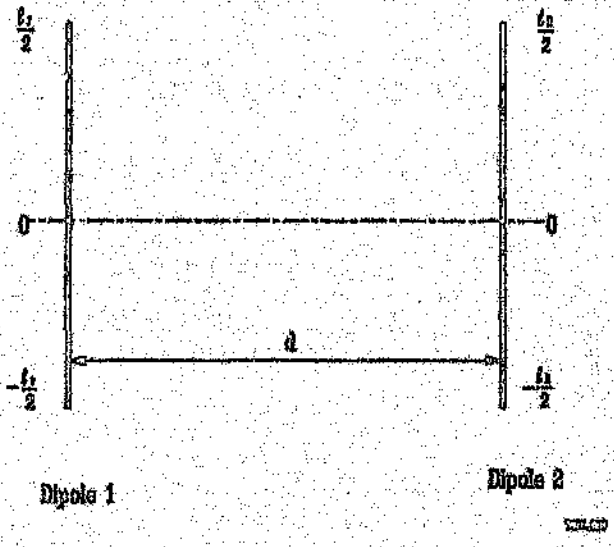
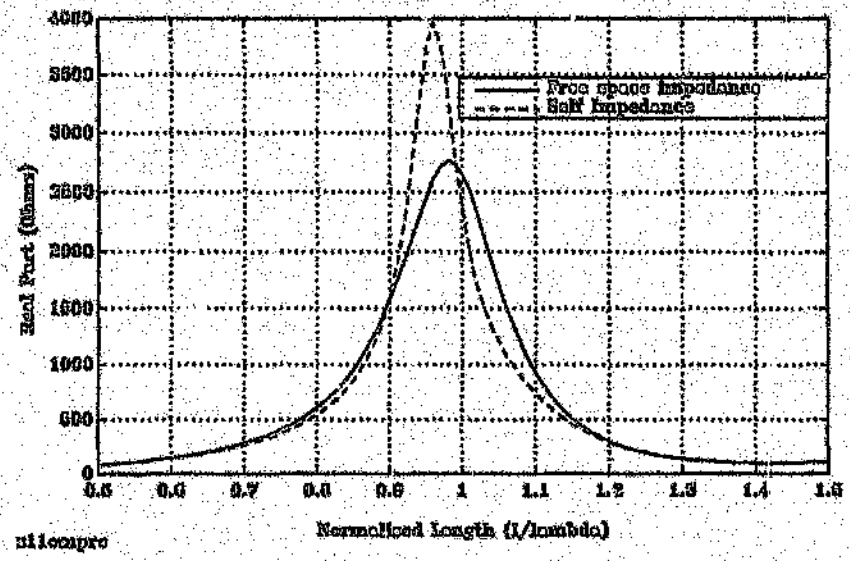


Figure 3.2: The self-impedance/free space impedance experimental geometry

Both dipole lengths were varied continuously from a half wavelength to one and a half wavelengths, ie starting and ending at case (a) and passing through case (b) as defined in figure 3.1. NEC2 was used to evaluate the input impedance under the two conditions:

- Dipole 2 not present (ie $Z_{11\text{Free}}$)
- Dipole 2 present, but open circuited. (ie Z_{11})



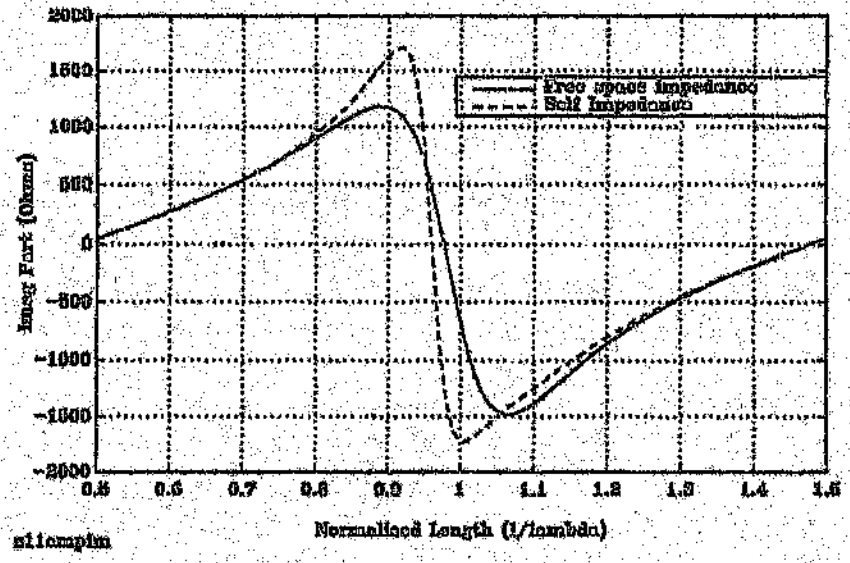


Figure 3.3: Comparison of Free space vs Self impedance of a dipole

Figure 3.3 shows the results of the simulation. Clearly the error is acceptable for much of the range, but not in the vicinity of the full wavelength case, as predicted by figure 3.1. There has also been a clear shift in the peak magnitude, probably due to the finite gap in the open circuited dipole - causing the sections to resonate at a slightly earlier point.

Define the percentage error, referenced to the free space impedance as:

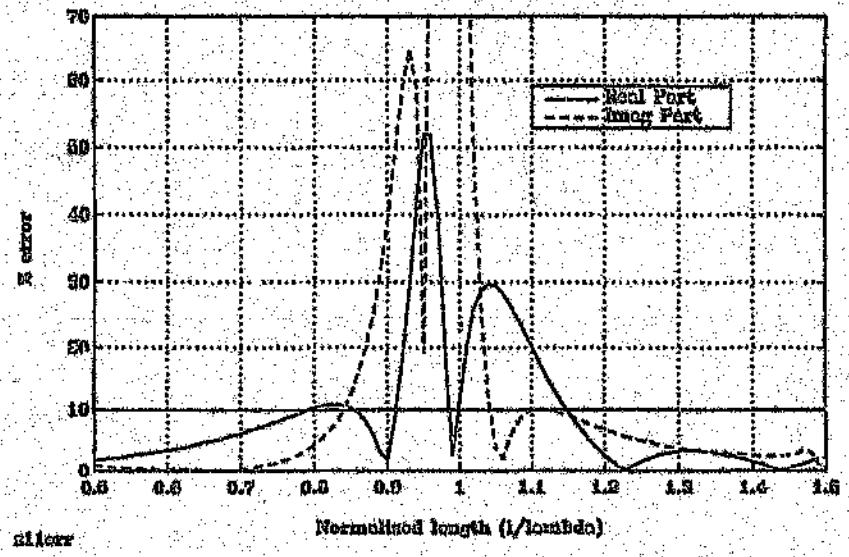


Figure 3.4: Percentage error in the use of Z_{11Free} instead of Z_{11}

$$\%\text{Error} = \left| \frac{Z_{11} - Z_{11Free}}{Z_{11Free}} \right| \qquad (3.1)$$

Assuming that a 10% error is acceptable, figure 3.4 shows that for this particular spacing of $d = \lambda/2$, the Z_{11Free} cannot be used instead of the Z_{11} from 0.84λ to 1.15λ.

The unacceptable error means that a method which relies on using the simple free space impedance values as self impedance values in the matrix equation (2.23) cannot be expected to analyse antennas which have elements that are a full wavelength long, such as will occur when analysing a log-periodic array.

Note that there are are many factors that have not been considered in this experiment, such as:

- How the error range varies for different spacings.
- The effect of changing the open circuit gap geometry.
- Whether the error is affected by radius of the dipoles.

However, it is clear that at first resonance, the free space impedance sufficiently approximates the self impedance required by equation (2.24).

3.2 Folded Dipole Self-Impedance

In section 2.3 on page 15 the transmission line method was presented which offers a simple method of obtaining the input impedance of the folded dipole. According to Thiele et al. (1980), however, the method can only be used with confidence if the separation of the dipole sides is less than one hundredth of a wavelength. He ascribes the failure of the method to transmission line equation breakdown. Clearly, however, transmission line theory *does* hold for larger separations – and a different explanation is given in (Clark & Fourie 1991) which is outlined in this section.

To illustrate the limitation of $s < \lambda/100$, consider that a typical commercial 150MHz folded dipole is made of 19mm diameter aluminium tubing (OD) and has a separation s of 95mm, or one twentieth of a wavelength. For this dipole, Thiele's transmission line model breaks down.

This section will present extensions to the transmission line method to be able to analyse dipoles with a separation of up to one sixth of a wavelength.

Wirelength and resonant length of a bent wire radiator

The transmission line component of the method takes the separation s into account only by its inclusion in the characteristic impedance expression. The characteristic impedance of a transmission line is not unique in that many different geometries of two wire line can have the same characteristic impedance, ie the separation is used as a ratio to the diameter. Thiele feels that at the larger separations, the transmission line nature of the folded dipole breaks down. A paper by Austin & Fourie (1988) which illustrates the wirelength concept alludes to a different explanation.

Figure 3.5 shows the geometry of their monopole and the results obtained.

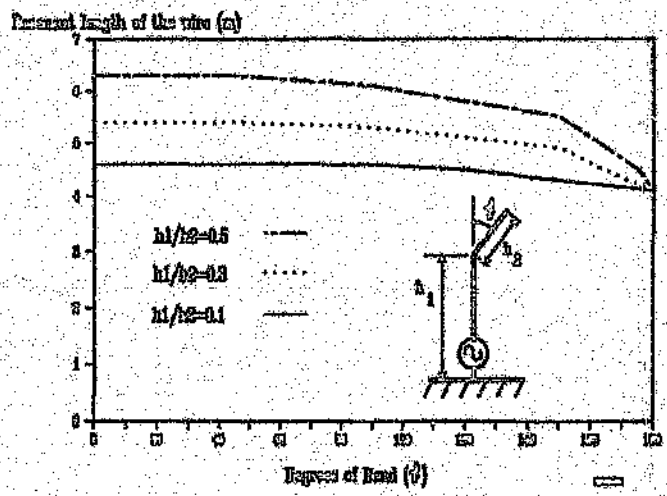


Figure 3.5: Resonant length of a bent wire

They showed that the resonant length of a bent monopole is essentially constant (and equal to $h_1 + h_2$) for bends of up to 90°for various configurations.

In essence their experiment showed that wires with a bend of less than 90°behave electrically like longer straight wires. Bends, such as the ones at the tips of a folded dipole, can hence be treated by extending the physical length of the antenna by a factor dependent on the inter-element spacing s.

The accuracy of the transmission line method should therefore improve if the overall length l is increased by an amount dependent on the additional wirelength at the tips of the folded dipole. The extension may not necessarily be the full separation s as suggested by figure 3.5 as the end-capacitance effects of a folded dipole are different to those of a monopole.

A numerical experiment was conducted to determine:

- the extended equivalent length l_{eq}.
- whether the extension applies to the transmission line mode, the antenna mode, or to both.

Clark & Fourie (1991) use as a first approximation,

$$l_{eq} = l + \alpha s \tag{3.2}$$

where

α = length extension factor, to be found

l = the original tip-to-tip length of the folded dipole

l_{eq} = the extended equivalent length of the dipole

and reports that

$$\alpha = 0.39 \tag{3.3}$$

gives acceptable results when applied to both the antenna and transmission line modes. It has since become apparent that a secondary correction factor is necessary to account for the radius a of folded dipole tubing. Thus, the extended length becomes (See appendix B):

$$l_{eq} = l + (0.4 - 20a)a \tag{3.4}$$

Thus it can be seen that the α value has simply been modified to account for the radius a, or

$$\alpha = 0.40 - 20a \tag{3.5}$$

The results of using the linearised equation (3.4) are shown in figures 4.7 to 4.9 on page 4.7ff.

3.3 Mutual impedance involving a folded dipole

An analytical expression for the mutual impedance between a dipole and a folded dipole has not yet been developed. However, the transmission line model of the folded dipole (Thiele et al. 1980) as discussed in section 2.3 on page 15 suggests a simple method of analysis that can be used to develop an expression for the mutual impedance.

3.3.1 Combining the transmission line model of the folded dipole and the induced-emf method

The induced-emf method as described in section 2.4 on page 17 is used to determine the mutual impedance between two antennas. The transmission line model of the folded dipole is used to determine the current structure on the folded dipole in order to use it in the induced-emf derivation to obtain the mutual impedance with a folded dipole (Clark & Fourie 1992).

Consider a dipole and a folded dipole as in figure 3.6:

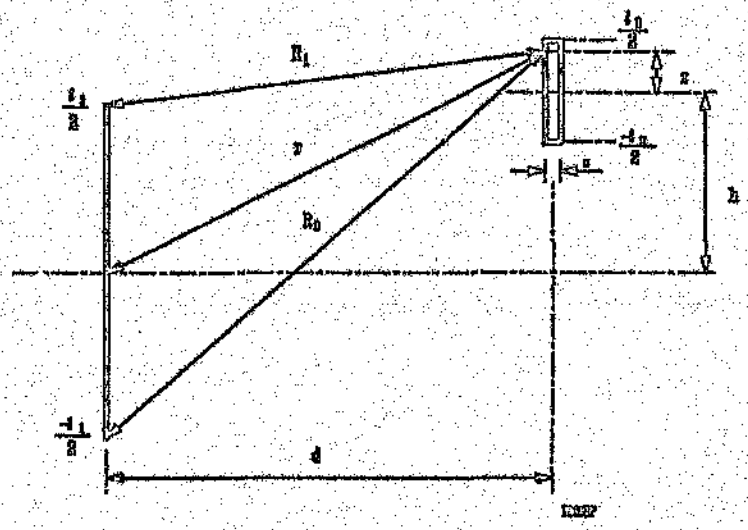


Figure 3.6: Coupling geometry with a folded dipole as the second antenna

The open circuit voltage induced in folded dipole 2 due to the radiation from dipole 1 excited by a current I_1 is expressed as: (See section 2.4 on page 17)

$$V_{21} = -\frac{1}{I_{1i}} \int_{\frac{-l_2}{2}}^{\frac{l_2}{2}} E_{z21}(z) I_2(z) dz \tag{3.6}$$

where the electric field component in the z-direction at folded dipole 2 due to the dipole 1 E_{z21} is of the standard form:

$$E_z = -j\frac{\eta I_m}{4\pi}\left[\frac{e^{-jkR_1}}{R_1} + \frac{e^{-jkR_2}}{R_2} - 2\cos\left(\frac{kl}{2}\right)\frac{e^{jkr}}{r}\right] \tag{3.7}$$

The current on the folded dipole is found by considering the transmission line mode current I_T and antenna mode I_A currents. Clearly the impressed electric field E_{z21} in the vicinity of folded dipole 2 causes an antenna mode current I_A to flow in each side of the folded dipole, which is of the form:

$$I_A(z) = I_m \sin\left[k\left(\frac{l}{2} - |z|\right)\right] \tag{3.8}$$

The actual current flow *in each side* of the folded dipole is modified by the transmission line component of the current I_T such that the current on the left hand side of the folded dipole is $I_T + I_A$ and $I_T - I_A$ on the right hand side.

However, the electric fields generated by the transmission line mode currents I_T cancel since they are in such close proximity and flow in opposite directions. It is therefore reasonable to postulate that the transmission line mode currents do not influence the mutual coupling. For the purposes of determining the mutual interaction between a dipole and a folded dipole, then, one can consider the folded dipole's sides as being collapsed to a filamentary current of value $2I_A$, or that the *effective current* in the second antenna as a whole is :

$$I_2(z) = 2I_A(z) = 2 \times I_m \sin\left[k\left(\frac{l}{2} - |z|\right)\right] \tag{3.9}$$

Now the mutual impedance is given as

$$Z_{21} = \frac{V_{21}}{I_1} \tag{3.10}$$

and it follows

$$Z_{21} = 2 \times j\frac{\eta I_{1m} I_{2m}}{4\pi I_{11} I_{21}} \int_{-\frac{l_2}{2}}^{+\frac{l_2}{2}} \sin\left[k\left(\frac{l_2}{2} - |z|\right)\right] \times \left[\frac{e^{-jkR_1}}{R_1} + \frac{e^{-jkR_2}}{R_2} - 2\cos\left(\frac{kl_1}{2}\right)\frac{e^{jkr}}{r}\right] dz \tag{3.11}$$

or substituting equation (2.35)

$$Z_{21\ \text{Folded Dipole to Dipole}} = 2 \times Z_{21\text{Dipole to Dipole}} \tag{3.12}$$

which is obtained by considering the transmission line model of the folded dipole when deriving the mutual impedances by the induced-emf method.

3.3.2 Folded dipole to folded dipole

The mutual impedance between two folded dipoles can then be obtained by extending the argument:

By reciprocity,

$$Z_{12} = Z_{21} \tag{3.13}$$

or, that the impedance would be the same if the folded dipole and the dipole were swapped in figure 3.6. It follows that the mutual impedance between a folded dipole and a folded dipole will again have twice the current moment, or:

$$Z_{21\ \text{Folded Dipole to Folded Dipole}} = 4 \times Z_{21\ \text{Dipole to Dipole}} \tag{3.14}$$

3.3.3 Using NEC2 to obtain mutual impedance

A standard is required against which the above theory can be measured. NEC2 cannot provide the mutual impedance between two antennas directly,[1] but the following procedure can be adopted:

Consider the coupling matrix in equation (2.23). If V_2 is set to zero (dipole two is short circuited):

$$\begin{aligned} V_1 &= Z_{11}I_1 + Z_{12}I_2 \\ 0 &= Z_{21}I_1 + Z_{22}I_2 \end{aligned} \tag{3.15}$$

Or

$$I_2 = -\frac{Z_{21}I_1}{Z_{22}} \tag{3.16}$$

the input impedance of the array (ie input impedance of antenna 1 in the presence of the parasitic short circuited antenna 2) is given by:

$$Z_{in} = \frac{V_1}{I_1} = \frac{Z_{11}Z_{22} - Z_{12}Z_{21}}{Z_{22}} \tag{3.17}$$

For a reciprocal network, $Z_{21} = Z_{12}$, and the mutual impedance Z_{21} is obtained by:

$$Z_{21} = \sqrt{Z_{11}Z_{22} - Z_{in}Z_{22}} \tag{3.18}$$

which ends the mathematical derivation. The practical implementation of this equation is a little more subtle. The quantity under the square root in equation (3.18) is a complex number. Finding the square root involves determining the arctangent of the imaginary part over the real part. A four quadrant arctangent must be used to determine the correct quadrant of the square root. But there remains the usual choice between two roots that are 180°out of phase. Normally, the choice is obvious due to a purely real nature etc, but mutual impedance can have negative real and imaginary parts – ie it can fall in any of the four quadrants in the Argand diagram.

[1] NEC2 can provide *Coupling* in dB's which is defined as the maximum coupling when both antennas are perfectly matched – but is *not* the mutual impedance as defined here.

To ensure a smooth phase transition when plotting the mutual impedance derived from this method the previous value of the argument needs to be inspected to choose the correct root[2]. There does not seem to be any other way of resolving this mathematical dilemma.

For every mutual impedance point calculated, there are three NEC2 evaluations – Z_{11}, Z_{22}, Z_{in}, the Z_{12} is calculated, and the root chosen. The procedure has been automated using SCAT as a pre and post processor to NEC2.

The method of obtaining the mutual impedance from NEC2 in this fashion is nevertheless very useful and a verification of it is offered in the results section 4.3 on page 49.

Chapter Summary

- The free space input impedance can be used instead of the rigorously defined self impedance, provided that the dipole lengths are not near a full wavelength. The simplification offers a significant saving of computational effort.
- A significant extension of the transmission line model of the folded dipole has been described by considering the wirelength extensions due to the inter-element separation.
- The transmission line model of the folded dipole is combined with the induce-emf method of deriving mutual impedance to obtain expressions for the mutual impedance involving folded dipoles.
- Since a standard is required against which to compare the mutual impedance expressions, a method of obtaining the mutual impedance from NEC2 between any two antennas is outlined.

[2]Obviously a change from $-\pi$ to π is allowable, but not a phase change of π which would imply a swap of quadrants.

Chapter 4

RESULTS

This chapter applies the theory developed in chapter three, and presents results of simulations performed against NEC2. Section 4.1 shows the degradation of Thiele's transmission line model for large separations, and shows the improvement obtained with the extensions presented in this thesis. Measurements of mutual impedance were performed to confirm the simulation results presented in section 4.3 – the details of the measurement setup are shown in section 4.2. Finally, section 4.4 shows the simulation results of a few simple arrays, using the theory developed in the thesis, versus NEC2 results.

4.1 Folded Dipole Self Impedance

4.1.1 Deterioration of accuracy of Thiele's transmission line model with increasing inter-element spacing.

A numerical experiment was used to show the deterioration in accuracy of Thiele's transmission line model as the inter-element separation s of the folded dipole was increased. In this experiment, a half-wavelength long folded dipole was evaluated from 2/3 centre-frequency, f_c, to 4/3 f_c. The radius of the folded dipole elements used was one two- thousandths of the wavelength at the centre-frequency, $r = \lambda_c/2000$, for all three simulations. The progression of the inaccuracy can be clearly seen as the separation s increases: figure 4.1 shows the comparison to NEC2 for a separation of $s = 0.015\lambda_c = 3\lambda_c/200$; figure 4.2 for a separation of $s = 0.05\lambda_c = \lambda_c/20$; and figure 4.3 for a separation of $s = 0.1\lambda_c = \lambda_c/10$. Also shown are the results (annotated as SCAT-0.39) of the equivalent length modification to the transmission line model given by:

$$l_{eq} = l + \alpha s \tag{4.1}$$

where

$$\alpha = 0.39$$

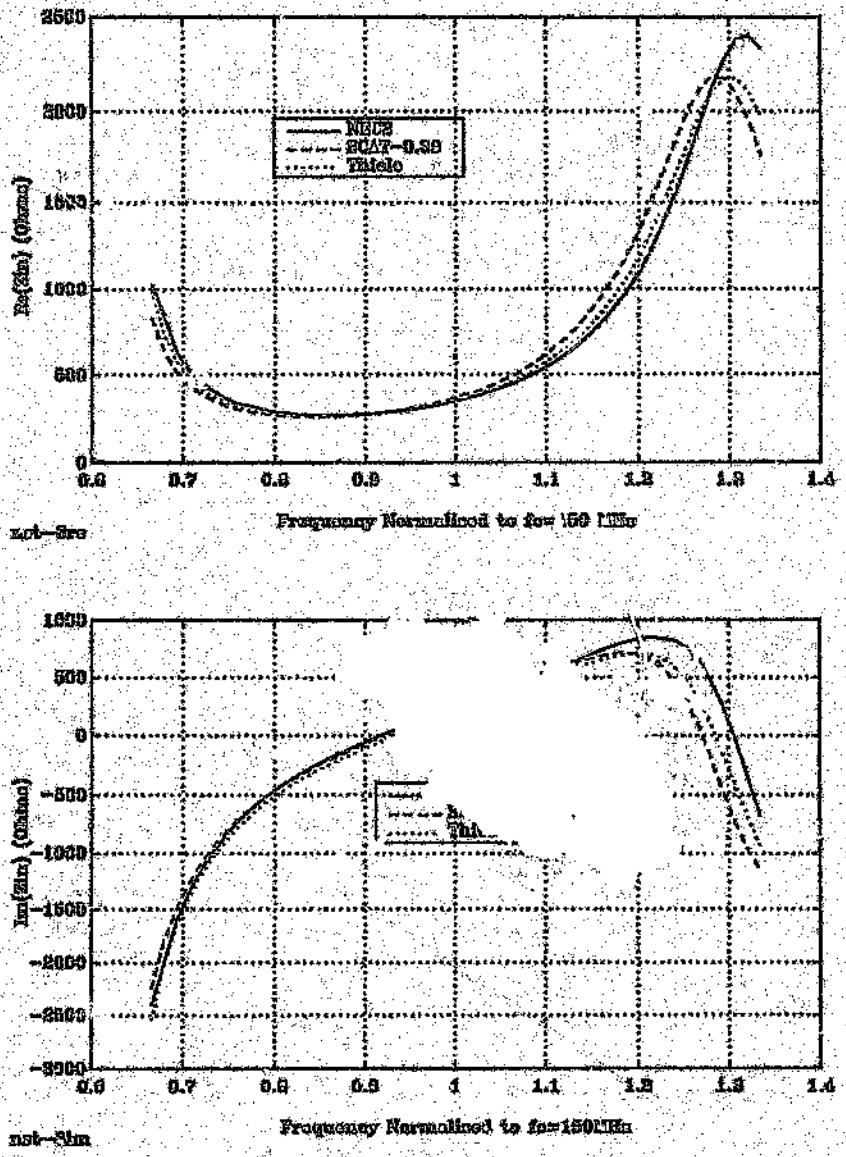


Figure 4.1: Compared folded dipole input impedance for $s = 3\lambda_c/200$. Thiele vs. NEC2 vs. SCAT $\alpha = 0.39$

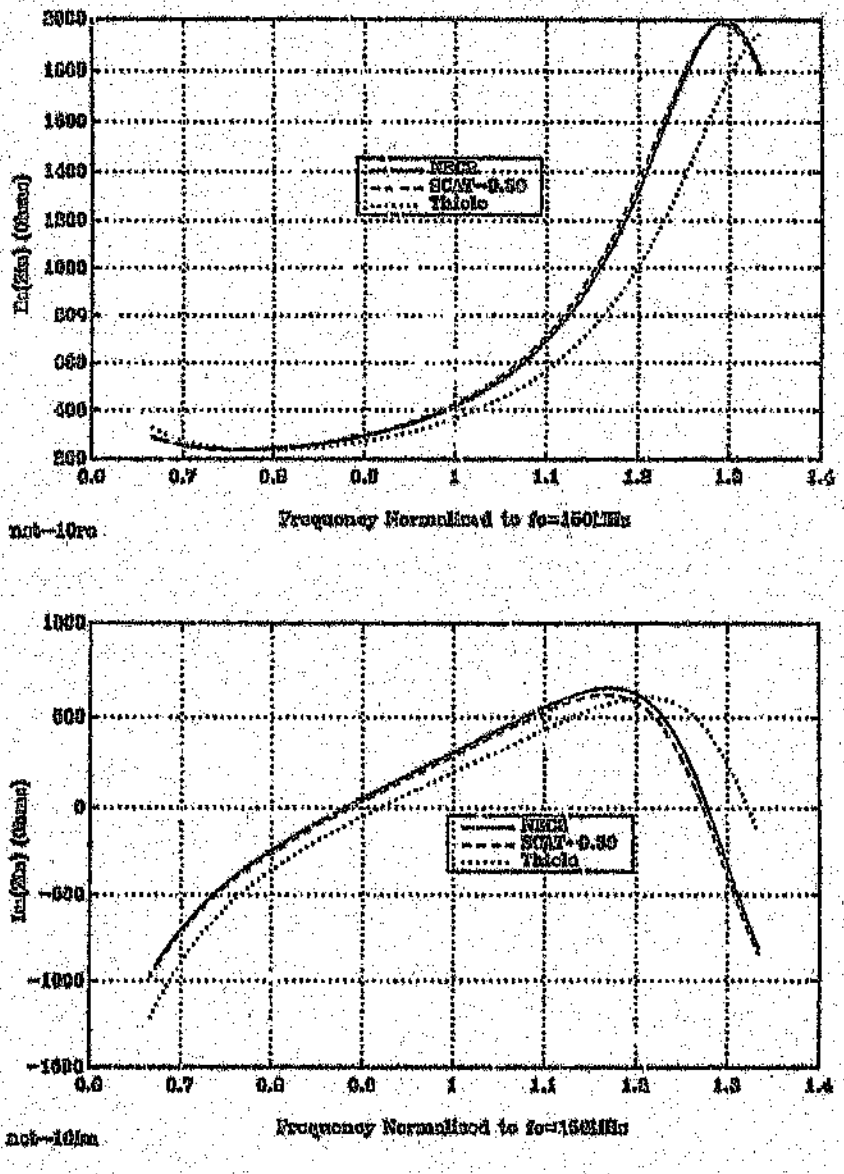


Figure 4.2: Compared folded dipole input impedance for $s = \lambda_o/20$. Thiele vs. NEC2 vs. SCAT $\alpha = 0.39$

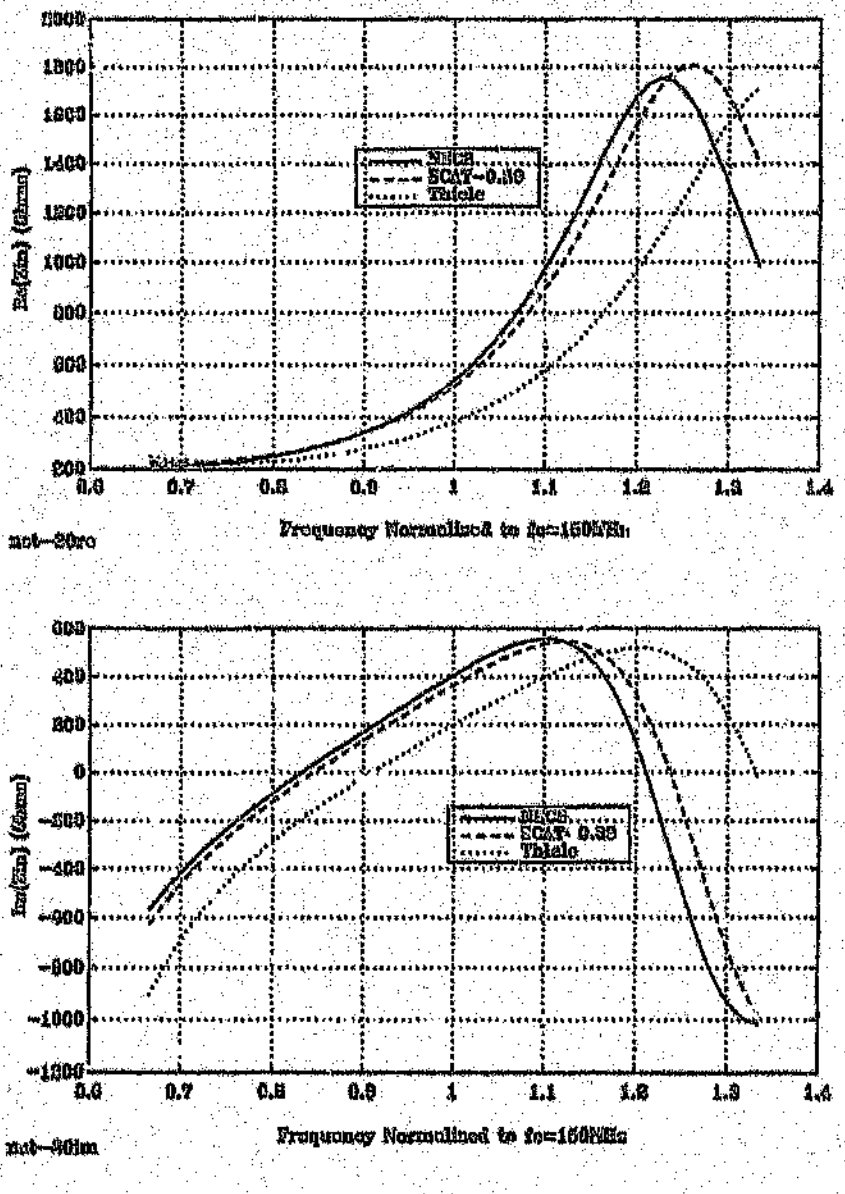


Figure 4.3: Compared folded dipole input impedance for $s = \lambda_o/10$. Thiele vs. NEC2 vs. SCAT $\alpha = 0.39$

In conclusion, the experiment has shown that Thiele's transmission line model is inadequate for folded dipoles with a separation greater than $s = \lambda_o/100$. It has also shown that the first-order modification to the equivalent length used in the transmission line model adequately compensates for this error, but only for the case of a fixed radius of $r = \lambda_o/2000$ (or 1mm at 150MHz).

4.1.2 The deterioration of accuracy of the first-order modification to the transmission line model with increasing radius.

The accuracy of the first-order compensation as given by equation (4.1) again degrades with thicker radius folded dipoles (See Section 3.2 on page 29). The following numerical experiment demonstrates the deterioration in accuracy. A half wavelength long folded dipole is analyzed from $2/3\,f_c$ to $4/3\,f_c$. The inter-element spacing is fairly large, at $s = 0.06\lambda_0$ (at 150MHz, $s = 120$mm) for all three simulations. The radius is $r = \lambda_c/400$ in figure 4.4 (ie 5mm at 150MHz); $r = 2\lambda_c/400$ in figure 4.5; and finally $r = 3\lambda_c/400$ in figure 4.6 (ie 15mm at 150MHz).

The error norm quoted in the figures is the mean absolute error norm, ie the absolute value of the difference in impedance magnitudes given by:

$$e = \frac{1}{N}\sum_{0}^{N} \| |Z_1| - |Z_2| \| \tag{4.2}$$

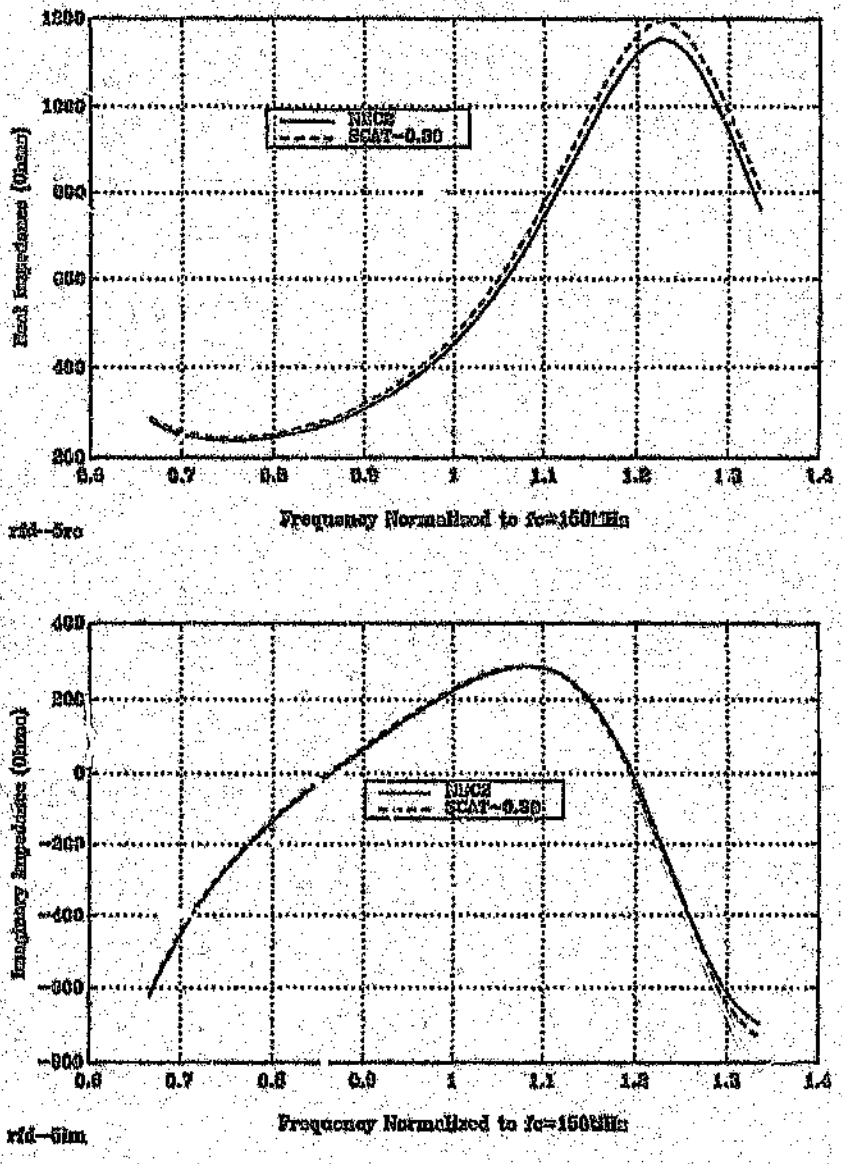
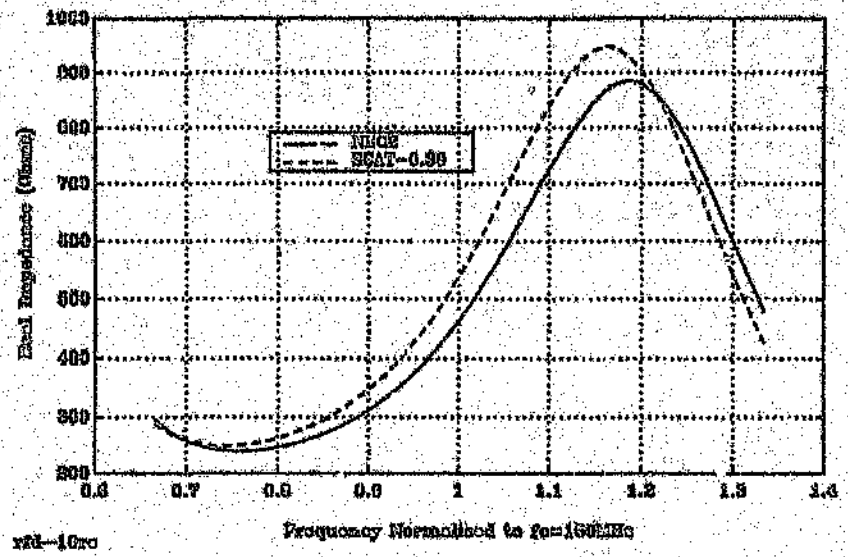


Figure 4.4: Compared folded dipole input impedance for $r = \lambda_c/400$ (e=22.4Ω)



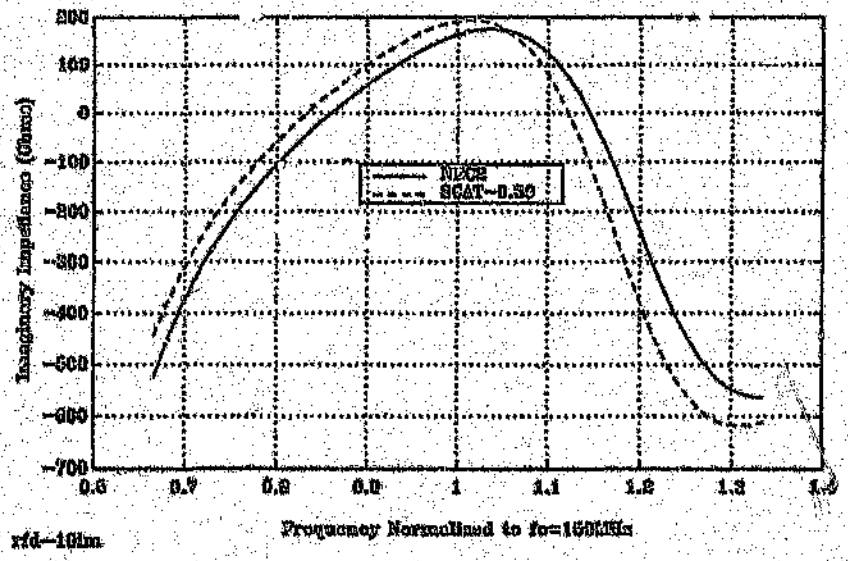
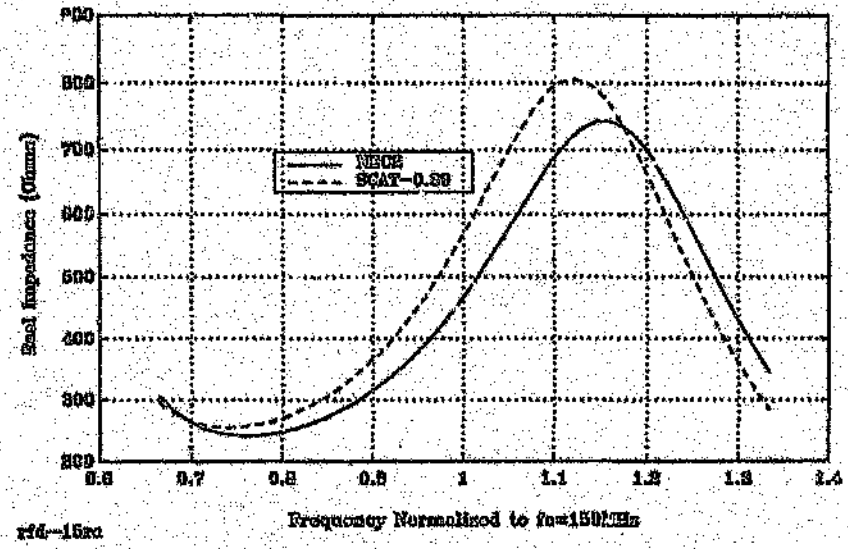


Figure 4.5: Compared folded dipole input impedance for $r = 2\lambda_o/400$ (e=53.5Ω)



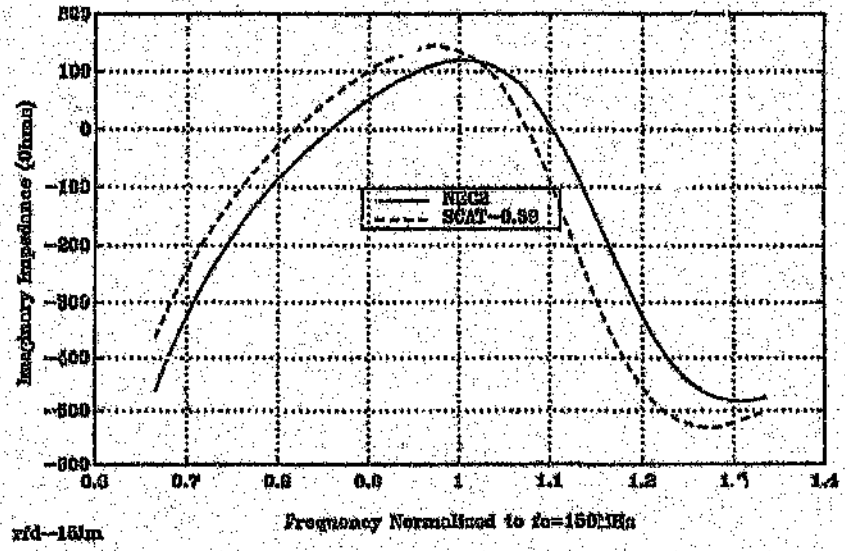


Figure 4.6: Compared folded dipole input impedance for $s = 3\lambda_c/400$ (c=56Ω)

In conclusion, the experiment has shown that the first-order correction does not adequately correct for thicker dipoles, and a secondary correction is needed to take the radius into account.

4.1.3 The final correction to the transmission line model

The need for the secondary correction introduced in section 3.2 is evident from the results shown in the previous section. The secondary correction to the equivalent length which incorporates the separation s and the radius r was given as:

$$l_{eq} = l + s(0.4 - 20a) \tag{4.3}$$

The simulations presented in the previous section were run again, with the full correction to the transmission line method. The results are shown in figures 4.7 to 4.9.

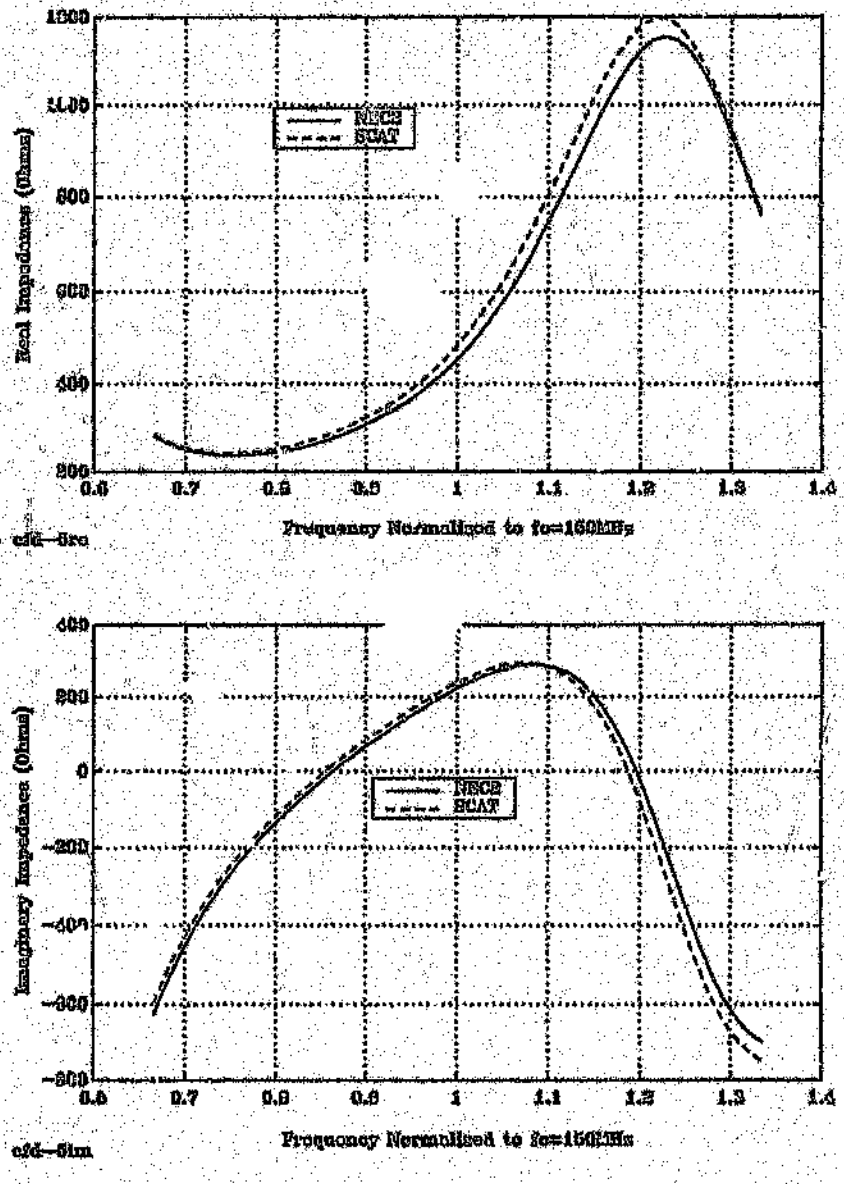
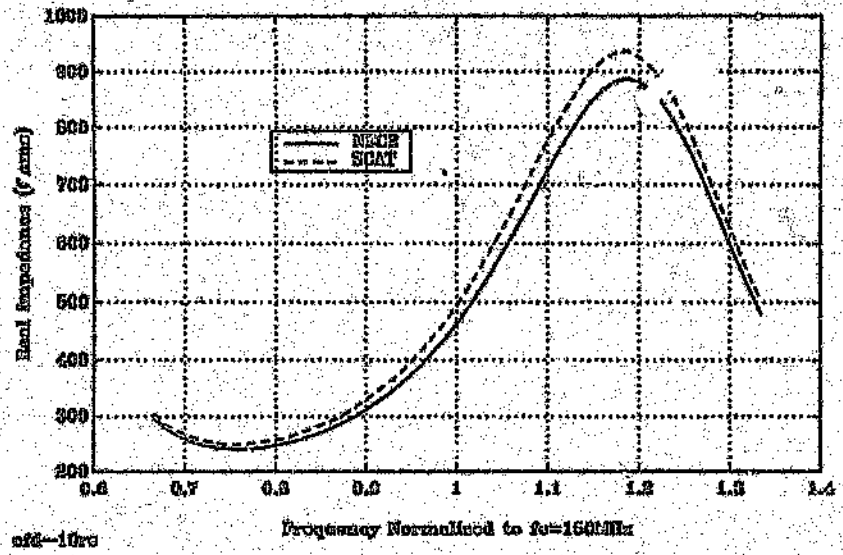


Figure 4.7: Compared FDZin using the full correction. $r = \lambda_c/400$ (e=32.3Ω)



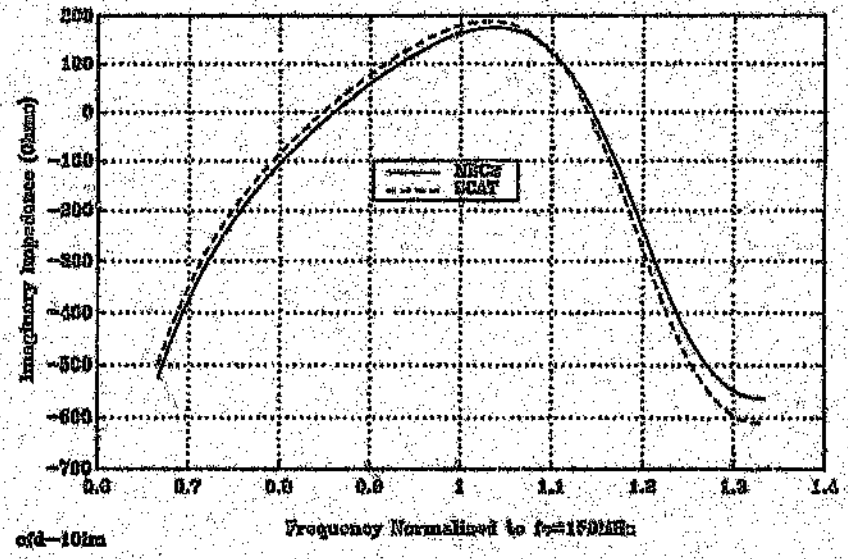
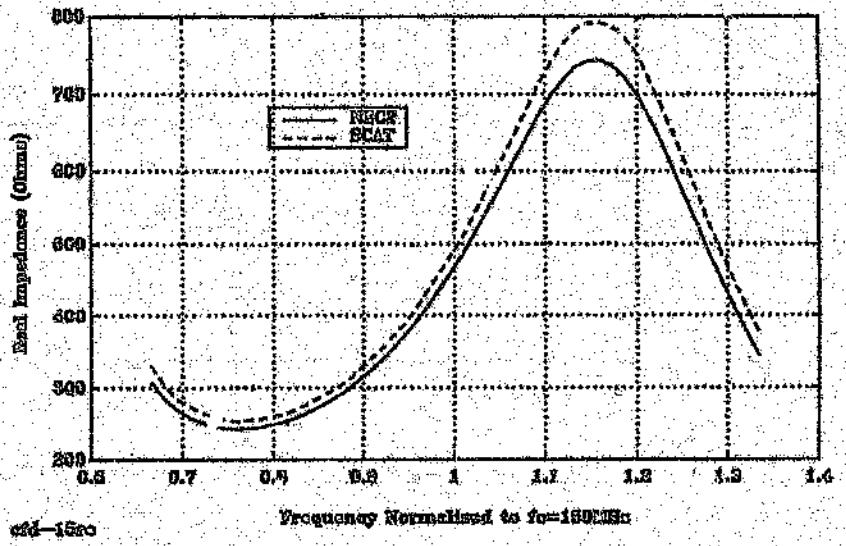


Figure 4.6: Compared FDZin using the full correction. $r = 2\lambda_o/400$ (e=33.0Ω)



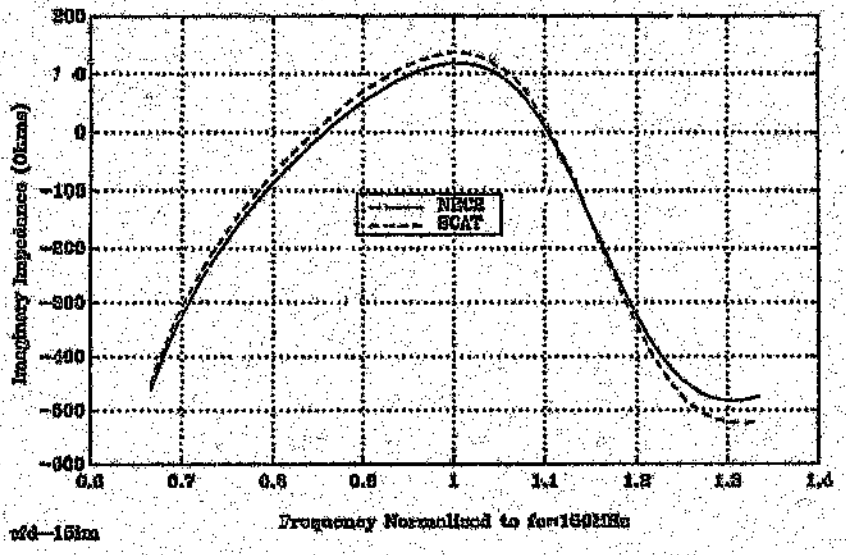


Figure 4.9: Compared FDZin using the full correction. $r = 3\lambda_c/400$ (e=28.68Ω)

In conclusion, the above simulations show that an acceptable comparison to the NEC2 folded dipole input impedance results are obtained with the modified transmission line model, across a wide range of element radi., and inter-element separations.

The development of equation (4.3) and further results are presented in appendix B on page 99

4.2 Measurement Procedure

NEC simulations were performed to test the validity of the simple results obtained from theory, viz. that the mutual impedance between a dipole and folded dipole is twice that between two dipoles and that the mutual impedance between two folded dipoles is four times that between two dipoles. The results of these simulations are presented in the next section. Although NEC can really be considered to be the validation tool, it was felt that measured results of the mutual impedance to validate NEC would be beneficial.

Unfortunately, mutual impedance (Z_{21}) cannot be directly measured, and has to be inferred, either from full S-parameter results, or by the Z-parameter method outlined in section 3.3.3 on page 34. Both methods have inherent numerical error due to the subtraction of two large numbers. However, the Z-parameter method requires that open and short circuits are defined, both of which are difficult to achieve (without end capacitance and series inductance) in the measurement setup. The S-parameter method was used for the measured results that are presented as this uses matched ports which are far easier to achieve accurately.

Sazonov (1990, ch3) shows the relation between the scattering matrix S and the normalized impedance matrix z as:

$$z = (I - S)^{-1}(I + S)$$

where I is the identity matrix of appropriate order.

The normalized mutual impedance z_{21} is thus given as:

$$z_{21} = \frac{2S_{21}}{(1 - S_{11})(1 - S_{22}) - S_{12}S_{21}}$$

which is multiplied by the system impedance.

The measurements presented were performed with a Hewlett-Packard HP8753C network analyser, in an anechoic chamber suitable for frequencies above 400 MHz. The instrument was calibrated with the aid of an N-type calibration kit HP85032D. All measurements were performed at 500MHz, with monopoles over a ground plane. Using a ground plane reduces the need for a balun, and also reduces error due to the proximity of the feed cables. The impedances thus obtained are simply multiplied by two to get the full dipole impedances.

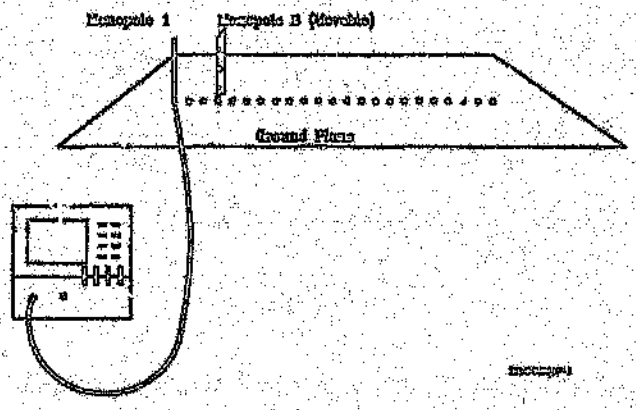


Figure 4.10: The Measurement Geometry

The ground plane used was 1.5λ by 3.0λ, the measurements being taken at 500MHz. The two antennas could be moved relative to one another down the central axis of the ground plane, as shown in figure 4.10.

The wire radius of the antennas was $r = 0.0005\lambda$ (0.3mm) and the inter-element separation of the folded monopole was $s = 0.0167\lambda$ (10mm). The calibration reference plane was established by Hewlett Packard 7mm to female N-type barrels. A full 2-port calibration was performed, eliminating the matching, tracking and directivity errors via the open, short, load and "thru" calibration standards. Isolation calibration was not performed, as the dynamic range is adequate.

After calibration, Greenpar male N-type to male BNC barrels were used to connect to coaxial dyleads that were *directly soldered* onto the ground plane. The measurement reference plane was adjusted via port extensions to an absolute short circuit on the ground plane. The antennas were mounted (one at a time) to check their input impedance.

The measurement problems associated with the coaxial feed arrangement are further discussed in Appendix D.

4.3 Mutual Impedance

4.3.1 Verification of the NEC2 method of obtaining mutual impedance

A method of obtaining the mutual impedance from NEC2 was outlined in section 3.3.3. Self-impedances Z_{11} and Z_{22} and the input impedance Z_{in} are used to calculate the mutual impedance Z_{21} from:

$$Z_{21} = \sqrt{Z_{11}Z_{22} - Z_{in}Z_{22}} \tag{4.4}$$

A numerical experiment was conducted to prove the validity of this method of obtaining the mutual impedance. Two dipoles were arranged as shown in figure 4.11, where the distance between them d was varied between 0.05λ and 2λ. The radius of the wires used in the NEC2 numerical experiment was very thin ($a = 5 \times 10^{-6}\lambda$) since the theoretical values against which the NEC2 results are compared are for infinitely thin wires. The length l of the dipoles is a half-wavelength $l = \lambda/2$.

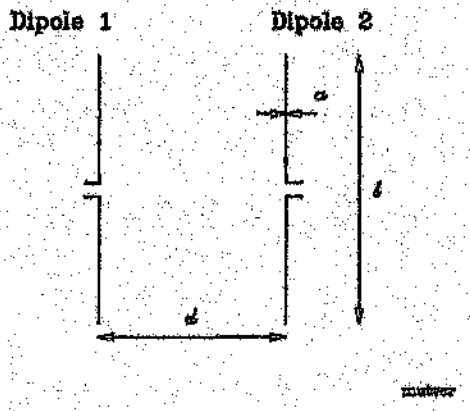


Figure 4.11: Geometry used for the NEC2 Z12 verification

Figure 4.12 shows the results of the experiment. The curve denoted SCAT is the theoretical curve, assuming infinitely thin wires. The measured results are limited to the range of the ground plane movement, ie the largest spacing is 1.15λ, and a wire radius of $a = 0.0005\lambda$ is used (0.3mm at 500MHz).

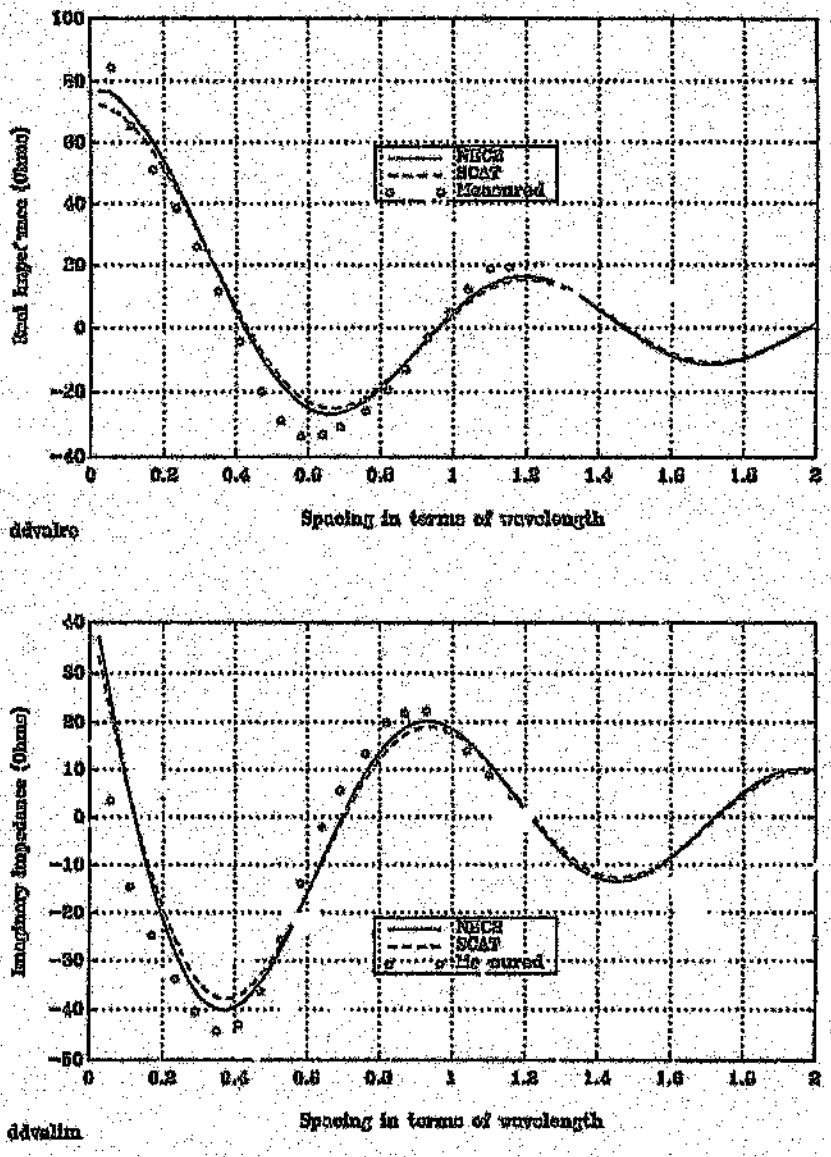


Figure 4.12: Comparison of mutual impedances obtained from NEC2, theoretical (labelled SCAT) and measurement.

In conclusion, the experiment has shown that the NEC2 method is a valid method of obtaining the mutual impedance, since its values compare favourably with the theoretically obtained results, with an error norm of only 1.45Ω. The measured results shown were obtained by the Z-parameter method, which has a higher inherent error than the S-parameter method; nevertheless, the measured results do track the theoretical results reasonably, with an error norm of 10.64Ω. These measurements used a wire radius of 0.0017λ (2mm 500MHz) and a later experiment shows the dependence of the mutual impedance on the wire radius, which also contributed to the error.

The method of obtaining the mutual impedance from NEC can thus be used with confidence to establish whether the mutual impedance involving folded dipoles is as proposed in section 3.3 on page 31.

4.3.2 Mutual impedance – folded dipole to dipole

The mutual impedance between a folded dipole and a dipole was shown to be twice that of two dipoles in section 3.3 on page 31, ie

$$Z_{21\ \text{Folded Dipole to Dipole}} = 2 \times Z_{21\text{Dipole to Dipole}} \tag{4.5}$$

The following numerical experiment was designed to verify the above equation. A folded dipole and a dipole were placed as shown in figure 4.13, where the dipole was moved such that the distance d was varied from 0.05λ to 2λ. The folded dipole was kept fixed as the feed antenna. As before $a = 5 \times 10^{-6}\lambda$ for the NEC2 numerical model, and in this case thinner monopoles ($a = 0.0005\lambda$) were used for the measured antennas. The folded dipole element separation s was 0.06λ

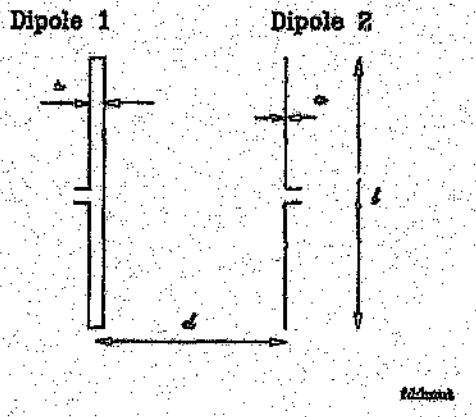


Figure 4.13: Folded Dipole to Dipole mutual impedance geometry

The results are shown in figure 4.14. The curve denoted SCAT is simply the standard theoretical mutual impedance between two infinitely thin half-wavelength long dipoles multiplied by two. Measured results are also shown which validate the NEC method.

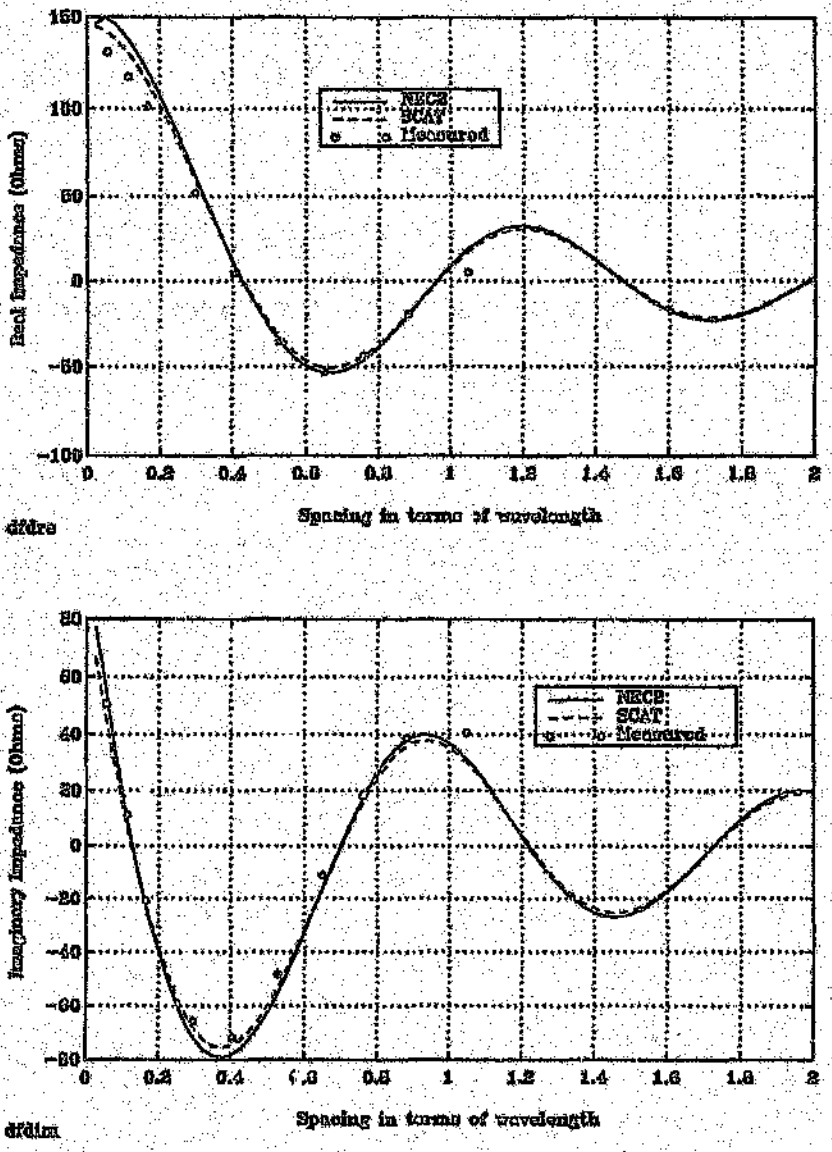


Figure 4.14: Folded dipole to dipole mutual impedance

As can be seen, the theoretical results and the NEC results are extremely close with an error norm of only 2.47Ω, thus the experiment has shown that the mutual impedance between a folded dipole and a dipole is twice that between two dipoles. (cf figure 4.12)

The measured results shown were obtained by the S-parameter method with the coaxial cables soldered to the ground plane. Extremely good correlation was obtained, with an error norm of 5.72Ω, which validates the NEC method. Using panel mount BNC connectors on the ground plane gave large errors (error norm of 20.33Ω), as shown in appendix D. Extreme care in the measurement procedure was needed to produce the results shown.

4.3.3 Mutual impedance between two folded dipoles

The mutual impedance between two folded dipoles was shown to be four times that of two dipoles, or:

$$Z_{21\ \text{Folded Dipole to Folded Dipole}} = 4 \times Z_{21\ \text{Dipole to Dipole}} \tag{4.6}$$

The experiment used the geometry as shown in figure 4.15.

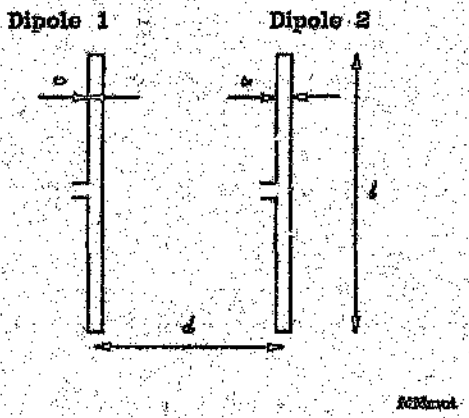
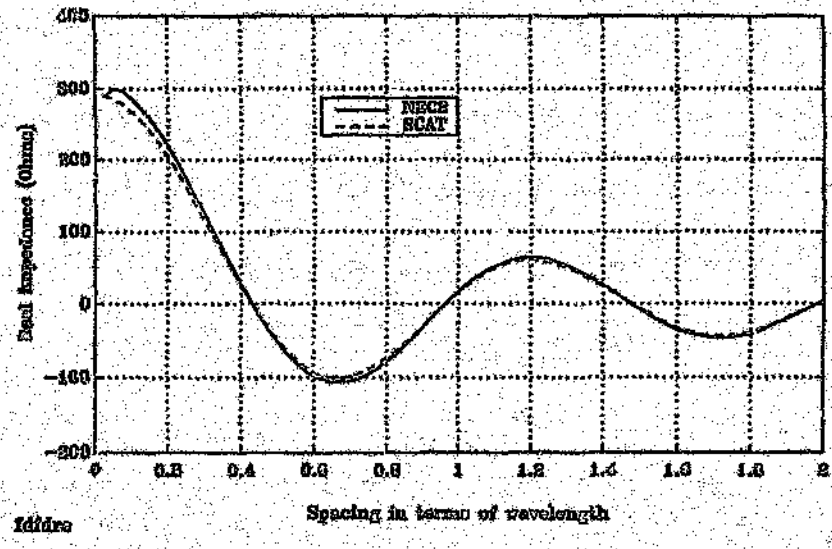


Figure 4.15: Geometry for the mutual impedance of two folded dipoles

The results are shown in figure 4.16, where the curve denoted SCAT is the theoretical mutual impedance between two infinitely thin half-wavelength long dipoles multiplied by four.



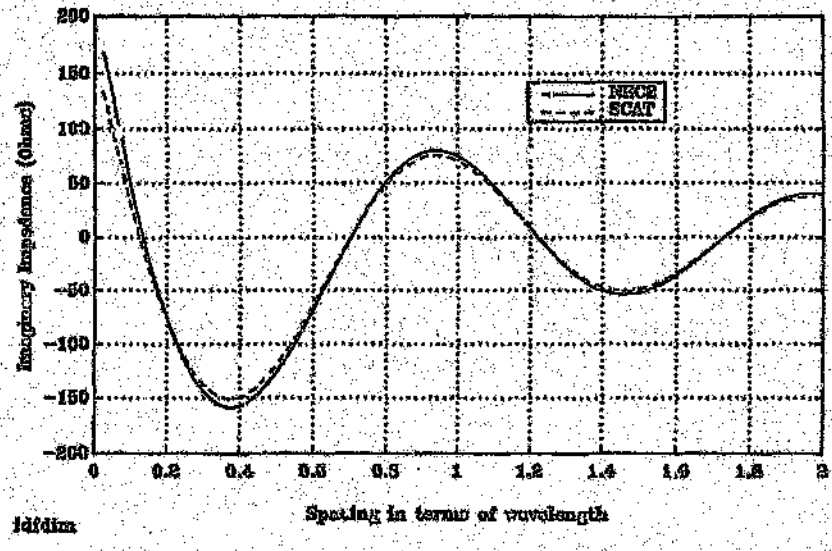


Figure 4.16: Folded dipole to folded dipole mutual impedance

In conclusion, the NEC and theoretical results compare well with an error norm of 6.13Ω, and show that the mutual impedance between two folded dipoles is simply four times that between two dipoles.

No measured results are shown, as the measurements in the previous section clearly show that the NEC method is a valid benchmark against which to test the theory.

4.3.4 An investigation of the effect of thickness on mutual impedance

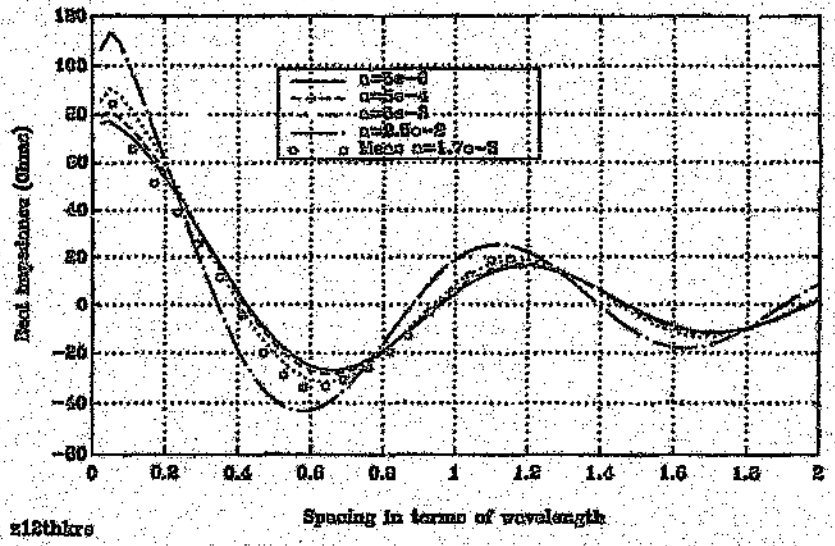
Clearly, the comparisons that have been presented validate the theory proposed in section 3.3 on page 31. The simulations were, however, performed with very thin wires ($a = 5 \times 10^{-6}\lambda$) since the theoretical values against which they were compared assume infinitely thin wires. However, the NEC2 method outlined can be used to obtain the mutual impedance between any two radiating structures, of any thickness.

The NEC2 was thus used to generate data on the mutual impedance between two dipoles for thicker radius wires to investigate the sensitivity of the mutual impedance to wire thickness, taking care not to violate NEC's segment length to radius ratio.

The geometry used for the numerical experiment was as shown in figure 4.11, ie two half-wavelength dipoles with the separation d between them being varied between 0.05λ and 2λ. The radius a of the simulations was:

- $a = 5 \times 10^{-6}\lambda$
- $a = 5 \times 10^{-4}\lambda$
- $a = 5 \times 10^{-3}\lambda$
- $a = 2.5 \times 10^{-2}\lambda$

The results of the simulations are shown in figure 4.17, together with the measured results, with a radius $a = 1.6 \times 10^{-3}\lambda$. Note that the axes in the graph are in units of lambda.



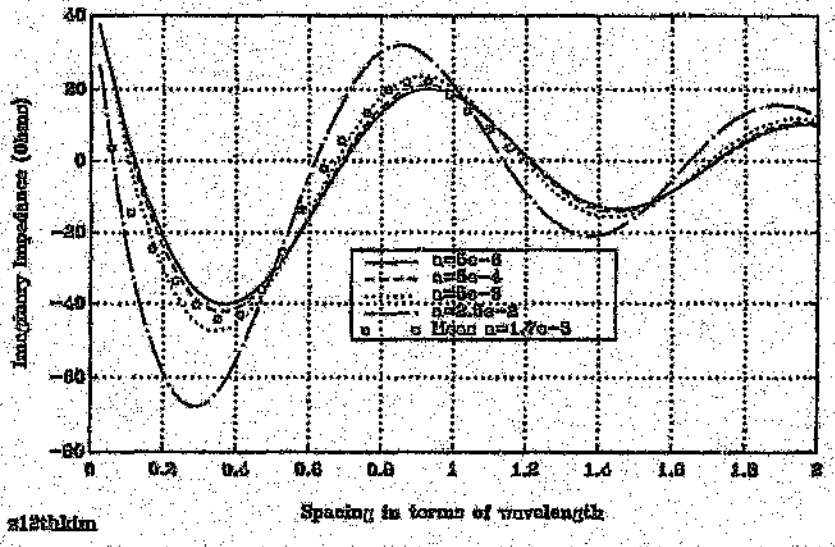


Figure 4.17: The effect of dipole thickness on mutual impedance – curves are obtained from NEC2 and measurement.

In conclusion, 4.17 shows that the radius of the antennas affects the value of the mutual impedance. Acceptable accuracy is obtained up to a radius of $a = 5\times10^{-3}$ which corresponds to a diameter of 40mm for a 1m long half-wave dipole at 150MHz. Clearly a correction factor will need to be incorporated into the mutual impedance expression for thicker dipoles, if desired. For the purposes of this thesis, however, the restriction is acceptable.

4.4 Array Analysis

The theory presented in this thesis is encoded in the computer programme SCAT, whose results are compared against those obtained from NEC2. Both input impedance and radiation pattern results are presented for a number of simple antennas.

4.4.1 Case 1 - 2 Element Yagi-Uda, dipole feed

The geometry of the 2 element Yagi is shown in figure 4.18, all dimensions being in metres; the feed element is the folded dipole. The Yagi was evaluated from 100MHz to 200MHz, the radiation pattern being performed at 150MHz. All results have been normalised to the centre frequency $f_c = 150$MHz.

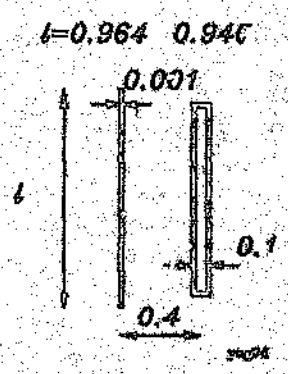
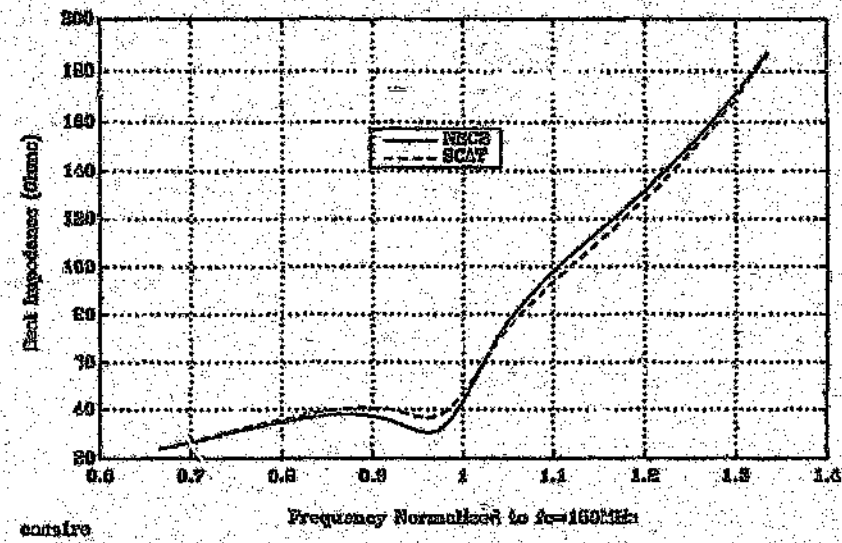


Figure 4.18: Geometry of two element Yagi-Uda array

Figure 4.19 shows the real and imaginary components of the input impedance and figure 4.20 shows the E and H plane radiation pattern ie the elevation and azimuth plots respectively, when the elements of the antenna are aligned in the elevation plane, when the folded dipole in figure 4.18 is replaced with a dipole.



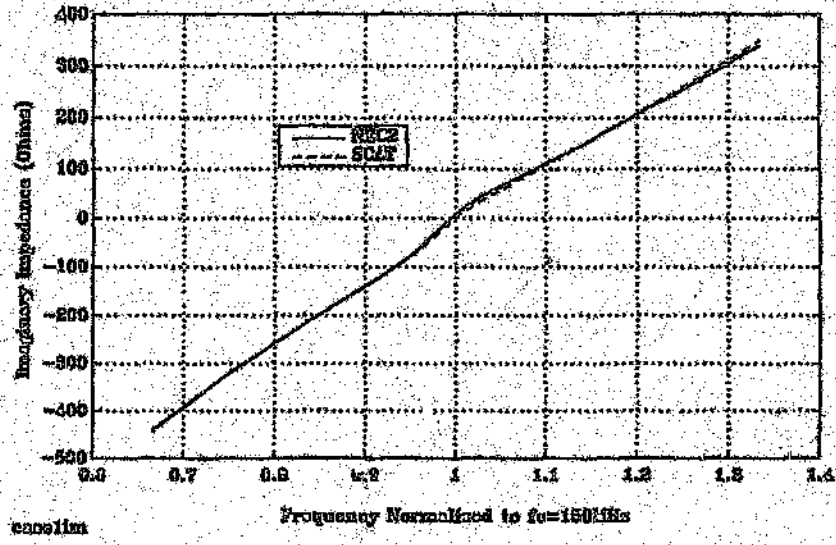
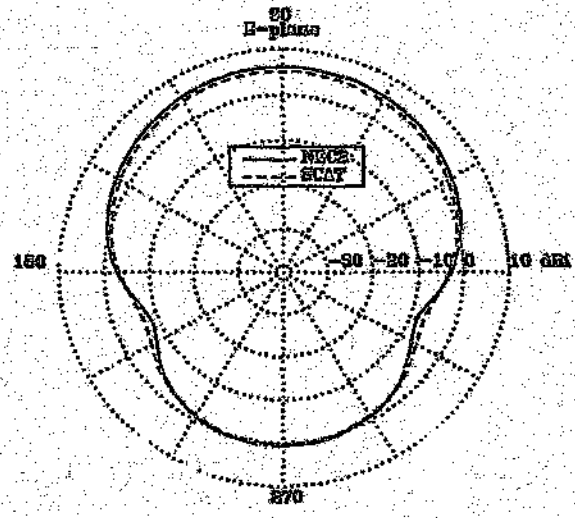
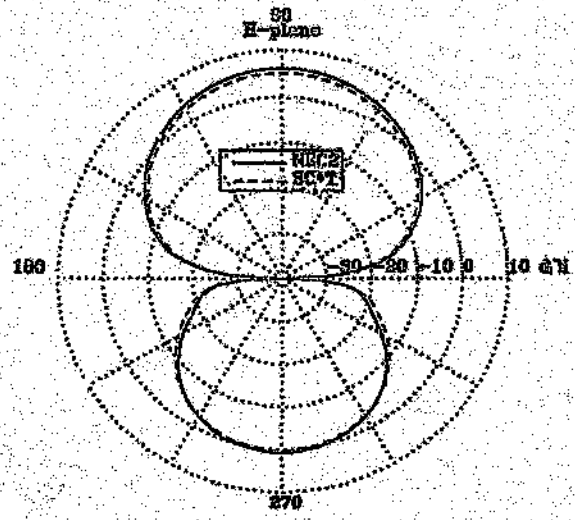


Figure 4.19: NEC vs SCAT input impedance – 2 element Yagi-Uda, dipole feed replacing the folded dipole; (error norm = 2.43Ω)



concair



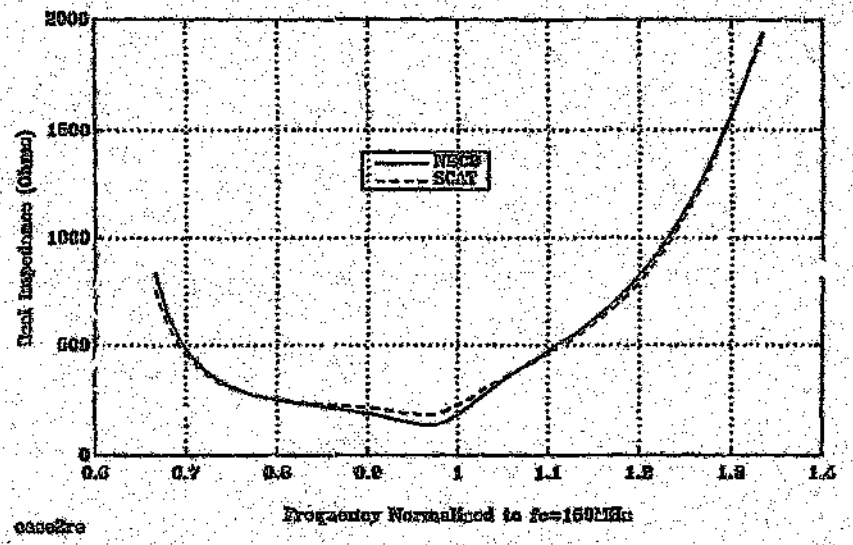
conclrh

Figure 4.20: NEC vs SCAT radiation pattern – 2 element Yagi-Uda, dipole feed replacing the folded dipole

In conclusion, it is clear that for the extremely simple case presented, the results compare well, with a mean absolute magnitude error of 2.43Ω.

4.4.2 Case2 – 2 element Yagi-Uda, folded dipole feed

Case 2 shows the same antenna with a folded dipole feed element, as shown in figure 4.18. The impedance comparisons are shown in figure 4.21, and the radiation patterns in figure 4.22.



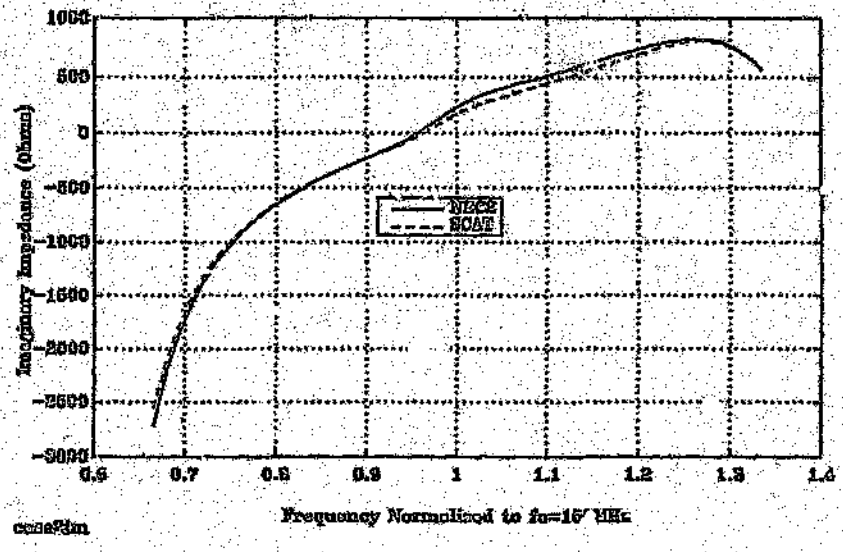


Figure 4.21: NEC vs SCAT input impedance – 2 element Yagi-Uda with a folded dipole feed; (error norm = 36.37Ω)

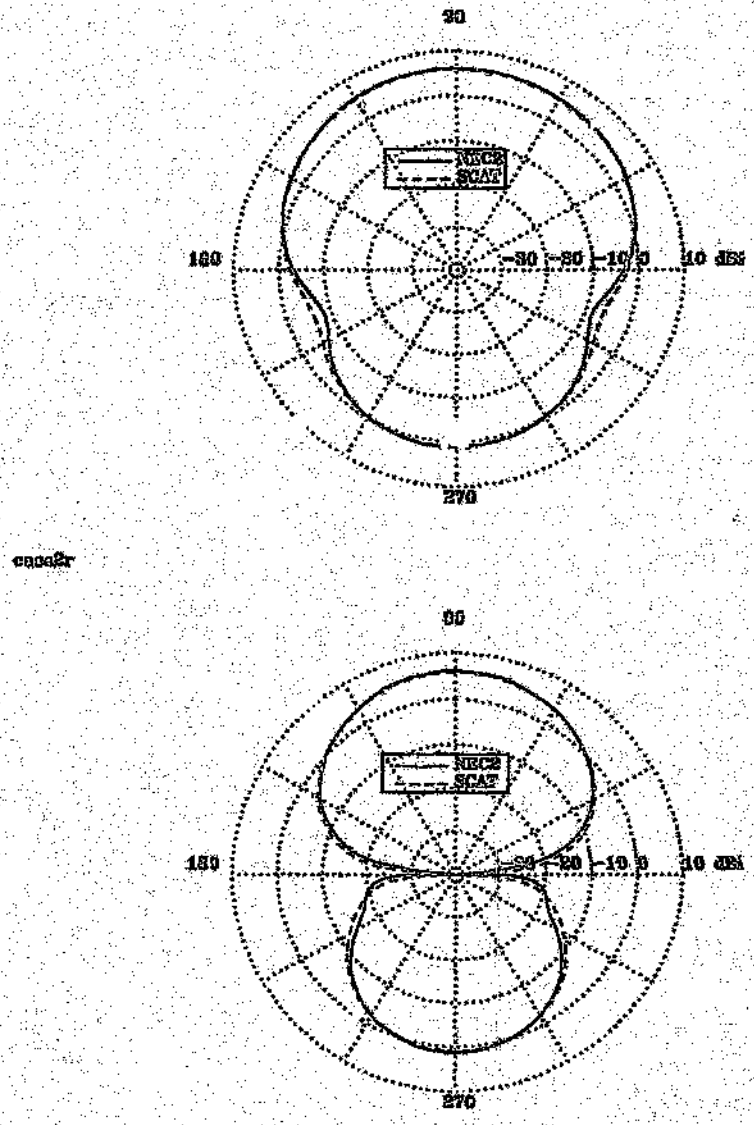


Figure 4.22: NEC vs SCAT radiation pattern – 2 element Yagi-Uda, folded dipole feed

Again, the input impedances and radiation patterns compare favourably. Although the e... is now 36.37Ω, the y axis scales are much higher (10 times for the real part), so this still represents a very low error.

4.4.3 Case 3 – 5 element Yagi-Uda, dipole feed

The geometry for this numerical experiment is shown in figure 4.23(again, the dimensions are in metres), except that the folded dipole feed element shown is replaced with a dipole feed element of the same dimensions.

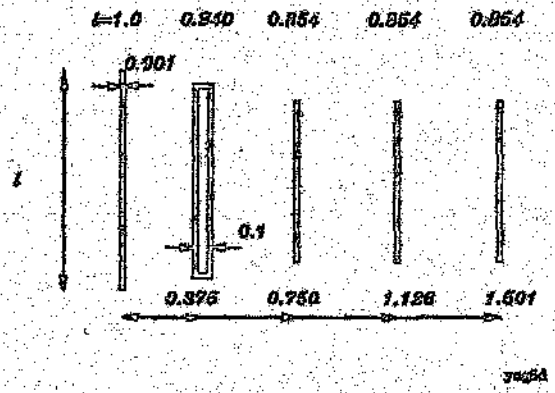
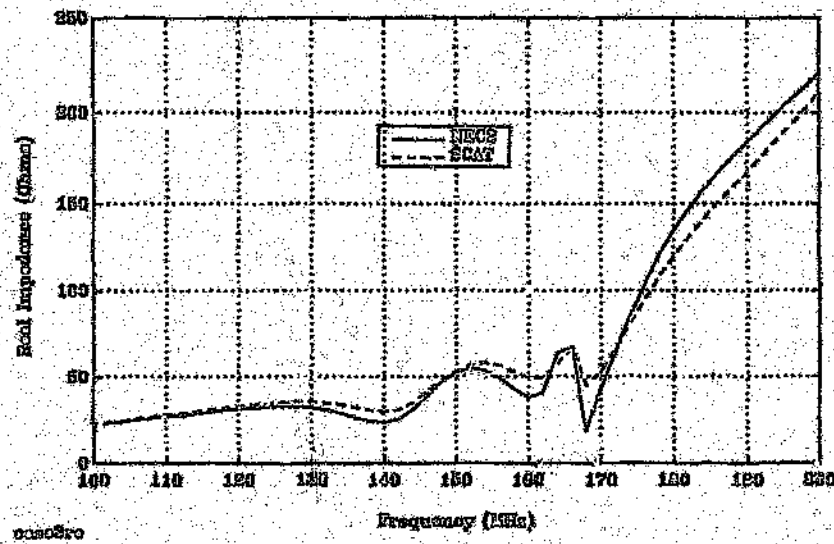


Figure 4.23: Geometry for the 5 element Yagi-Uda

Figure 4.24 & 4.25 show the impedance and radiation pattern results respectively.



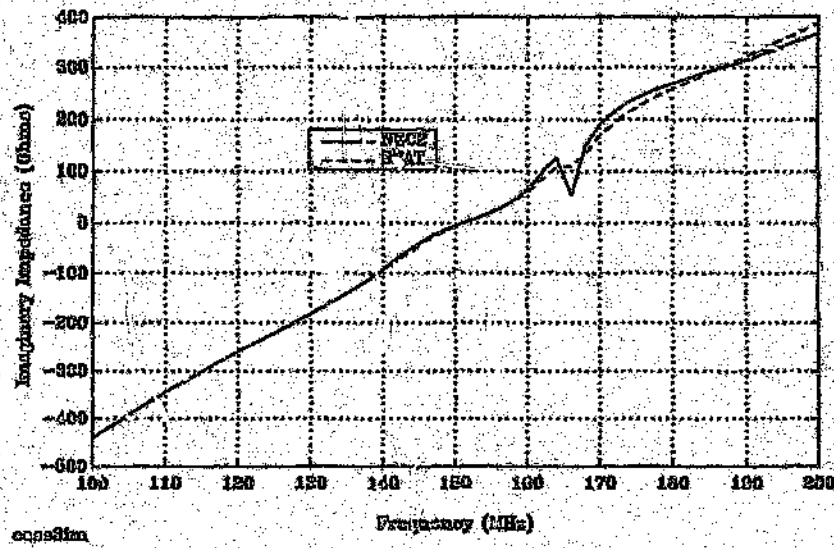


Figure 4.24: NEC vs SCAT impedance – 5 element Yagi-Uda, dipole feed replacing the folded dipole; (error norm = 6.12Ω)

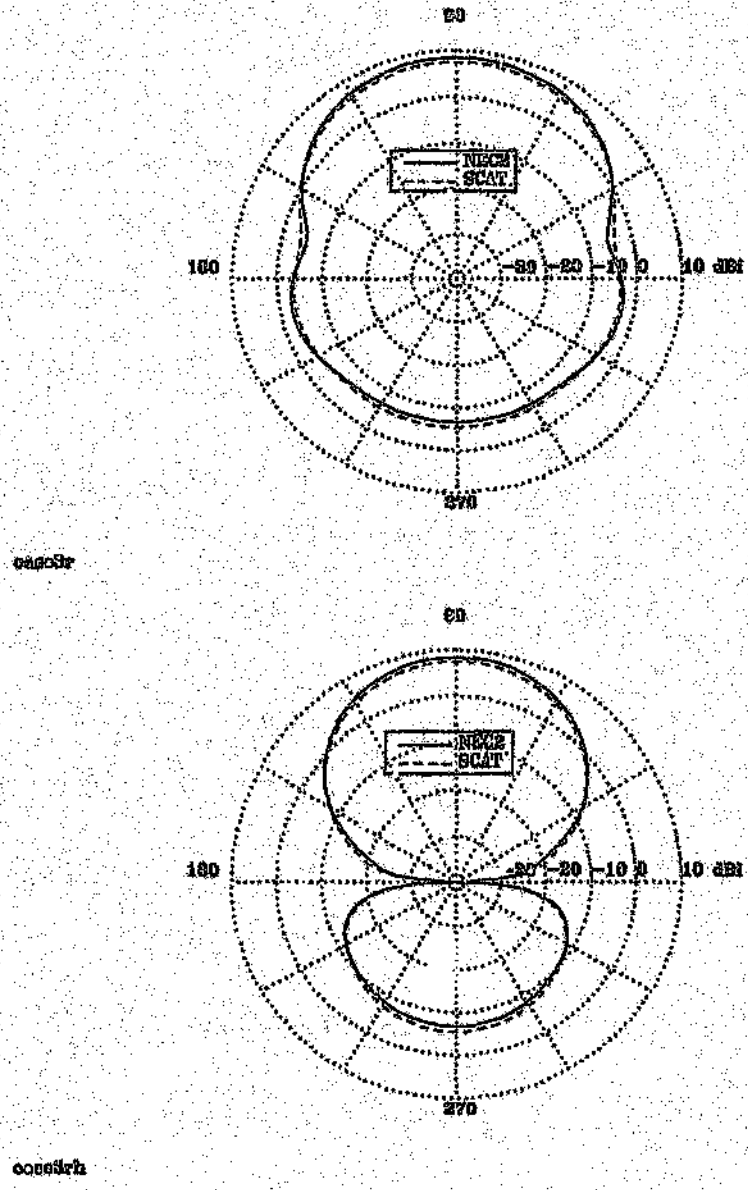


Figure 4.25: NEC vs SCAT radiation pattern - 5 element Yagi-Uda, dipole feed replacing the folded dipole

Clearly, the results still compare favourably, with the impedance results even tracking the geometrical resonance at $1.15\,f_c$, although not with the same magnitude as the NEC results. The disturbance in the otherwise smooth impedance curve is an anomaly of the design, and not a numerical error. The antenna presented has been optimized for superior front-to-back ratio at the expense of bandwidth.

4.4.4 Case 4 – 5 element Yagi-Uda, folded dipole feed

Case 4 is the same antenna as case 3, but with a folded dipole feed, as shown in figure 4.23.

Impedance results are shown in figure 4.26 and radiation pattern results in figure 4.27.

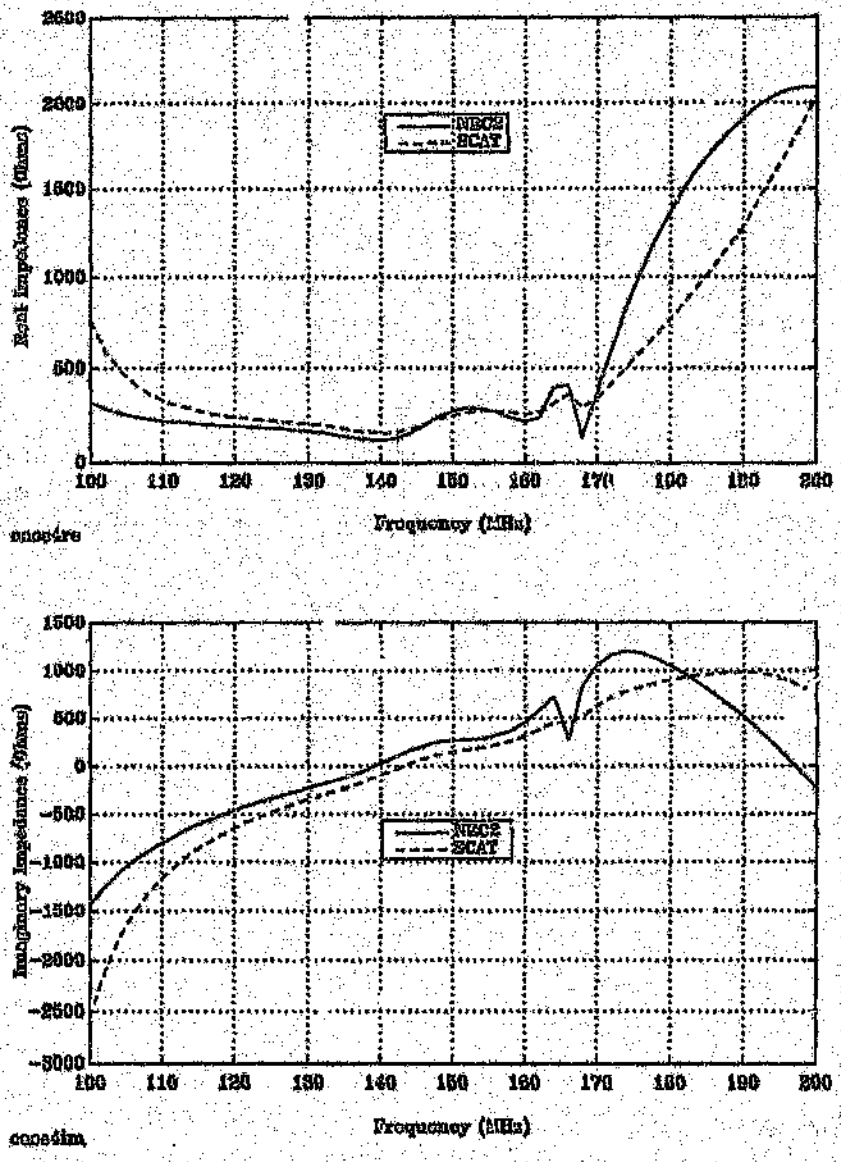


Figure 4.26: NEC vs SCAT impedance – 5 element Yagi-Uda folded dipole feed; (error norm = 278.85Ω)

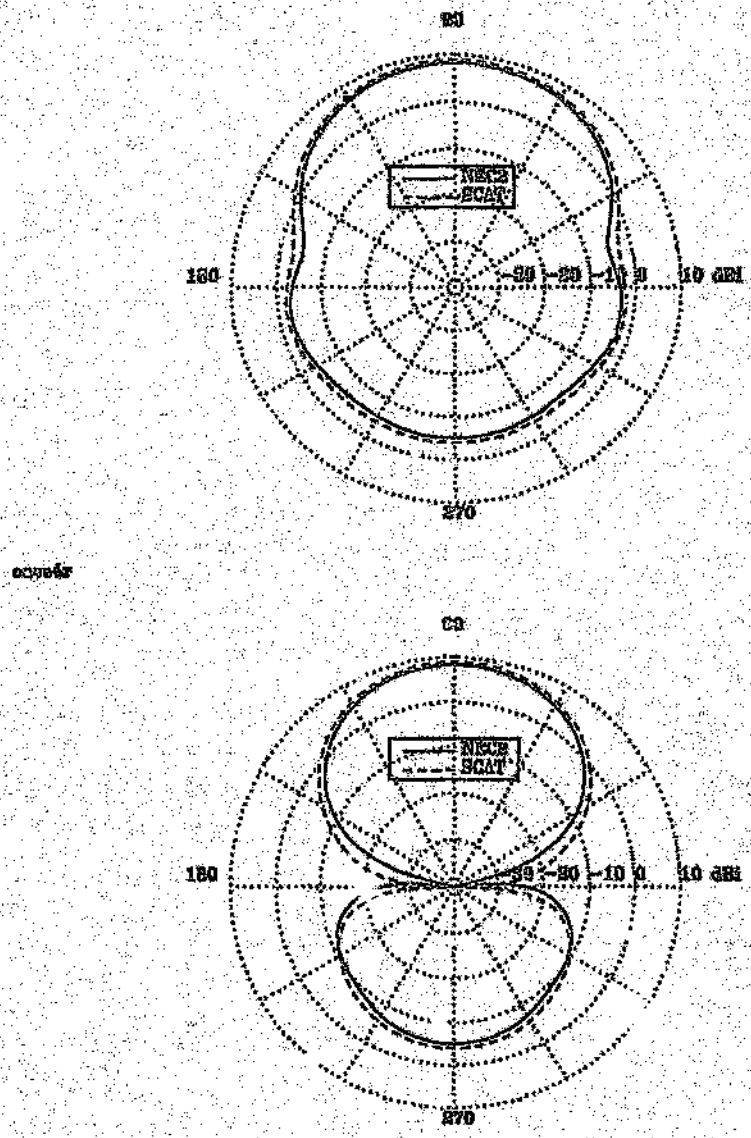
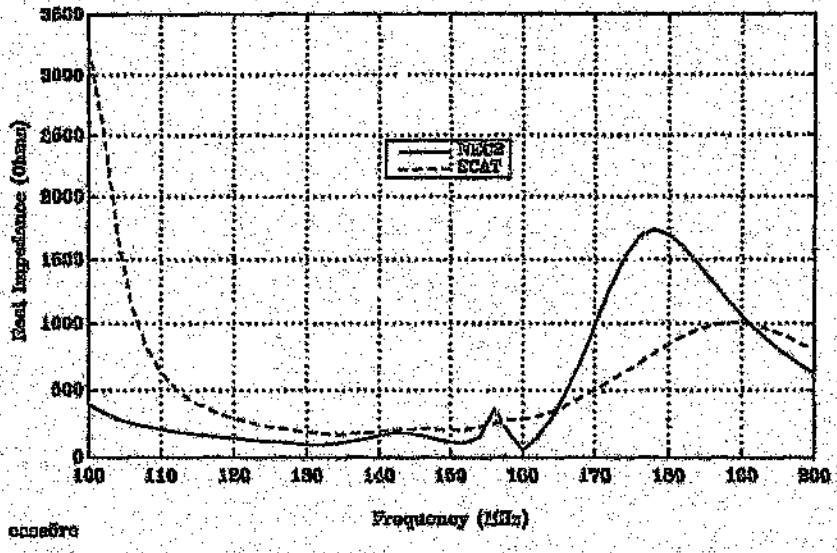


Figure 4.27: NEC vs SCAT radiation pattern – 5 element Yagi-Uda, folded dipole feed

Here the impedance results compare favourably up to 1.15 f_c, including tracking the geometrical resonance of the structure, but immediately thereafter there is a large, unexplained discrepancy.

4.4.5 Case 5 -- 5 element Yagi-Uda, folded dipole feed, 19mm diameter

Case 5 is the same antenna as in case 4, shown in figure 4.23 but using a more realistic value of element diameter, namely 19mm (ie a radius $a = 0.00475\lambda_c$). Results of this simulation are shown in figures 4.28 & 4.29.



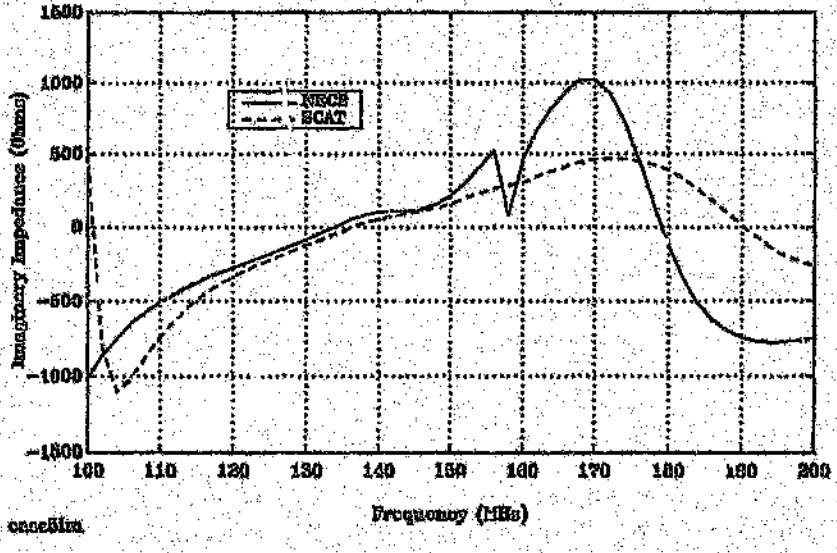


Figure 4.28: NEC vs SCAT impedance -- 5 element Yagi-Uda folded dipole feed, 19mm diameter tubing. (error norm = 382.53Ω)

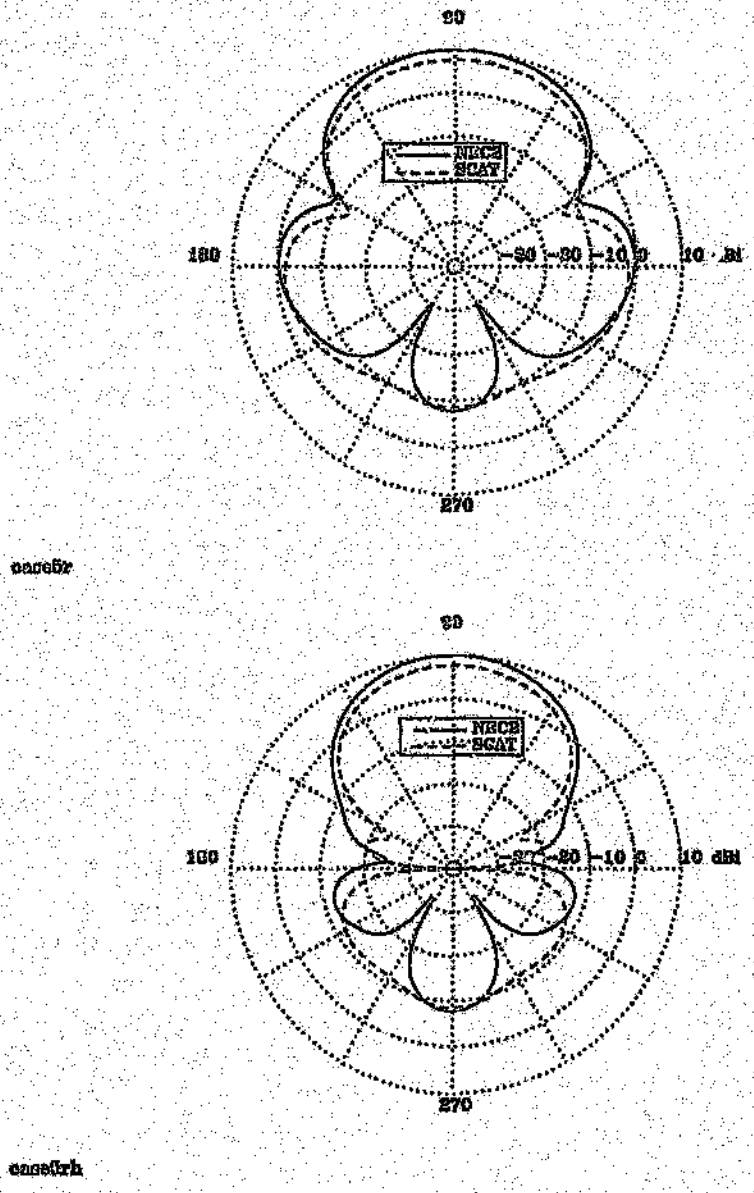


Figure 4.29: NEC vs SCAT radiation pattern – 5 element Yagi-Uda, folded dipole feed, 19mm diameter tubing.

It is clear from the results of this experiment versus those of case 4 that the thickness of the dipole elements has adversely affected the calculation of the mutual impedances of the array. (Error norm of 382.53Ωvs 278.85Ωfor the thinner case). It is to be noted that thickness is taken into account in the self-impedances of the array, and it is only in the calculation of the mutual impedances that a filamentary current is assumed.

4.4.6 Array Analysis timing results

One emphasis in the discussion of the importance of the problem addressed by the thesis is that a simpler method of analysis should provide a faster and more efficient analysis method. The execution times for the cases presented above are shown in table 4.1, as run on an IBM compatible, 80386-SX machine.

Case#	NEC2 Runtime	SCAT Runtime	Speed-up Factor
1	26.133	0.350	74.66
2	71.583	0.350	204.52
3	157.150	2.467	63.71
4	252.233	2.483	101.58
5	252.250	2.467	102.25

Table 4.1: Runtimes for case studies presented on 386SX-25

The execution times presented in table 4.1 were obtained from running NEC2 on a 25 MHz 80386-SX IBM compatible machine, without co-processor. The implementation of NEC2 used throughout was supplied by the Applied Computational Electromagnetics Society (ACES), recompiled to support machines without co-processors.

Note that the greatest speed-up occurs for antennas with folded dipoles, as the SCAT runtimes are proportional to the number of antenna elements, whereas NEC2 runtimes are dependent on the number of wire segments.

Chapter Summary

- A numerical experiment showed the decreasing accuracy of Thiele's transmission line model of the folded dipole as the inter-element spacing increased, and showed that the error was unacceptably large for most practically dimensioned folded dipoles. It also showed the significant improvement in accuracy obtained by a simple first order modification to the transmission line model.
- A numerical experiment showed that the first order modification was not sufficient to cope with a large range of element radius. A further correction factor was introduced, and results were presented for a large range of inter-element spacing and radius.
- The measurement procedure has been outlined as many of the results presented have been verified by measurement.
- The method of obtaining the mutual impedance between any two antennas from NEC2, as outlined in chapter 3, was verified by measured and to theoretical results.

- The mutual impedance between a dipole and a folded dipole (and the reciprocal arrangement) as well as between two folded dipoles has been presented, and verified against measured results, and NEC2.
- The NEC2 was used to investigate the effect of element thickness on the mutual impedance values and the variation in the values have been presented.
- Several simple arrays have been analysed and the radiation pattern and input impedance results have been compared against those obtained from NEC2. Good comparison is obtained for dipole and folded dipole fed arrays but less so with thicker radius antennas.
- The faster execution times for the method are compared to those of NEC2.

Chapter 5

CONCLUSIONS

5.1 Document Summary

A considerable number of antennas are composed of simpler elements such as dipoles and folded dipoles. When designing these antennas, it is important to be able to determine the input impedances for correct matching to the transmitting or receiving system and also to determine the radiation pattern of the antenna.

Coupling theory has been used to characterize such antennas in terms of the self and mutual impedances of the antenna elements. The thesis has been mainly concerned with defining these self and mutual impedances, particularly with folded dipoles.

The self impedance of a dipole in an array has been shown to be different to its free space input impedance. Within the scope of a simplified analysis method, however, these impedances are assumed to be equal. A numerical experiment was presented which defined the range of validity of this assumption for a particular geometry. In general, the impedances are comparable when the dipoles are not approaching an integer wavelength in length.

The standard expression for mutual impedance between dipoles assumes an infinitely thin dipole, and sinusoidally varying current distribution, implying that at a full wavelength, a numerical singularity will occur.

The simplified method must therefore be restricted to antennas where the dipole lengths are not approaching an integer wavelength long.

The self impedance of a folded dipole has been found by applying the transmission line model of the folded dipole. Various extensions to the model were proposed to take the inter-element spacing of the folded dipole into account. It has been shown that the extensions to the model provide accurate input impedances up to an inter-element spacing of one-sixth of a wavelength.

The mutual impedance between a folded dipole and dipole has been defined. This has been

verified against the NEC2 and measured results. It is shown that the mutual impedance between a folded dipole and a dipole is twice the mutual impedance between dipoles. It is also shown that the mutual impedance between two folded dipoles is four times that between two dipoles.

The simplified analysis techniques presented in this thesis was embodied in a computer program called SCAT, which was used to analyze several simple antennas. For thin radius antennas, the comparative input impedance and radiation pattern results were good, implying a close modelling of self and mutual impedances, even with folded dipoles. However, for dipoles of larger radius, the mutual impedances are no longer accurately modelled, and the degradation in accuracy is clear.

It has been shown that the execution speed of the SCAT program is greatly improved over the NEC2 program, justifying the thesis of faster execution for simplified analysis methods. However, the method has had to be severely limited in scope to achieve this, although there are still many types of antenna that can be analysed by SCAT.

5.2 Original Contribution

The original contribution of the thesis is re-iterated here for the purposes of clarity.

- The mutual impedance involving a folded dipole has been analytically defined, by considering the transmission line model of the folded dipole when using the induced-emf method of determining the mutual impedance. An expression for the mutual impedance between a dipole and a folded dipole has been defined in this manner, analogous to the mutual impedance between two dipoles. The expressions are for infinitely thin wires, however, and it has also been shown how the mutual impedance varies with thickness of the antennas, which has been confirmed by numerical experiment and measurement. Some of this work has been published (Clark & Fourie 1992)
- It was shown that the self impedance of a dipole in an array is significantly different from the dipole's free space input impedance when the dipole is a full wavelength long. Within the scope of a simplified analysis method, the free-space impedance must be used in place of the self- impedance which precludes the analysis of full wavelength dipoles. Published in (Clark & Fourie 1990)
- The transmission line model of the folded dipole has been shown to be inadequate for the analysis of folded dipoles with an inter-element spacing of more than one hundredth of a wavelength. The model has been extended by the inclusion of the inter-element separation into the equivalent length of the folded dipole to enable the accurate analysis of folded dipoles with inter-element separations of up to one-sixth of a wavelength. This aspect of the work has been published in the open literature. (Clark & Fourie 1991)

5.3 Recommendations for further investigation

The two major problems encountered with the self and mutual impedance when the dipoles are an integer wavelength long need to be addressed.

The mutual impedance for dipoles needs to be extended in order to take the thickness of the dipoles into account. It has been shown that the mutual impedance is sensitive to the thickness of the dipoles, and that as a result, the simplified method's accuracy degrades when analysing thicker antennas.

The SCAT program is not optimized for speed of execution. The numerical methods used in it were chosen for their simplicity in order to test the theory that was developed. More complex and faster integration methods could be adopted.

The restriction of parallel z-directed currents can be removed by simply considering the parallel components of the radiated fields. The basic data structure of SCAT will need to be changed, however.

One of the aims of this research was to see how well the sinusoidal current assumption, with its attendant coupling theory, could accurately predict performance as compared to a full current expansion method like NEC. The problems outlined in this thesis seem to indicate that the limit has been reached, and that increased accuracy of the simplified method will only be brought about by increased complexity. It is thus recommended that other techniques are investigated to increase the execution speed of NEC; for example admittance matrix interpolation or sparse matrix techniques, etc.

Appendix A

SCAT MANUAL

A.1 Overview

The SCAT computer software package was written as a tool to explore the theory developed in this thesis. SCAT is an acronym for *S*imple *C*omputational Antenna *A*nalysis *T*echniques. An overview of the package is given, followed by a description of the user interface and the internal Units.

Features and Capabilities:

Language Turbo Pascal Version 6.0, but without using Object Oriented Extensions

Source Size The total package is 6943 lines of Pascal source code

Executable Size SCAT compiles to 185kBytes of executable, non- overlaid code. This can reduce if the overlays are enabled.

- Analysis of antenna arrays comprising dipoles and folded dipoles
- Radiation Pattern Prediction
- Input Impedance prediction similar to the accuracy of NEC2
- Mutual impedances derived from NEC for any geometry
- Theoretical mutual impedances for dipoles
- Speed of computation can be several times less than NEC2 for the equivalent computation
- Post Processing of NEC results – collects Input Impedance data to file in a plottable form. Also collects NEC radiation pattern data.
- Post processing of SCAT results – Outputs impedance and radiation pattern data in a similar form to the NEC post-processing.

- Comparison plotting. Accepts NEC or SCAT files and plots them against each other to allow for comparison. Plots Smith Charts, Radiation Patterns in Polar, Elevation Only, or Rectangular formats.

A.2 User Interface

A.2.1 Description of the parts of the screen

Although SCAT was written using Turbo Pascal 6.0, the bulk of it was written in Turbo Pascal 4.0, so the convenience of the Turbo Vision interface with automatic mouse support and drop-down menu's was not utilized. Instead, a screen management utility, based in concept on Walker (1986) (but extensively modified) was used. The various screens presented to the user are now described.

The Menu Screen

The menu screen is placed upon the desktop with a highlighted bar which scrolls through the menu options using the arrow keys. Pressing Enter will select the highlighted menu option.

The first letter of the menu option is Bold – indicating that typing the letter will auto-select that item.

Some menu options will lead to further menus being placed on the screen. Other options will pop-up a prompt screen to capture user input - often these options will have a default value, shown right justified on the menu screen. If the default value is suitable, the option can obviously be bypassed.

The Function Key Screen

The very last line of the screen can display a Function key menu, where the options are selected by pressing the appropriate Function key. Since this largely duplicates the functionality of the Menu Screens, and is generally more cryptic, they are not often used.

The Status Screen

The second last line of the screen is a Status screen – This is used to convey information to the user about the currently running process; for example the frequency being worked on in a frequency sweep analysis.

The Prompt Screen

All user input is captured via Prompt screens (similar in concept to the modern "Dialog Box"). The prompts are pop-up windows containing the prompt string and space to fill in the response. The default values of the items are also sometimes shown, and simply pressing Enter will accept them. The input is type-checked (if numeric data is needed, alphabetic characters are not accepted), and the input can be edited with the backspace key.

The Error Screen

This is also a pop-up screen, typically conveying information about a fault condition, and requiring a keystroke to remove it from the desktop.

A.2.2 Environment Variables

There is only one Environment variable that SCAT responds to in order to suppress the beeping sounds made on error conditions, and when finishing an analysis task. From the Dos prompt, issue: `Set SCAT=NOSOUND` to keep it quiet.

A.2.3 The Configuration File

The Configuration file can be used to set up the screen colour scheme, and the paths to the '.bgi' Borland Graphics Interface files needed in order to plot Smith Charts, Radiation patterns etc in graphics mode.

Only those variables that you wish to change need be put into the .cfg file (No attention need to be paid to capitalization etc). The variables that can be set, together with their default values (in square brackets) are given below:

DeskTopBack [Black] Background colour of the Desktop

DeskTopText [LightGray] Text colour. (Note use of Gray not Grey, since these variables are parsed directly into the Borland equivalent colours–using American spelling)

ESText [White] Error screen text colour

ESBack [Red] Error screen background colour

SSText [Yellow] Status screen

SSBack [Brown]

MSText [Lightgray] Menu screen

MSBack [Black]

FSText [Lightgray] Function screen

FSBack [Black]

PSText [Green] Prompt screen

PSBack [Magenta]

BGIPATH [=.] (ie Dos Current Path) Path to the Graphics Interface Files.

OverLayPath [=.] Path to the Overlay Files

MONO The existence of this keyword anywhere in the configuration file results in a black-and-white colour scheme for the User Interface suitable for Hercules monitors, and monochrome monitors on colour cards.

A.2.4 Description of the menus

This section will describe the various functions of the menus.

Main Menu of SCAT

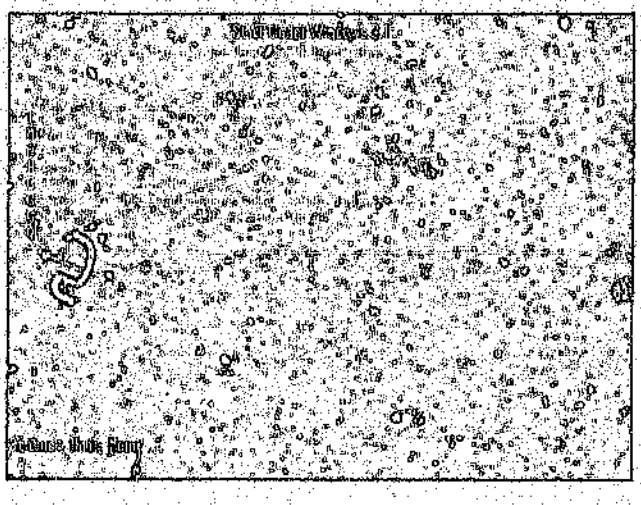


Figure A.1: Main menu

SCAT Analysis of Dipole Structures Calls the "SCAT Input Impedance" menu which allows for the entry of a geometry and runs SCAT on the array

Impedance Manipulations - vswr etc. Calls up the "Impedance Manipulation Menu" which allows the manipulation of impedances in files, conversions etc..

Mutual Impedance of arrays Calls up the "Mutual Impedance Menu" which evaluates the mutual impedances

Automated NEC mutual impedance Calls up the "NEC Z12 Batch Menu" which runs NEC in batch mode to evaluate mutual impedances

Radiation Pattern from NEC file Prompts for the name of a NEC output file, which it searches for a Radiation Pattern to plot. It then calls up the first Function Screen Menu, described below.

Get Nec Zin vals and append to a single file Calls up the "NEC Zin Search" menu which does NEC Post processing – searches NEC Output files for impedance data – can handle multiple impedances in multiple files.

Get HP4195A Data and plot a Smith Chart. Prompts for the name of a file of measured data and enables a Smith Chart Plot

Quit this menu Quits SCAT after the usual "Are you sure" prompt

SCAT array analysis menu

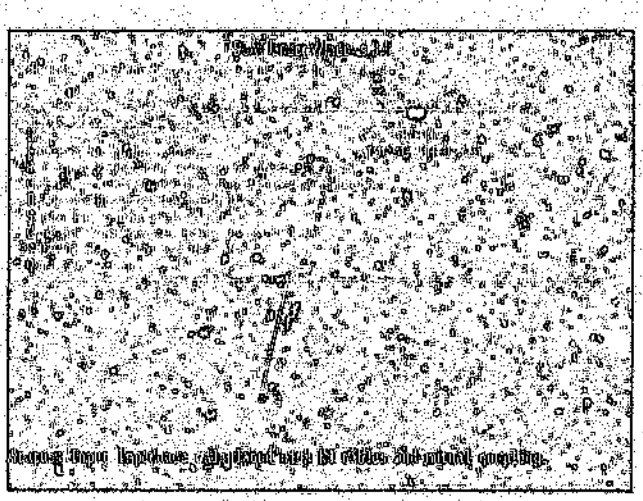


Figure A.2: Array analysis menu

Add a Wire to the Geometry Calls up the "Wire Geometry Data Entry" menu which can add a wire to the existing geometry

Enter a Single Frequency Prompts for a frequency at which to evaluate the input impedance of the antenna array stored in the geometry for a single frequency point only

Enter a frequency Sweep Prompts for the Start frequency, End frequency and the frequency increment of a frequency sweep, to evaluate the current geometry.

Set up a Radiation Pattern Request Calls up the "Radiation Pattern Specification" menu to specify the points in space at which to calculate the Radiation pattern of the stored geometry.

Calculate the input impedance for the geometry Prompts for an output file name, and runs SCAT on the geometry and control that has been entered

Read in the Geometry from Disc Prompts for a file name and reads in a Stored geometry

Store Geometry to Disc Prompts for a file name and stores the current geometry to disc

Convert SCAT output files to plot files Prompts for a SCAT output file and converts the impedance data into the standard form used for plotting and outputs into a file

SPECIAL Fn - Plot vs NEC2 file Calls up the "SCAT vs NEC2 Plots" menu

Quit this menu Goes back to the "Main Menu of SCAT"

Impedance Manipulation Menu



Figure A.3: Impedance manipulation menu

Automated enter,match,vswr,plot An automation of the other functions.

Enter input impedance coefficients Prompts for number and value of impedance values (Entered in real-and-imaginary form)

Impedance in parallel with 54" whip (Historic!) does the parallel computation for a standard 54" whip

Convert polar to rectangular form Converts all impedances

Edit input impedance coefficients Allows the impedances to be edited.

Calculate the best match Avg of the real parts

Calculate the VSWR's Does the VSWR wrt the Z0 entered

Plot the VSWR's Plots to screen

File input Reads the coeffs from ASCII file

File Output writes the coeffs to an ASCII file

Enter Z0 The Z0 value to calculate the VSWR to.

Quit Go back to the Main Menu

Mutual impedance menu



Figure A.4: Mutual impedance menu

Linear separation of the dipoles (d) Enter a value for the initial separation of the two dipoles

Height separation of the dipoles (h) Enter a value for the initial height offset of the two dipoles

Overall length of dipole 1 (l1) Enter the tip-to-tip length of the first dipole

Overall length of dipole 2 (l2) Enter the tip-to-tip length of the second dipole

Frequency of operation (MHz) Enter the freq.

The accuracy of the integration Enter the "epsilon" figure that will satisfy the Romberg Convergenge criteria

The Damping Factor of integration A non-zero value here adds a damping factor to the denominator of the integral, eliminating the singularity at full wavelength

Vary the linear separation (d) Evaluates the mutual impedance integral for varying d. Prompts for max d and increment

Vary the height separation (h) Evaluates the mutual impedance integral for varying h. Prompts for max h and increment

Plot the results of a sweep Plots ...

Input from file Pulls in impedance data from an ASCII file

Output to file writes the impedance data to an ASCII file

Quit this menu Back to Main Menu

Automated NEC mutual impedance menu

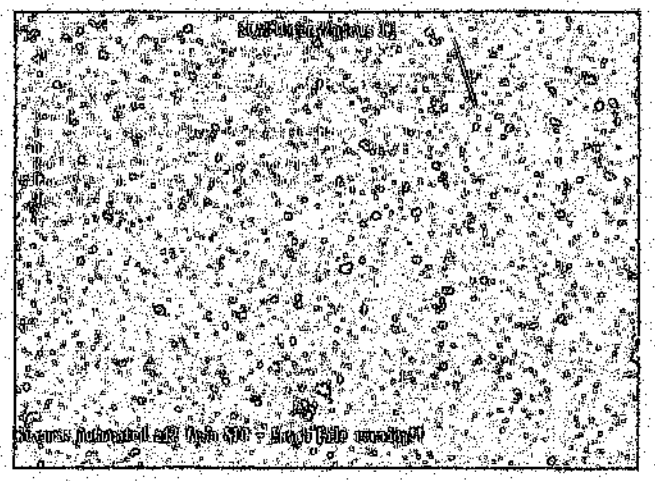


Figure A.5: Automated NEC mutual impedance menu

Primary NEC File Name Enter the filename of the primary (stationary) geometry and control cards for the NEC run

Secondary NEC File Name Enter the filename of the secondary (movable) geometry

The mutual Coupling Data Output File Name Enter a filename to use for the mutual impedance output

Assume that z11=z22? If the antennas are identical, then their self impedances are equal, and a NEC run per data point is saved, shortening run times by a third

Run: Vary the d spacing, and run NEC. Runs NEC three times for each data point required. Prompts for start, end and increment of d

Run: Vary the length l of both dipoles - get z12 Prompts for start, end and increment of the dipole length l

Quit this menu Back to the Main Menu

Get NEC Zin vals...menu

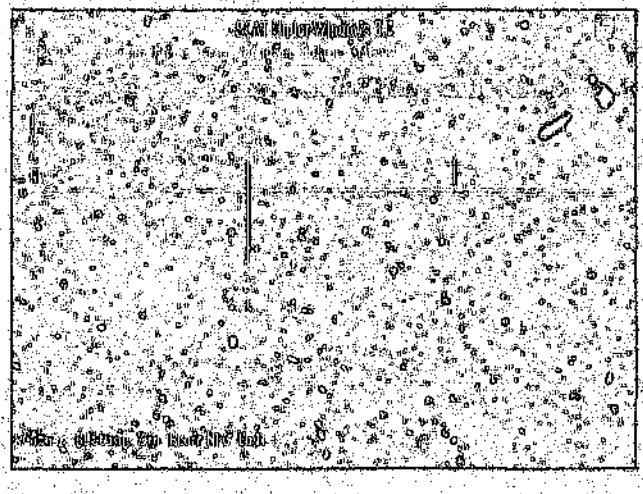


Figure A.6: Get NEC Zin vals...menu

File to Append to ie the Output file

File to look for Zin Scan file

Get One Zin in the current file Only searches for one Zin

Get all Zin's in the current file ...

Quit Back to Main Menu

Wire Geometry Data Entry menu

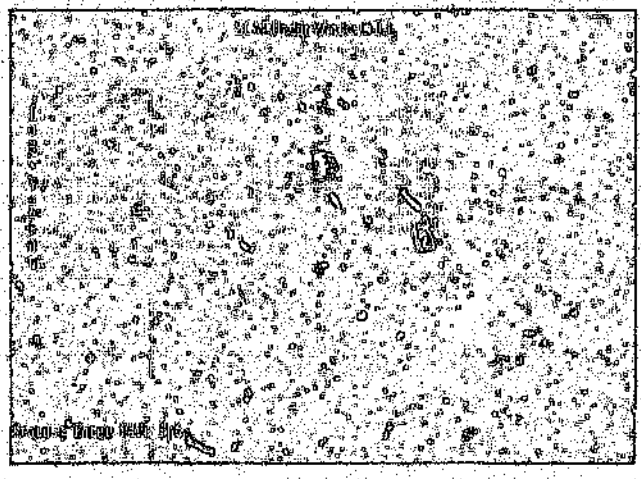


Figure A.7: Wire Geometry Data Entry menu

The total length of the dipole (l) Enter the tip to tip length of the dipole of folded dipole that is being added to the existing geometry

The radius of the dipole ie the radius of the tubing, whether dipole of folded dipole

Ordinary of Folded Dipole Flag

Folded Dipole Element Spacing Enter the inter-element separation of teh folded dipole. Disabled if not applicable

x coordinate of the dipole centre ...

y coordinate of the dipole centre ...

z coordinate of the dipole centre ...

Excitation Voltage - real part If the wire is to be fed, enter the voltage, converting mag and phase to real and imag first

Excitation Voltage - imag part ...

Abort this wire specification Do not add the wire to the linked list of wires that make up the current geometry, and go back to the Analysis menu

Quit and save the wire definition Add the wire defn to the linked list, and go back to the Analysis menu

Radiation Pattern Specification

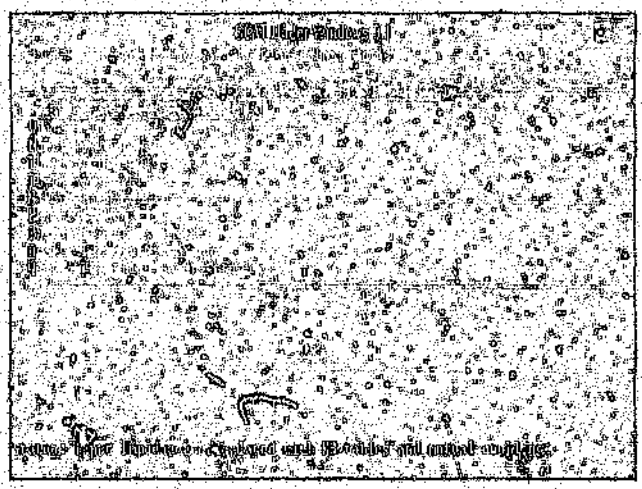


Figure A.8: Radiation Pattern Specification

Read in a pattern spec from file ...

Write Pattern Spec out to file ...

No of theta points Theta is the angle from the zenith

Theta Start Angle in degrees

Theta increment ...

No of Phi points Phi is the angle from the x axis in the xy plane

Phi Start Angle ...

Phi increment ...

Abort this specification do not add this specification to the control list for the analysis run, and return to the Analysis menu

Quit & use this specification abd Go back to the Analysis menu

A.3 Unit Hierarchy

SCAT consists of 12 Self-Authored UNIT's. Their Functions are briefly described:

A.3.1 Unit Description

SMLCLRK The Screen management unit. Provides a set of procedure calls to enable simple but effective screen management. This is based on Walker (1986) Screen Management Library, but has been extensively modified

IMPDANCE Impedance conversion utilities: polar to rectangular, Best Impedance match, VSWR from Zin, and the "varying by distance" mutual impedance user interface.

PLOTUNIT to plot rectangular, and polar pattern , elevation only polar graphs esp. from NEC2 Outputs.

ZIN_COUP The Mutual Coupling calculation Unit.

NEC_Z12 Contains the NEC file PostProcessing. Can extract radiation patterns suitable for plotting; impedance data from a multifrequency NEC run, and convert to an output format suitable for Smith chart plotting. This Unit also contains the automation necessary to produce mutual impedance data using NEC. For this purpose, it runs NEC in a batch mode three times for each mutual impedance data point.

RAD_PAT Does Radiation Pattern calculations from the currents on the structure

HP4195A Convert measured data stored on disc from the HP4195A Hewlett-Packard Vector Network Analyser data format to a form plottable by SMITHPLT

MATHUTIL Mathematical Utilities to get round the lack of complex number capabilities in Pascal. Also includes the Romberg Integration routine essential to the mutual impedance calculation.

FILEUTIL A collection of the File Opening / Closing utilities - can be seen as a logical extension of the SMLCLRK user interface

COMP_NUM Does the Complex Numbered Gaussian Elimination required for the LU Decomposition part of the N-port matrix calculations. It does a standard LU Decomposition, with Partial Pivoting; and Back Substitution. No attempt is made to take advantage of the matrix's obvious symmetry, or its sparsity.

SMITHPLT Does a Smith Chart, based on data fed to it.

CARD_OBJ A type definition for a NEC Card Object. Dangerous mix of a very small OOP code fragment in an otherwise OOP ignorant program!

DOS_ETC Returns an intelligible Dos Error message instead of the usual number!

SCAT Main Program

A.3.2 Unit Dependency

SCAT started life in Turbo Pascal Version 3, migrated to 4, skipped 5 & 5. 5 and landed up at 6. This implies that many of the features (such as Object Orientation) are not used

in SCAT. (The objective was not Software Engineering, but a Theory Testbed!) Thus the Unit Dependencies are of the Interface type only. No Implementation Circular references were used. The Interface dependencies are:

SCAT Uses: Graph, Crt, Overlay, SmlClrk, Impdance, PlotUnit, Zin_Coup, Nec_Z12, Rad_Pat, HP4195A

SMLCLRK Uses: Crt, Graph, Dos, Uin

IMPDANCE Uses: MathUtil, Dos, PlotUnit, FileUtil, SmlClrk

PLOTUNIT Uses: Graph, Crt, SmlClrk, MathUtil

ZIN_COUP Uses: Dos, FileUtil, MathUtil, Comp_Num, PlotUnit, SmlClrk

NEC_Z12 Uses: crt, dos, dos_etc, SmlClrk, FileUtil, MathUtil, Objects, Card_Obj, Plotunit

RAD_PAT Uses: FileUtil, SmlClrk, PlotUnit, Dos, Crt

HP4195A Uses: Graph, SmlClrk, MathUtil, FileUtil, SmithPlt

MATHUTIL Uses: None

FILEUTIL Uses: Dos, Crt, SmlClrk

COMP_NUM Uses: MathUtil

SMITHPLT Uses: Graph, Crt, SmlClrk, MathUtil

CARD_OBJ Uses: None

DOS_ETC Uses: None

A.3.3 Unit Interface Listing

The listing of the program cannot be presented here as it consumes of the order of 120 pages printed in an 8 pt font!. However, the unit interfaces are presented here with all public procedures. The full listing, and executable code can be found on a floppy disc at the back of the thesis.

SCAT

```
{$M 64000, 0, 30000}
(* Put the usual $define precompiler switches here *)
(* as an example, use {$DEFINE Overlay} to use Overlays *)

Program Simple_Computational_antenna_Analysis_Techniques; (* SCAT *)

{*****************************************************************}
(*                          STATEMENT                            *)
```

```
(*                                                                  *)
(*  A program to analyse simple antennas using simple analytical   *)
(*  techniques, as opposed to purely numerical techniques. (MOM)    *)
(*  Note that this is a rough and ready shell, and is thus          *)
(*  definitely a THROW AWAY DESIGN. The purpose of this shell       *)
(*  is to  determine the requirements of a multipurpose antenna     *)
(*  shell. - A.R.Clark       March 1989                             *)
(*******************************************************************)

Uses
  Graph,
  Crt,

{$IFDEF Overlay}
  overlay,
{$ENDIF}

  Calcirh,
  Impdance,
  Plotunit,
  Zin_comp,
(*  Doc_zout,*)
  Doc_z12,
  Rad_Pat,
  HP4195A;

(* Overlay all units to conserve .EXE size *)

{$IFDEF Overlay}
  {$O plotunit}
  {$O zin_comp}
  {$O doc_z12}
  {$O HP4195A}
  {$O Impdance}
{$ENDIF}

Var
  exitsave                                : pointer; (* Graceful Crashing *)

Procedure Main_menu;
(*****************************************************************)
(* Simply calls the relevant procedures in their varie-  'ite - note  *)
(* no data passing at this level - minimises g'...ll        variables *)
(*****************************************************************)

Var
  nop, opt              : integer;
  ch                    : char;
  quit                  : boolean;

Begin
  quit := false;
  Repeat
    ms_menu ('scatt000', nop);
    ms_write ('Main Menu');
    ms_options (o,z, nop);
```

```
    Case opt Of
      0: Zi\_by_mutuals;
      1: Impedance_manipulation;
      2: Mutual_impedance;
      3: Automated_s12_from_UUT;
      4: Radiation_pattern;
      5: Current_plot;
      6: Get_UUT_Zin_and_append;
      7: Get_HP4195A_and_Smith;
      8: Begin
           blast;
           ps_ofay ('Do you really want to leave SCAT??', ch);
           If ch In ['y','Y'] Then quit := true;
         End;
    End;
    Until quit;
  End;

Procedure Crash_fairly_gracefully; far;
{**********************************************************************}
{* This is not much of an attempt at an error handler, but it does *}
{* get the screen out of graphics mode - so that at least you can  *}
{* actually SEE the error message provided & dont have to go about *}
{* resetting the machine!!!!!!    12 June 1988                     *}
{**********************************************************************}

Var
  i : integer;
Begin
  If erroraddr <> NIL Then Begin
    For i := 300 downto 5 Do Begin
        sound (i);
        delay(3);
      End;
      nosound;
      window (1, 1, 80, 25);
      clrscr;
      writeln;
      writeln ('WHEEEEE - Clunk Bang - I''ve been bulletted by an');
      writeln ('Outer Mongolian Batter Pudding. Actually, you have');
      writeln ('managed to confound an unconfoundable ClarkDare');
      writeln ('product!! - Please read error message below, if any!');
      writeln;
    End;
  exitproc := exitsave;
End;


Begin {* SCAT main prog *}
  exitsave := exitproc;
  exitproc := @crash_fairly_gracefully;
  sml_clrk_init ('scat.cfg');

{$IFDEF Overlay}
  ovrinit (overlay_path + 'scat.ovr');
{$ENDIF}
```

```
  main_menu;
  banner;
End.
```

SmlClrk

```
Unit smlclrk;
{*****************************************************************************}

Interface

Uses
  Crt,
  graph,
  dos,
  vin;

Type
  screen_message = string; {* Gets rid of the one liner restriction *}

{* Publically accessible screen procs *}
Procedure scr_format;
Procedure bleat;
Procedure fn_check (file_name              : screen_message;
                    Var file_status        : boolean);
Procedure file_check (file_name            : screen_message;
                      Var file_status      : boolean);
Procedure cr; {* Carriage Return *}
Procedure ms_clear;
Procedure ms_menu (filename                : screen_message;
                   Var no_of_options       : integer);
Procedure ms_default (option               : integer ;
                      default              : screen_message);
Procedure no_options (Var this_option      : integer;
                      no_of_options        : integer);
Procedure ms_load (filename                : screen_message);
Procedure ms_msg (message                  : screen_message);
Procedure ms_output_window (x1, y1, x1, y2 : integer);
Procedure ms_output_close;
Procedure ss_clear;
Procedure ss_write (messag:                : screen message);
Procedure ss_mandi (message                : screen_message;
                    val                    : integer);
Procedure ss_mandr (message                : screen_message;
                    val                    : real);
Procedure ps_clear;
Procedure ps_wait;
Procedure ps_write (message                : screen_message);
Procedure ps_ufi (message                  : screen_message:
                  Var this_value           : integer);
Procedure ps_ufr (message                  : screen_message;
                  Var this_value           : real);
Procedure ps_ufsy (message:                : screen_message;
```

```
                    Var this_symbol          : char);
Procedure ps_ofst (message                   : screen_message;
                    Var this_string          : screen_message);
Procedure ss_clear;
Procedure ss_write (message                  : screen_message);
Procedure fs_clear;
Procedure fs_options (Var this_option        : integer;
                      no_of_options          : integer);
Procedure fs_name (filename                  : screen_message;
                    Var no_of_options        : integer);
Procedure ac; (* Clears all one line screens *)
Procedure banner;
Procedure graphics_to_text;
Procedure text_to_graphics;
Procedure zal_clrk_init (config_file_name    : string);

Procedure home;
Procedure set_cp (row, column                : integer);


Var
  overlay_path                               : string;

Implementation
```

Impdance

```
Unit Impdance;
(*************************************************************************)
(* A unit containing the impedance manipulation utilities                *)
(* for converting polar to rect, finding the best match to zin,          *)
(* and the corresponding VSWR etc. Also has the mutual                   *)
(* impedance generation routines (user interfaces) for th                *)
(* "Varying by distance" runs.                                           *)
(* 860 lines of code.                                                    *)
(*************************************************************************)

Interface

Uses
  mathutil,
  dos,
  plotunit,
  filesutil,
  calclrk;

Const
  max_no_of_coeffs = 400;

Type
  complex_array = ARRAY [1..max_no_of_coeffs] of complex;
  real_array    = ARRAY [1..max_no_of_coeffs] of real;

Procedure Mutual_impedance;
```

```
Procedure Impedance_manipulation;


Implementation
```

PlotUnit

```
Unit PlotUnit;
(*************************************************************************)
(* A Unit with two plotting routines - my & polar plots in an            *)
(* "intelligent" fashion. December 1988 - Alan Robert Clark.             *)
(*************************************************************************)

Interface

Uses graph,
     crt,
     calcirk,
     mathutil;

Const
  max_points = 366;

Type

  multiplotarray = Array [1..max_points, 1..6] of real;



(*************************************************************************)
(*              A Generalised x-y plotting procedure.                    *)
(*          Alan Robert Clark Nov '88 Turbo 4 Graph Unit                 *)
(* plot_array is an input array of two dimensions, x is in [1,1]         *)
(* & y is in [1,2]. The no_of_points to be plotted can be input,         *)
(* or if not to zero, the procedure will plot any points until           *)
(* BOTH x and y coords are zero, ie it will automatically find           *)
(* which points are valid to plot.                                       *)
(*************************************************************************)

Procedure Multiple_plot (
                  mult_plot_array       : multiplotarray;
                  no_of_plots           : integer;
                  no_of_points          : integer;
                  header_text           : screen_message;
                  x_text, y_text        : screen_message;
                  legend_1, legend_2,
                  legend_3, legend_4,
                  legend_5              : screen_message);

(*************************************************************************)
(*          A Fairly Generalised polar plotting package.                 *)
(*                Alan Robert Clark Dec '88                              *)
```

```
(* plot_array [1,1] contains the angle IN DEGREES and [1,2] should      *)
(* contain the magnitude with the qualifications below.                 *)
(* By Fairly I mean that it has been created for doing NEC plots        *)
(* and then expects its magnitude values to lie between -40 & 20 or so  *)
(* All values below -40 dBi are truncated to be -40dBi, and if you go   *)
(* much above +40dBi or so , it will still be scaled in to fit, by the  *)
(* circles will look stupid as they stop at 0dBi !!!- it will still plot *)
(* though !!                                                            *)
(**********************************************************************)

Procedure Multiple_Polar_plot
                  (mult_plot_array        : multiplotarray;
                  no_of_plots             : integer;
                  no_of_points            : integer;
                  header_text             : screen_message;
                  elevation_only          : boolean;
                  legend_1, legend_2,
                  legend_3, legend_4,
                  legend_5                : screen_message);




Procedure Current_plot;

Implementation
```

Zin_comp

```
Unit zin_comp;(* -ling theory included *)
(**********************************************************************)
(* This unit contains the wherewithall to calculate the input impedance *)
(* of an array of dipoles, based on their all freespace (NEC tables)    *)
(* values, and the all given by the seat formulation. It has all the    *)
(* special handling for the folded dipole input impedances, and folded  *)
(* dipole mutuals. At 1040 lines, this is really the "meat" of the      *)
(* analysis part of SCAT                                                *)
(*                                                                      *)
(* It has only one PUBLIC proc, and it is called without parms.         *)
(**********************************************************************)

Interface

Uses
  dos,
  filutil,
  mathutil,
  comp_num,
  plotunit,
  crtclrk;
```

```
Procedure zin_by_mutuals;

Implementation
```

Nec_Z12

```
Unit NEC_Z12;

(*****************************************************************)
(* This unit handles the NEC batch file processing - get mutual  *)
(* impedances from NEC, handles the NEC radpats & impedance file *)
(* gathering. ie NEC PostProcessing. The impedance data is output *)
(* in a form suitable for Smith Charting.                        *)
(* 3 Procs; 820 lines of Code.                                   *)
(*****************************************************************)

Interface


Uses
  crt,
  dos,
  dos_etc,
  mathutil,
  calclrk,
  filoutil,
  Objects,
  Card_Obj,
  plotunit;


Procedure Automated_Z12_from_NEC;
Procedure Get_NEC_Zin_and_append;

Implementation
```

Rad_Pat

```
Unit rad_pat;
(* Contains JUST the radiation Pattern bit *)
Interface

Uses filoutil, calclrk, plotunit, Dos, Crt;

Procedure Radiation_Pattern;


Implementation
```

HP5195A

```
Unit HP4195A;
(*****************************************************************************)
(* A unit to get the Smith Chart Output from a an ascii file containing      *)
(* Gamma x and Gamma y, and to convert it to a smith chart plottable form    *)
(* & to do a spot of further manipulation. The SCM utility brings it into    *)
(* Manuscript                                                                *)
(* One PUBLIC Proc without Parms 225 lines of Code.                          *)
(*****************************************************************************)

Interface

Uses
  graph,
  calcirk,
  mathutil,
  filesutil,
  smithplt;

Procedure Get_HP4195A_and_Smith;

Implementation
```

MathUtil

```
Unit mathutil;

(*****************************************************************************)
(* 25 PUBLIC Procs with parms.  465 lines of Code                            *)
(*****************************************************************************)
Interface

Type
  complex = Record
              re,
              im : real;
            End;
(* All pgms using complex numbers will USE this unit obviating their  *)
(* own complex type declarations.                                     *)

  parameters = Array [1..10] of real;
(* An array of bloody parameters because Turbo 4 did not allow procedural *)
(* parameters - now turbo 5.5 does, but I havent converted them yet!!!    *)


Procedure rtheta          (Var rth : complex);
Procedure cart            (Var xy : complex);
Procedure add             (x,y : complex; Var ad : complex);
Procedure sub             (x,y : complex; Var su : complex);
Procedure mult            (x,y : complex; Var mu : complex);
Procedure divide          (x,y : complex; Var di : complex);
Procedure Square_Root     (x : complex; Var y : complex);
Function tan              (x : real) : real;
```

```
Function re                 (x : complex) : real;
Function im                 (x : complex) : real;
Function modd               (x : complex) : real;
Function arg                (x : complex) : real;
Function DegreeToRadian     (x : real) : real;
Function RadianToDegree     (x : real) : real;
Function Cosh               (x : real) : real;
Function Sinh               (x : real) : real;
Procedure C_Tanh            (x : complex; Var y : complex);
Procedure C_Sinh            (x : complex; Var y : complex);
Procedure C_Cosh            (x : complex; Var y : complex);
Function Tanexp             (x : real) : real;
Function Si                 (x : real) : real; {using Trapezoidal Rule}
Function Cin                (x : real) : real;
Function Ci                 (x : real) : real;
Function power              (a, b : real) : real; {*Raises a to the power b*}
Procedure romberg_integration(fn_type : integer; a, b : real; P : parameters;
                              Var extrap : real);


Implementation
```

FileUtil

```
Unit fileutil;

{*********************************************************************}
{* A simple unit to handle the repeated opening of input and output  *}
{* text files - with the usual checking features, anti-overwritten etc *}
{* and finds a given filename in the PATH environment Variable       *}
{* useful for finding Configuration files etc etc                    *}
{*                                                                   *}
{* Three PUBLIC Procs with Parms. 265 Lines of Code.                 *}
{*                                                                   *}
{* For use with the SMLCLRK Screen Management Library under TP6.0    *}
{*********************************************************************}

Interface

Uses
  dos,
  crt,
  smlclrk;


Procedure open_file_input  (Var infile : text;
                                ext : screen_message;
                        Var file_exists : boolean);


Procedure open_file_output (Var out_file : text;
                                   ext : screen_message;
                           Var file_ok : boolean);
```

```
Procedure find_file_in_any_DOS_PATH
          (filename                          : string;
           Var current_path                  : string);


(*****************************************************************)
(* Documentation:                                                *)
(*                                                               *)
(* Procedure open_file_input                                     *)
(*                                                               *)
(* Opens a file for input and checks that it exists              *)
(* It adds the extension .ext to the file name if it             *)
(* is not supplied by the user. ext can be anything              *)
(* can do a Wherois type or a directory search for               *)
(* the file.                                                     *)
(*                                                               *)
(* Procedure open_file_output                                    *)
(*                                                               *)
(* Opens a file for output, and checks that it does not exist.   *)
(* If it does then you can either overwrite, abort, or try       *)
(* another name                                                  *)
(*                                                               *)
(* Procedure find_file_in_any_DOS_PATH                           *)
(*                                                               *)
(* This procedure searches the currently active DOS directory    *)
(* and all directories defined in the Dos PATH Environment       *)
(* Variable for the filename input parameter specified.          *)
(* The output is the path string where the file is found with    *)
(* terminating backslash.                                        *)
(* If the file is not found, the string is filled with           *)
(* "<not found>"                                                 *)
(* If the file is in the currently active Dos directory the      *)
(* string is returned empty.                                     *)
(* This results in the fewest test cases: simply test for the    *)
(* presence of "<" in pos (1) If not then - simply use!!!        *)
(*****************************************************************)

Implementation
```

Comp_Num

```
Unit comp_num;
(*****************************************************************)
(* A unit to do Complex Gaussian Elimination - without the need to *)
(* go to a 2N by 2N matrix method - A.R.Clark 17 May 1989        *)
(*                                                               *)
(* One Public Proc with Parms. 210 Lines of Code.                *)
(*****************************************************************)

Interface
Uses
  mathutil;
```

```
Const
  max_complex_array_size = 15;


Type
  complex_vector = array [1..max_complex_array_size] of complex;
  complex_matrix = array [1..max_complex_array_size] of complex_vector;

Procedure complex_gaussian_elimination (dimen          : integer;
                                        impedances     : complex_matrix;
                                        excitations    : complex_vector;
                                        Var currents   : complex_vector;
                                        Var error      : integer);



Implementation
```

SmithPlt

```
Unit SmithPlt;

(*****************************************************************)
(* This unit plots a Smith Chart on Screen from a bunch of arrays  *)
(* previously filled prob. by the HP4195A Unit - but not nece.     *)
(*****************************************************************)
Interface

Uses Graph,
     Crt,
     SmlClrk,
     Mathutil;

Type
  Smith_arrays = Array [1..405, 1..10] of Real;

Procedure smith_plot
                  (mult_plot_array       : smith_arrays;
                   no_of_plots           : integer;
                   no_of_points          : integer;
                   header_text           : screen_message;
                   legend_1, legend_2,
                   legend_3, legend_4,
                   legend_5              : screen_message);


Implementation
```

Card_Obj

```
Unit Card_Obj;
Interface
Uses Objects;
```

```
{**********************************************************}
{* Simply holds the DOS Dock card definitions - to be used in *}
{* an instance of a TCollection                              *}
{**********************************************************}
Type
  PCard = ^Card;
  Card = Object (TObject)
    data_ptr : PString;
    Constructor Init (Data : String);
    Destructor Done; Virtual;
  End;
Implementation
```

Dos_Etc

```
Unit Dos_etc;
{**********************************************************}
{* 1 Proc simply returns an intelligeable error message in Slim. *}
{**********************************************************}
Interface

Function DosErrorStr (DosError : Integer) : String;
Implementation
```

Appendix B

Extension factor derivation for Folded Dipole transmission line model

From section 3.2 on page 29 the first order approximation for the equivalent length was (Clark & Fourie 1991):

$$l_{eq} = l + \alpha s \tag{B.1}$$

where

l_{eq} = the equivalent (or extended) length.
l = original length of the dipole.
s = separation of the folded dipole sides.

However, it became apparent that for larger radii, the value of α required further adjustment. NEC2 was used to generate results for folded dipoles of different separations and radii, and the α values were optimised for good comparison. These values are presented in table B.1 and the related equivalent dipole lengths are shown in table B.2.

From the table of equivalent length in table B.2, a column-wise linear regression, gives:

Each equation in the above table gives the linear regression (or linear interpolation using a least squares fit) for the equivalent length, l_{eq}, of the folded dipole as it varies with radius, a. If the above equations are of the form $y = mx + c$, then c is very linear with s and is given as:

$$c = 0.5164s + 0.9852 \tag{B.2}$$

m is given as:

$$m = -13.05s - 1.0315 \tag{B.3}$$

Using logical deduction, it is clear that both constants in the new equations are 1, and hence are the length of the dipole, l. The equivalent length can then be expressed as:

Table B.1: Optimized α values

Optimized α values				
mm	120mm	100mm	80mm	50mm
1	0.40	0.39	0.35	0.25
2	0.36	0.34	0.30	0.20
3	0.32	0.28	0.25	0.15
5	0.25	0.25	0.15	0.10
8	0.21	0.16	0.10	0.08
10	0.17	0.10	0.05	0.05
12	0.13	0.08	0.02	0.02
15	0.10	0.05	0	0

Table B.2: Equivalent lengths

Related l_{eq}				
mm	120mm	100mm	80mm	50mm
1	1.0480	1.0390	1.0280	1.0125
2	1.0432	1.0340	1.0240	1.0100
3	1.0384	1.0280	1.0200	1.0075
5	1.0300	1.0250	1.0120	1.0050
8	1.0252	1.0160	1.0080	1.0040
10	1.0204	1.0100	1.0040	1.0025
12	1.0156	1.0080	1.0016	1.0010
15	1.0120	1.0050	1.0000	1.0000

Table B.3: Linear regression in the s plane

s (m)	Linear Regression on s's column.
0.050	$l_{eq} = -0.825\alpha + 1.0111$
0.080	$l_{eq} = -2.022\alpha + 1.0264$
0.100	$l_{eq} = -2.444\alpha + 1.0377$
0.120	$l_{eq} = -2.544\alpha + 1.0469$

$$l_{eq} = (-13.05s - l)a + (0.5164s + l) \tag{B.4}$$

which, after rounding the values, and some re-arrangement, becomes:

$$l_{eq} = l(1 - a) + s(0.5 - 13a) \tag{B.5}$$

clearly, since $a \ll 1$

$$l_{eq} = l + s(0.5 - 13a) \tag{B.6}$$

which gives the form of the secondary compensation to α that is required. Several iterations have been performed, and the closest comparison with the original table of equivalent lengths is obtained from:

$$l_{eq} = l + s(0.4 - 20a) \tag{B.7}$$

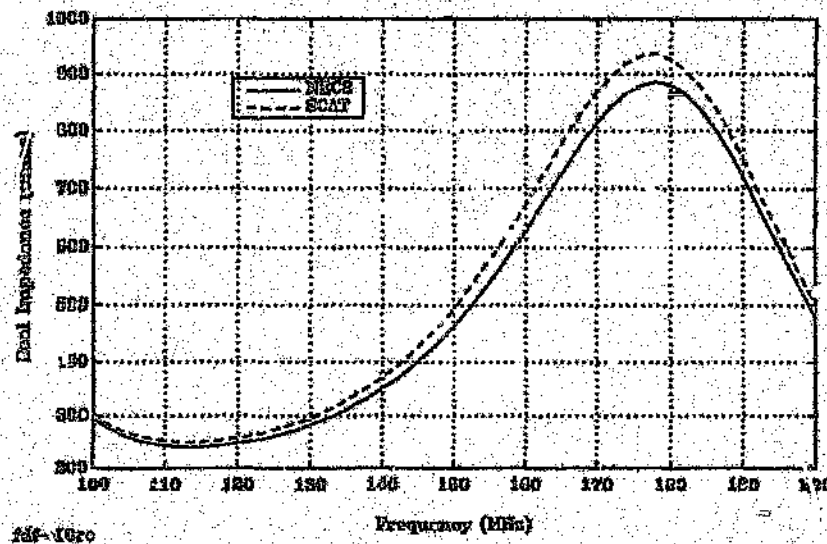
ie $\alpha = 0.4 - 20a$ or

that $\alpha_{new} = \alpha_{old} - 20a$. So the $-20a$ simply modifies the previous value of alpha. The table of equivalent lengths that this produces is shown in table B.4 which, for the simplicity of the adjustment, compared well with the values shown in table B.2.

Table B.4: Linearized equivalent lengths

a (mm)	120mm	100mm	80mm	50mm
1	1.0456	1.0380	1.0304	1.0190
2	1.0432	1.0360	1.0288	1.0180
3	1.0408	1.0340	1.0272	1.0170
5	1.0360	1.0300	1.0240	1.0150
8	1.0288	1.0240	1.0192	1.0120
10	1.0240	1.0200	1.0160	1.0100
12	1.0192	1.0160	1.0128	1.0080
15	1.0120	1.0100	1.0080	1.0050

The results for a 10mm radius folded dipole are shown for a separation ranging from 120mm to 50mm in figures B.1 to B.4. It is clear that the comparisons are acceptable over most of the range.



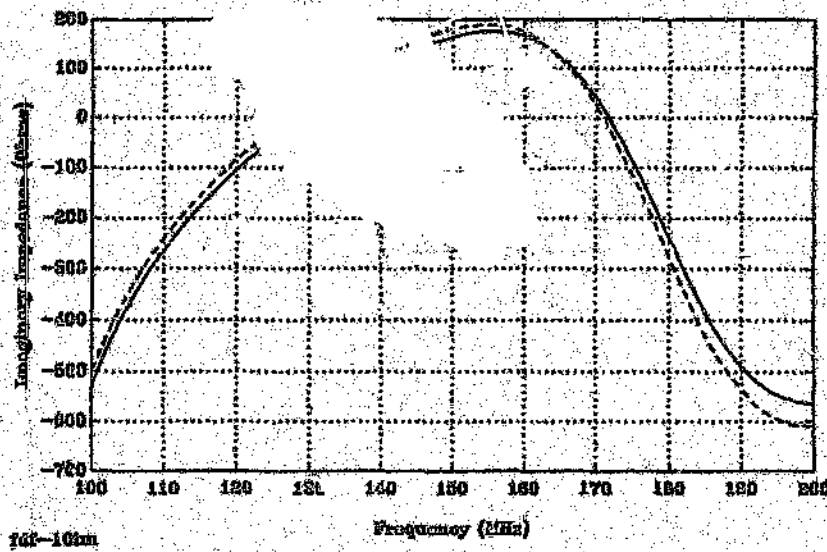
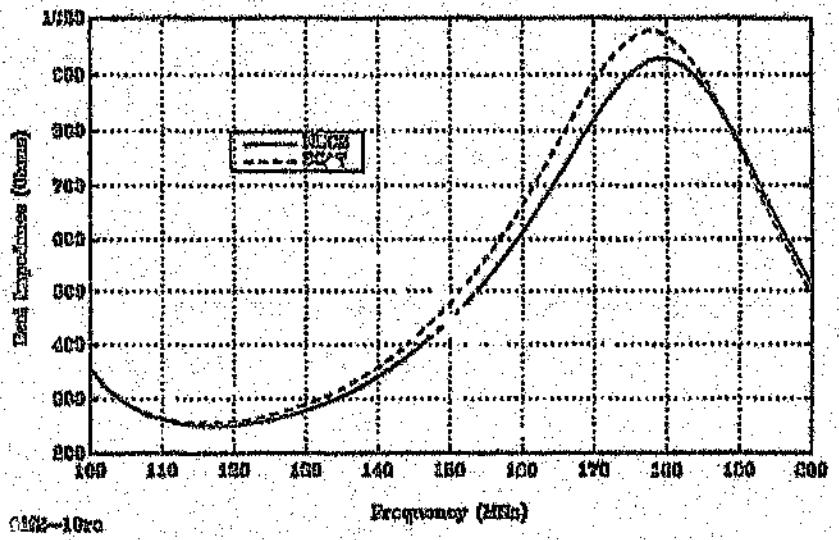


Figure B.1: Compared fd zin $r = 10\text{mm}$ $s = 120\text{mm}$



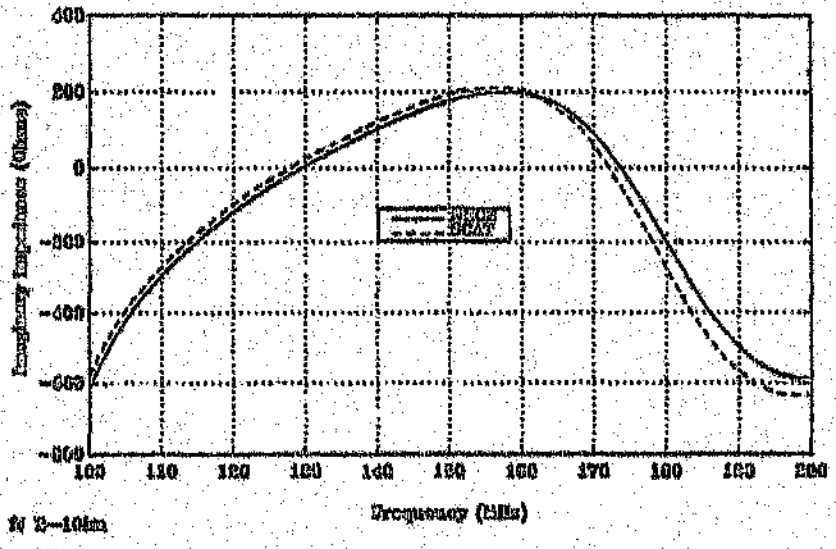
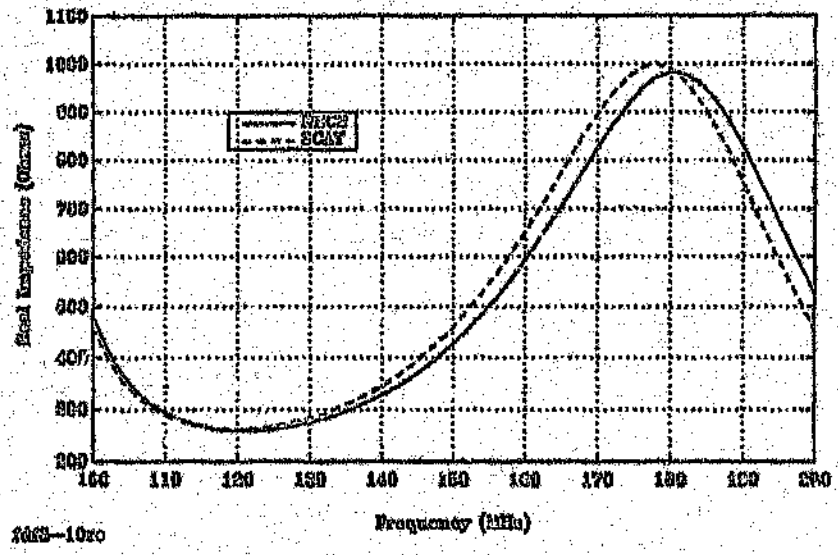


Figure B.2: Compared fd zin $r = 10\text{mm}$ $s = 100\text{mm}$



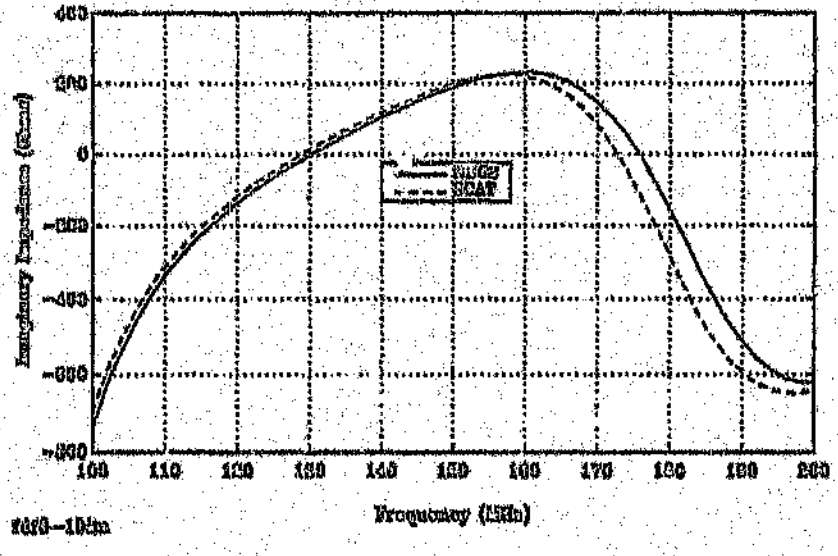
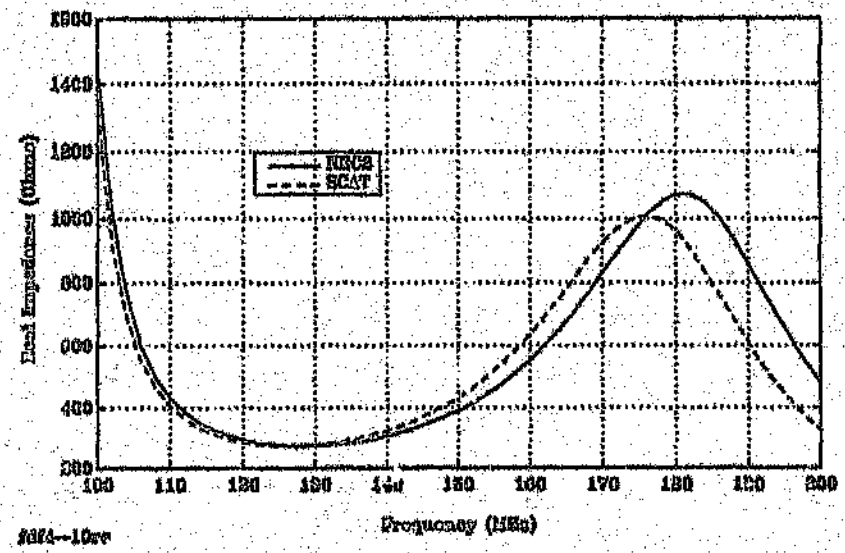


Figure B.3: Compared fd sin $r = 10$mm $a = 80$mm



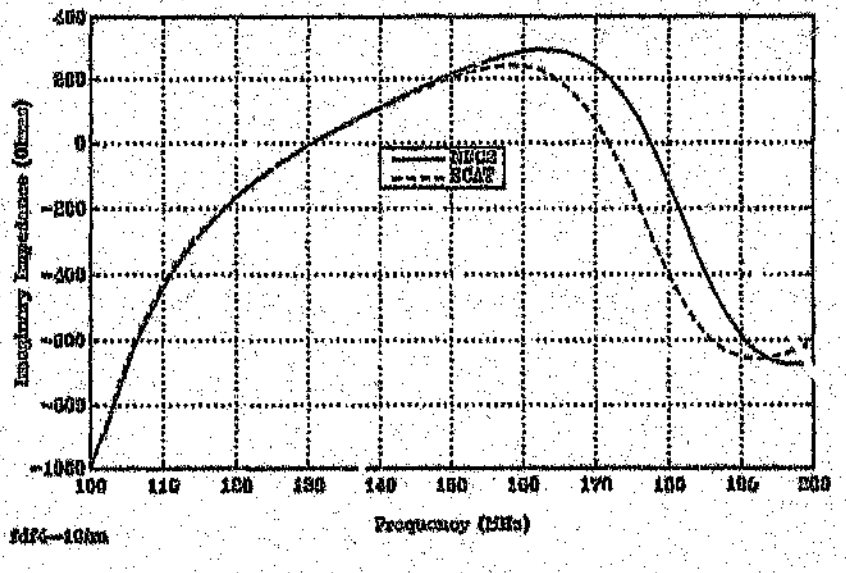


Figure B.4: Compared fit sin $r = 10mm$ $s = 50mm$

Appendix C

Tables of Input Impedance of the Cylindrical Dipole

Tables of input impedance are often tabulated in terms of tlickness factor Ω and electrical length k_0h. ($k_0 = \beta = k$, used elsewhere), hence the same convention has been adopted here.

where

$\Omega = 2\ln\left(\frac{2h}{a}\right)$, the Thickness Factor

$k_0h = \frac{2\pi h}{\lambda}$

a = dipole radius

h = dipole half-l---gth

NEC2 was used to generate tables of input impedances similar to those of King & Harrison (1969) for two reasons:

- The King-Harrison tables do not give values for the thicker dipoles. These are needed for the input impedances of folded dipoles where the impedance of an equivalent thicker dipole is used in the transmission line model.
- To ensure that a valid comparison was being made between NEC2 and SCAT, it is imperative that SCAT's self-impedances are derived from NEC2, so that the differences observed in the outputs are due only to the methods.

The tables are listed for increasing k_0h values and separate tables are used for the different Ω values. A two dimensional linear interpolation is performed by SCAT to find a particular Ω and k_0h combination from the two dimensional grid.

Thickness factor $\Omega = 5$		
$k_0 h$	$\Re(Z_{in})$	$\Im(Z_{in})$
0.5	4.857	-208.577
0.6	7.4371	-162.934
0.7	10.6884	-128.234
0.8	15.4711	-100.271
0.9	21.5319	-76.7807
1	29.5107	-56.5905
1.1	39.9245	-39.2719
1.2	53.2723	-25.0623
1.3	69.795	-14.9923
1.4	89.0042	-10.6215
1.5	109.075	-13.7402
1.6	126.621	-25.0937
1.7	137.707	-43.0447
1.8	139.998	-63.5468
1.9	134.138	-82.0966
2	122.929	-95.8961
2.1	109.461	-104.354
2.2	95.9397	-108.251
2.3	83.5304	-108.781
2.4	72.6729	-107.029
2.5	63.4119	-103.309
2.6	55.6234	-99.6781
2.7	49.1327	-94.9948
2.8	43.7711	-89.9837
2.9	39.3986	-84.7815
3	35.9111	-79.4713
3.1	33.2399	-74.1706
3.2	31.3496	-68.7291
3.3	30.2332	-63.383
3.4	29.9066	-58.1279
3.5	30.3983	-53.0513

Thickness factor $\Omega = 6$		
$k_0 h$	$\Re(Z_{in})$	$\Im(Z_{in})$
0.5	5.48003	-315.611
0.6	8.22446	-247.214
0.7	11.7575	-195.292
0.8	16.2556	-153.617
0.9	21.9467	-118.041
1	29.1381	-88.2509

continued on next page

continued from previous page		
k_0h	$\Re(Z_{\text{in}})$	$\Im(Z_{\text{in}})$
1.1	38.1823	-61.2055
1.2	49.5566	-36.8235
1.3	62.7951	-14.8964
1.4	81.4746	4.31324
1.5	103.092	20.0005
1.6	126.825	30.7481
1.7	153.113	34.5612
1.8	180.133	29.2363
1.9	218.44	13.2419
2	241.386	-12.9963
2.1	253.659	-46.2506
2.2	253.305	-81.1597
2.3	241.599	-112.329
2.4	222.088	-136.293
2.5	198.77	-152.044
2.6	174.814	-160.32
2.7	152.186	-162.614
2.8	131.858	-160.482
2.9	114.157	-155.231
3	99.0652	-147.843
3.1	86.4184	-139.019
3.2	76.0081	-129.24
3.3	67.6418	-118.634
3.4	61.1653	-108.032
3.5	56.4702	-97.0088

Thickness factor $\Omega = 7$		
k_0h	$\Re(Z_{\text{in}})$	$\Im(Z_{\text{in}})$
0.5	5.73352	-428.905
0.6	8.51819	-336.68
0.7	12.0322	-267.129
0.8	16.4068	-211.56
0.9	21.8103	-165.106
1	28.4563	-124.872
1.1	36.6149	-89.0149
1.2	46.6267	-56.3511
1.3	58.9114	-26.1403
1.4	73.9869	2.00392
1.5	92.4731	28.1242
1.6	115.06	51.8894
continued on next page		

continued from previous page

$k_0 h$	$\Re(Z_{in})$	$\Im(Z_{in})$
1.7	142.457	73.4877
1.8	175.227	88.4993
1.9	213.477	97.7859
2	256.336	97.5302
2.1	301.267	84.6489
2.2	343 644	56.8771
2.3	376.92	14.4307
2.4	394.648	-38.6169
2.5	393.211	-94.7306
2.6	373.666	-145.541
2.7	341.017	-184.996
2.8	301.6[illegible]	-210.802
2.9	261.0[illegible]	-223.782
3	222.85	-226.33
3.1	188.836	-221.154
3.2	159.676	-210.614
3.3	135.348	-196.526
3.4	115.516	-180.195
3.5	99.7541	-162.524

Thickness		$\Omega = 8$
$k_0 h$	$\Re(Z_{in})$	$\Im(Z_{in})$
0.5	5.81747	-545.861
0.6	8.59302	-429.659
0.7	12.0557	-342.229
0.8	16.3104	-272.596
0.9	21.4898	-214.623
1	27.7619	-164.594
1.1	35.3373	-120.131
1.2	44.4801	-79.0518
1.3	55.522	-42.0747
1.4	66.8784	-6.66398
1.5	85.0683	27.0348
1.6	104.734	59.2191
1.7	128.659	89.797
1.8	157.767	118.308
1.9	193.086	143.777
2	235.616	164.514
2.1	286.024	177.865

continued on next page

continued from previous page

$k_0 h$	$\Re(Z_{in})$	$\Im(Z_{in})$
2.2	344.054	180.029
2.3	407.527	166.214
2.4	471.134	131.636
2.5	525.809	79.8429
2.6	560.202	-4.10114
2.7	565.158	-91.967
2.8	538.886	-175.123
2.9	488.223	-240.861
3	424.621	-283.194
3.1	358.772	-302.902
3.2	297.725	-304.519
3.3	244.848	-293.38
3.4	201.001	-274.044
3.5	165.74	-249.666

Thickness factor $\Omega = 9$		
$k_0 h$	$\Re(Z_{in})$	$\Im(Z_{in})$
0.5	5.83589	-664.959
0.6	8.58984	-524.503
0.7	12.0011	-419.063
0.8	16.1581	-335.31
0.9	21.1728	-265.752
1	27.1856	-205.909
1.1	34.3714	-152.879
1.2	42.9498	-104.703
1.3	53.1948	-60.0147
1.4	65.4527	-17.8281
1.5	80.1607	22.5681
1.6	97.8717	61.6639
1.7	119.289	99.7455
1.8	145.301	136.808
1.9	177.025	172.781
2	215.831	206.785
2.1	263.328	237.492
2.2	321.223	262.463
2.3	390.91	277.705
2.4	472.512	277.176
2.5	563.081	252.764
2.6	654.027	195.843

continued on next page

continued from previous page		
$k_0 h$	$\Re(Z_{in})$	$\Im(Z_{in})$
2.7	729.359	101.84
2.8	768.586	-22.8258
2.9	756.819	-157.424
3	695.659	-274.675
3.1	602.793	-355.342
3.2	500.317	-395.557
3.3	404.348	-402.546
3.4	322.554	-386.895
3.5	256.624	-357.79

Thickness factor $\Omega = 10$		
$k_0 h$	$\Re(Z_{in})$	$\Im(Z_{in})$
0.5	5.83592	-784.704
0.6	8.5702	-619.959
0.7	11.941	-496.474
0.8	16.0266	-398.638
0.9	20.9255	-317.385
1	26.7611	-247.71
1.1	33.6859	-186.103
1.2	41.8914	-130.251
1.3	51.6165	-76.514
1.4	63.1618	-29.6989
1.5	76.9095	17.1112
1.6	93.3461	62.6053
1.7	113.098	107.309
1.8	136.975	151.578
1.9	166.033	195.583
2	201.647	239.224
2.1	245.598	281.979
2.2	300.154	322.622
2.3	368.064	358.739
2.4	452.317	385.949
2.5	555.247	396.788
2.6	676.273	379.626
2.7	807.424	319.061
2.8	927.523	201.306
2.9	1001.62	27.5366
3	996.706	-172.645
3.1	908.701	-349.66
		continued on next page

continued from previous page		
k_0h	$\Re(Z_{\text{in}})$	$\Im(Z_{\text{in}})$
3.2	768.473	-466.125
3.3	616.879	-516.263
3.4	481.066	-515.866
3.5	371.047	-484.799

Thickness factor $\Omega = 11$		
k_0h	$\Re(Z_{\text{in}})$	$\Im(Z_{\text{in}})$
0.5	5.83357	-904.32
0.6	8.55313	-715.314
0.7	11.6948	-573.83
0.8	15.93	-461.725
0.9	20.7485	-368.964
1	26.4619	-289.46
1.1	33.2088	-219.271
1.2	41.1615	-156.742
1.3	50.5363	-96.9698
1.4	61.604	-41.5597
1.5	74.7093	11.5708
1.6	90.2926	63.2811
1.7	108.923	114.268
1.8	131.346	165.104
1.9	158.542	216.229
2	191.822	267.931
2.1	232.946	320.248
2.2	284.269	372.788
2.3	347.03	424.374
2.4	431.317	472.37
2.5	536.202	511.476
2.6	668.723	531.735
2.7	830.775	515.881
2.8	1013.36	438.281
2.9	1118.99	272.701
3	1282.12	18.6993
3.1	1251.29	-268.604
3.2	1096.14	-501.127
3.3	882.278	-628.137
3.4	676.252	-659.379
3.5	505.921	-630.179

Thickness factor $\Omega = 12$		
$k_0 h$	$\Re(Z_{\text{in}})$	$\Im(Z_{\text{in}})$
0.5	5.83253	-1023.58
0.6	8.54204	-810.388
0.7	11.8631	-650.919
0.8	15.863	-524.675
0.9	20.6246	-420.318
1	26.2521	-330.966
1.1	32.8738	-252.216
1.2	40.6496	-181.001
1.3	49.7794	-115.194
1.4	60.5139	-53.1978
1.5	73.1717	6.22348
1.6	88.1609	64.0804
1.7	106.01	121.215
1.8	127.412	178.364
1.9	153.289	236.176
2	184.883	295.21
2.1	223.893	355.899
2.2	272.667	418.438
2.3	332.486	482.546
2.4	413.932	546.972
2.5	517.306	608.474
2.6	652.798	659.832
2.7	829.54	686.167
2.8	1051.28	663.525
2.9	1303.06	536.143
3	1523.15	279.451
3.1	1602.7	-109.46
3.2	1473.52	-489.445
3.3	1199.3	-733.402
3.4	903.319	-817.061
3.5	657.854	-793.841

Thickness factor $\Omega = 13$		
$k_0 h$	$\Re(Z_{\text{in}})$	$\Im(Z_{\text{in}})$
0.5	5.83328	-1142.52
0.6	8.53577	-905.163
0.7	11.8426	-727.733
0.8	15.8 [illegible]9	-587.383
0.9	20.5375	-471.436
1	26.1027	-372.279

continued on next page

continued from previous page

$k_0 h$	$\Re(Z_{\text{in}})$	$\Im(Z_{\text{in}})$
1.1	32.6334	-284.925
1.2	40.2807	-206.023
1.3	49.2325	-133.174
1.4	59.7252	-64.5928
1.5	72.0589	1.11423
1.6	86.6174	65.089
1.7	103.899	128.31
1.8	124.56	191.685
1.9	[illegible]9.473	255.939
2	179.623	321.939
2.1	217.244	390.387
2.2	264.026	461.919
2.3	323.436	536.932
2.4	400.191	615.239
2.5	501.156	695.301
2.6	636.187	772.523
2.7	818.631	835.619
2.8	1063.24	859.403
2.9	1374.46	793.9
3	1711.51	562.737
3.1	1940.12	119.508
3.2	1889.23	-423.718
3.3	1566.64	-828.193
3.4	1163.69	-989.224
3.5	823.75	-975.923

Thickness factor $\Omega = 14$		
$k_0 h$	$\Re(Z_{\text{in}})$	$\Im(Z_{\text{in}})$
0.5	5.83523	-1261.05
0.6	8.53293	-999.64
0.7	11.8295	-804.261
0.8	15.785	-649.639
0.9	20.4751	-522.339
1	25.9936	-413.362
1.1	32.4563	-317.426
1.2	40.0069	-230.835
1.3	48.8251	-150.943
1.4	59.136	-75.7759
1.5	71.226	-3.76806
1.6	85.4611	66.2944

continued on next page

continued from previous page		
$k_0 h$	$\Re(Z_{in})$	$\Im(Z_{in})$
1.7	102.317	135.57
1.8	122.419	205.047
1.9	146.604	275.687
2	176.01	348.448
2.1	212.212	424.31
2.2	257.438	504.262
2.3	314.902	589.287
2.4	389.336	679.894
2.5	487.838	776.078
2.6	621.142	876.479
2.7	805.261	970.429
2.8	1062.27	1040.52
2.9	1414.31	1037.36
3	1851.49	864.714
3.1	2248.14	404.209
3.2	2331.33	-299.841
3.3	1982.98	-909.002
3.4	1455.04	-1176.38
3.5	1000.88	-1176.45

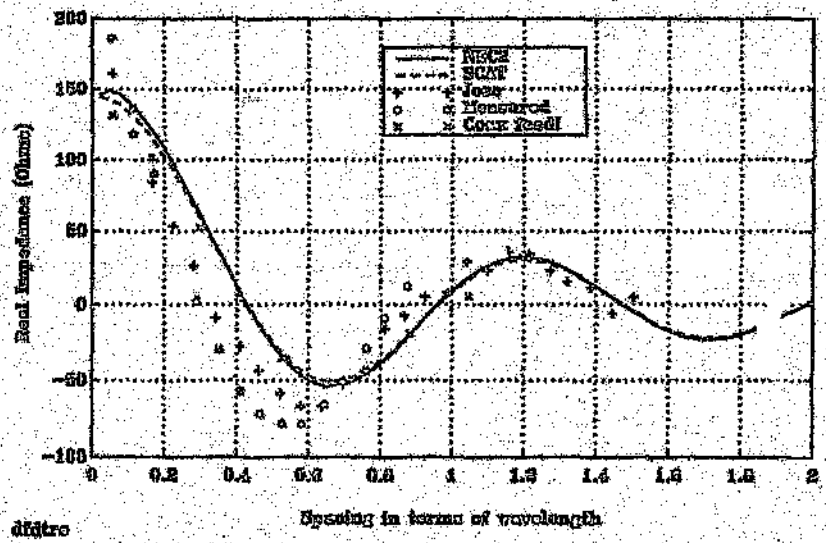
Thickness factor $\Omega = 15$		
$k_0 h$	$\Re(Z_{in})$	$\Im(Z_{in})$
0.5	5.83796	-1379.41
0.6	8.53243	-1193.9
0.7	11.521	-880.656
0.8	15.7625	-712.136
0.9	20.4294	-573.076
1	25.912	-454.284
1.1	32.3219	-349.773
1.2	39.7976	-255.49
1.3	48.5121	-168.552
1.4	58.6821	-86.7956
1.5	70.5829	-8.52685
1.6	84.5669	67.6557
1.7	101.092	142.97
1.8	120.76	218.544
1.9	144.379	295.471
2	173.047	374.874
2.1	208.291	457.941
	continued on next page	

continued from previous page		
$k_0 h$	$\Re(Z_{in})$	$\Im(Z_{in})$
2.2	252.273	565.963
2.3	308.163	640.317
2.4	380.639	742.364
2.5	476.877	853.093
2.6	608.067	972.144
2.7	791.823	1095.17
2.8	1055.2	1207.02
2.9	1434.4	1265.09
-	1952.1	1166.18
3.1	2519.03	729.796
3.2	2788.3	-116.452
3.3	2447.22	-972.436
3.4	1776.49	-1379.16
3.5	1187	-1395.38

Appendix D

Feed geometry sensitivity of the measured results

This appendix refers to the measured results of mutual impedance between a folded dipole and a dipole, as shown in chapter 4 of the thesis. The results are shown in real and imaginary form, as usual, but also in magnitude and phase form – which provides additional insight into the error mechanisms.



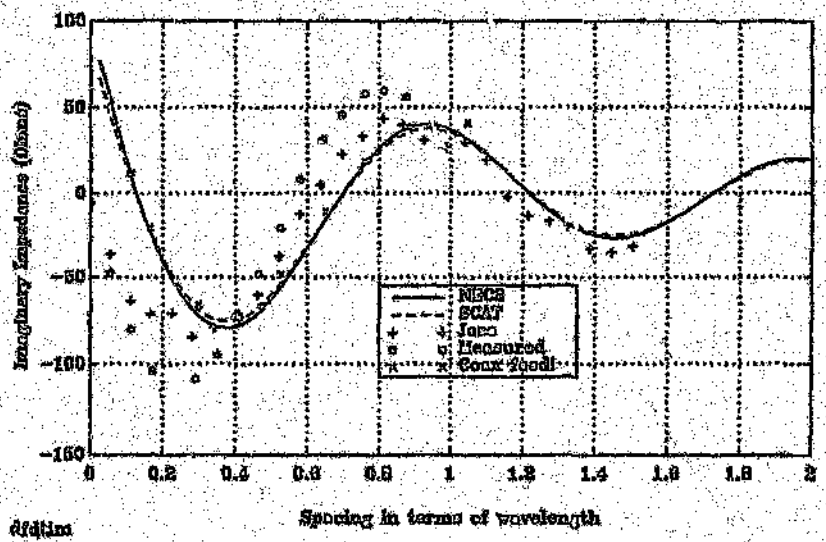


Figure D.1: Real and imaginary impedance

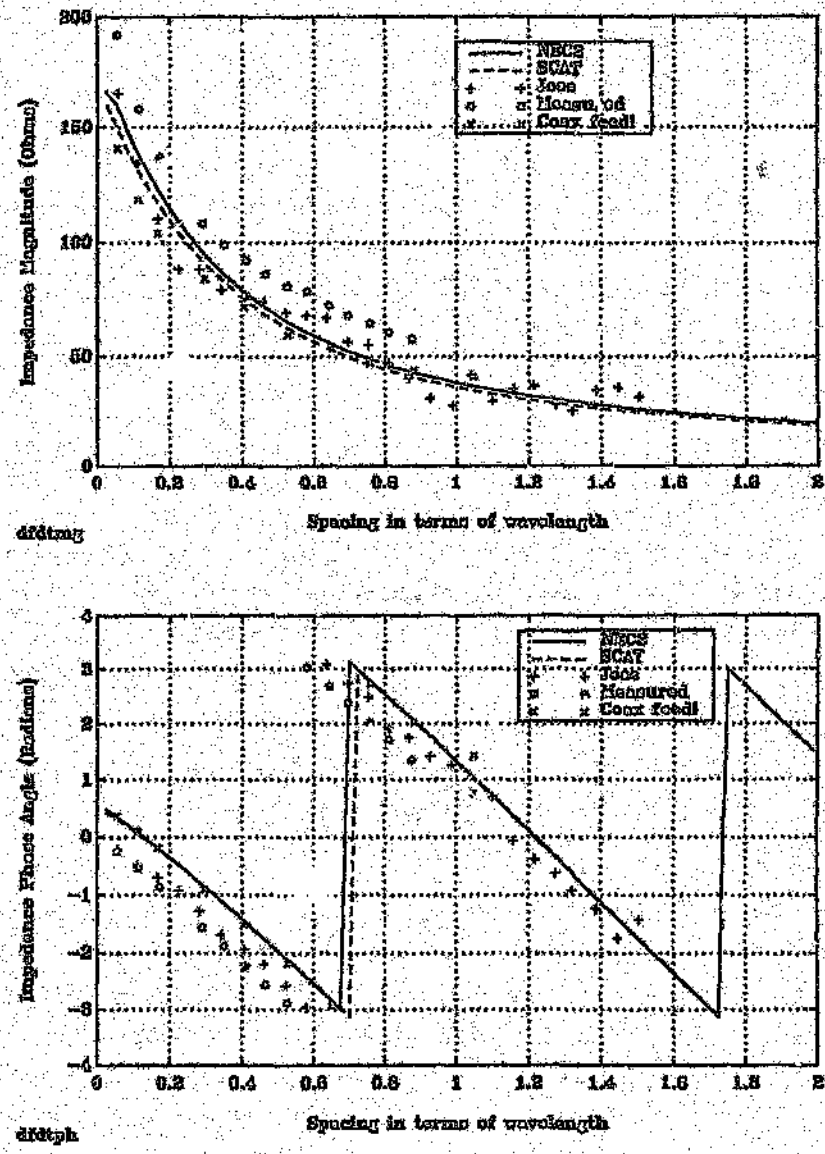


Figure D.2: Magnitude and phase impedance

As before, there is the theoretical curve, denoted SCAT; the curve derived from NEC, denoted NEC; and the final set of measured results, here denoted Coax Feed.

In addition, there are two other sets of results: one denoted Measured, which were measured by the S-parameter method, but using panel mount BNC connectors; and the other denoted Jose, which was the original set of results taken by the Z-Parameter method (no S-parameter test set at that stage).

The mean absolute magnitude errors (note that this norm ignores phase – but is usually used for complex impedance values) are given as compared to the theoretical, SCAT values

as:

Curve	mean($\|\|Z_1\| - \|Z_2\|\|$)
Measured	20.63Ω
Jose	6.61Ω
Coax Feed	5.72Ω
NEC	2.57Ω

It is interesting to view the original "Jose" results ('+') in magnitude and phase form — the magnitude results show quite an acceptable "scatter" around the theoretical results, but there is a very definite phase shift.

The poor comparison of the original measurements at the smaller spacings prompted a new set of measurements which was performed using the S-parameter method ('*'), which were far worse than the original measurements! — with a definite phase shift again, and a magnitude error. Note that these measurements were conducted in the anechoic chamber, as described, with full 2-port calibration, and port extensions to an absolute short circuit on the ground plane panel mount BNC connector.

The "Coax Feed" ('x') results were obtained by eliminating the BNC panel mount connector, and soldering the braid directly to the ground plane, and keeping all feed geometries as small as possible. Excellent comparison to theoretical results was obtained.

The error is introduced in the differences in the feed geometry of the source models. The NEC model uses an applied tangential E-field to excite the dipole/monopole — ie perpendicular to the ground plane. In reality, however, the coaxial feed applies an E-field coaxially parallel to the ground plane. It is only fringing flux that changes this to a tangential excitation. For this reason, the magnetic frill source is preferred for such coaxial feed arrangements. By scaling down the feed geometry (A BNC connector is considerably larger in diameter than the RG58 cable used), this anomaly is reduced. A further effect is that the short circuit is better defined, with less series inductance, which improves the calibration model of the instrument (For the port extension calibration).

In conclusion, it is imperative that great care is taken to accurately model the feed geometry in numerical simulations, if good comparison to measured results is to be achieved.

References

Austin, B. A. & Fourie, A. P. C. (1988), Numerical modelling and design of loaded broadband wire antennas, *in* "IEE Fourth International Conference on HF Communication Systems and Techniques", pp. 125–128. Conference Publication 284.

Balanis, C. A. (1982), *Antenna Theory - Analysis and Design*, Harper & Row Publishers, New York, chapter 7: Self and Mutual Impedances of Linear Elements and Arrays, and Finite Diameter Effects, pp. 283–304.

Brown, G. H. (1937), "Directional antennas", *Proceedings of the IRE* 25(1), 78–145.

Burke, G. J. & Poggio, A. J. (1981), Numerical electromagnetics code (NEC) - method of moments, Tech. doc. 116, Naval Oceans Systems Centre, San Diego, CA.

Carter, P. S. (1932), "Circuit relations in radiating systems and applications to antenna problems", *Proceedings of the IRE* 20(6), 1004–1041.

Chiodini, T. (1989), "Moment method predicted impedances compared to actual measured impedances of directional arrays", *IEEE Transactions on Broadcasting* 35(2), 190–192.

Clark, A. R. & Fourie, A. P. C. (1989), Problems with thin wire emulation of thicker wires using NEC2, *in* "5th Annual Review of Progress in Applied Computational Electromagnetics", Naval Postgraduate School, Monterey, California, pp. 584–593.

Clark, A. R. & Fourie, A. P. C. (1990), Dipole antenna analysis - the use of simplified techniques, *in* "SAIEE Third Joint Symposium on Antennas and Propagation & Microwave Theory and Techniques", Somerset West, pp. 275–282.

Clark, A. R. & Fourie, A. P. C. (1991), "An improvement to the transmission line model of the folded dipole", *IEE Proceedings Part H* 138(6), 577–579.

Clark, A. R. & Fourie, A. P. C. (1992), Mutual coupling and folded dipoles, *in* "Proceedings of the Antennas and Propagation & Microwave Theory and Techniques Symposium, Durban", pp. 92–95.

Collin, R. E. (1985), *Antennas and Radiowave Propagation*, Mc Graw-Hill Book Company, New York.

Cox, C. R. (1947), "Mutual impedance between vertical antennas of unequal heights", *Proceedings of the IRE* 35(November), 1367–1370.

Cox, J. W. R. (1993), "Some remarks on the current slope discontinuity source as described in the nec manual", *Applied Computational Electromagnetics Society Newsletter* 8(1), 11 – 13.

Elliott, R. S. (1981), *Antenna Theory and Design*, Prentice-Hall, Inc. New Jersey.

Givati, O., Clark, A. R. & Fourie, A. P. C. (1989), Intelligent pre-processor for NEC antenna design software, *in* "Fifth Annual Review of Progress in Applied Computational Electromagnetics", Naval Postgraduate School, Monterey, CA, pp. 572–583.

Harrington, R. F. (1968), *Field Computation by Moment Methods*, Macmillan, New York.

Jordan, E. C. & Balmain, K. G. (1968), *Electromagnetic Waves and Radiating Systems*, Second edn, Prentice-Hall, Inc. New Jersey.

King, H. E. (1957), "Mutual impedance of unequal length antennas in eschelon", *IRE Transactions on Antennas and Propagation* AP-5(7), 306–313.

King, R. W. P. (1969), Cylindrical antennas and arrays, *in* R. E. Collin & F. J. Zucker, eds, "Antenna Theory – Part 1", Mc Graw-Hill Book Company, New York.

King, R. W. P. & Harrison, C. W. (1969), *Antennas and Waves - a Modern Approach*, MIT Press, Mass, chapter Appendix 4 - Tables of Impedance and Admittance of Electrically Long Antennas - Theory of Wu, pp. 740–757.

Kraus, J. D. (1988), *Antennas*, second edn, McGraw Hill Book Company, New York, chapter 5: The Electric Dipole and Thin Linear Antennas, pp. 200–225.

Kubina, S. J. (1983), Numerical modelling methods for predicting antenna performance on aircraft, *in* "AGARD Lecture Series No 131", pp. 9–1 to 9–38.

Lawson, J. L. (1986), *Yagi Antenna Design*, The American Radio Relay League, Newington, CT. Publication 72.

Ludwig, A. C. (1987), "Wire grid modelling of surfaces", *IEEE Transactions on Antennas & Propagation* AP-35(9), 1045–1048.

Mahony, J. D. (1989), "Planar array design: Approximation to mutual impedance between two remotely spaced 'half-wavelength' dipoles.", *Electronics Letters* 25(25), 1711–1712.

Mayhan, J. T. (1990), "Characteristic modes and wire grid modeling", *IEEE Transactions on Antennas & Propagation* 38(4), 457–469.

Pages, J. L. (1987), "Numerical modelling of feedpoints at wire junctions", *Journal of Electrical & Electronic Engineers, Australia* 7(4), 257–260.

Pocklington, H. C. (1897), "Electrical oscillations in wires", *Cambridge Philisophical Society Proceedings* 9, 324 – 332.

Richmond, J. H. & Geary, N. H. (1970), "Mutual impedance between coplanar-skew dipoles", *IEEE Transactions on Antennas & Propagation* AP-18(5), 414–416.

Richmond, J. H. & Geary, N. H. (1975), "Mutual impedance of nonplanar-skew sinusoidal dipoles", *IEEE Transactions on Antennas & Propagation* AP-23(5), 412–414.

Sazonov, D. M. (1990), *Microwave Circuits and Antennas*, Mir Publishers, Moscow.

Tai, C. T. (1948), "Coupled antennas", *Proceedings of the IRE* 36(April), 487–500.

Thiele, G. A. (1973), Wire antennas, *in* R. Mittra, ed., "Computer techniques for Electromagnetics", Pergamon Press, chapter 2, pp. 7–19.

Thiele, G. A., Ekelman, E. P. & Henderson, L. W. (1980), "On the accuracy of the transmission line model of the folded dipole", *IEEE Transactions on Antennas & Propagation* AP-28(5), 700–703.

Walker, A. J. (1986), *A Screen Management Library, Version 2.0*, Dept. Elec. Eng. University of the Witwatersrand. Johannesburg, South Africa.

Walker, F. E., Sorensen, E. A. & Kenney, J. S. (1989), Supertab interface for NEC, *in* "5th Annual Review of Progress in Applied Computational Electromagnetics; Naval Postgraduate School, Monterey,Ca.", pp. 806 – 818.

Bibliography

Baker, H. C. & LaGrone, A. H. (1962), "Digital computation of the mutual impedance between thin dipoles", *IRE Transactions on Antennas and Propagation* AP-10(March), 172–178.

Ballantine, S. (1929), "Reciprocity in electromagnetic, mechanical, acoustical, and interconnected systems", *Proceedings of the Institute of Radio Engineers* 17(6), 929–951.

Boswell, A. G. P. (1989), "Analysis of curtain arrays for HF broadcasting", *IEE Proceedings, Part H* 136(2), 179–181.

Carson, J. R. (1929), "Reciprocal theorems in radio communication", *Proceedings of the Institute of Radio Engineers* 17(6), 952–956.

Chang, V. W. H. & King, R. W. P. (1968), "On two arbitrarily located identical parallel antennas", *IEEE Transactions on Antennas & Propagation* AP-16(3), 309–317.

Chuang, C. W., Richmond, J. H., Wang, N. & Pathak, P. H. (1990), "New expressions for mutual impedance of nonplanar-skew sinusoidal monopoles", *IEEE Transactions on Antennas & Propagation* 38(2), 275–276.

Jordan, E. C. & Everitt, W. L. (1941), "Acoustic models of radio antennas", *Proceedings of the IRE* 29(April), 186–194.

King, R. W. P. & Middleton, D. (1946), "The cylindrical antenna; current and impedance", *Quarterly of Applied Mathematics* 3(January), 302–355.

Koksal, A. & Kauffman, J. F. (1991), "Mutual impedance of parallel and perpendicular coplanar surface monopoles", *IEEE Transactions on Antennas & Propagation* 39(8), 1251–1256.

Lechtrek, L. W. (1968), "Effects of coupling accumulation in antenna arrays", *IEEE Transactions on Antennas & Propagation* AP-16(1), 31–37.

Lee, K. M. & Chu, R. S. (1991), "Analysis of mutual coupling between an infinited phased array of horizontal dipoles and vertical wires", *IEEE Transactions on Antennas & Propagation* 39(5), 591–599.

Lee, R. Q., Talty, T. & Lee, K. F. (1991), "Mutual coupling between electromagnetically coupled rectangular patch antennas", *Electronics Letters* 27(6), 532–533.

Lewin, L. (1951), "Mutual impedance of wire aerials", *Wireless Engineer* 28(December), 352–355.

Liu, K., Balanis, C. A. & Barber, G. C. (1991), "Exact mutual impedance between sinusoidal electric and magnetic dipoles", *IEEE Transactions on Antennas & Propagation* 39(5), 684–686.

Lo, K. W. & Vu, T. B. (1987), "Reduction of mutual coupling effects on the receiving pattern of a phased array using guard elements", *Journal of Electrical & Electronic Engineers, Australia* 7(4), 306–309.

Medhurst, R. G. (1951), "Dipole aerials in close proximity", *Wireless Engineer* 28(December), 356–358.

Richmond, J. H. (1970*a*), "Admittance matrix of coupled V antennas", *IEEE Transactions on Antennas & Propagation* AP-18(November), 820–821.

Richmond, J. H. (1970*b*), "Coupled linear antennas with skew orientation", *IEEE Transactions on Antennas & Propagation* AP-18(September), 694–696.

Schwering, F., Puri, N. N. & Butler, C. M. (1986), "Modified diakoptic theory of antennas", *IEEE Transactions on Antennas & Propagation* AP-34(11), 1273–1280.

Yang, H. Y., Alexopoulos, N. G., Lepeltier, P. M. & Stern, G. J. (1990), "Design of transversely fed EMC microstrip dipole arrays including mutual coupling", *IEEE Transactions on Antennas & Propagation* 38(2), 145–151.

Author: Clark Alan Robert.
Name of thesis: Development of self and mutual impedance theory to analyse arrays comprising halfwave dipole and folded dipole elements.

PUBLISHER:
University of the Witwatersrand, Johannesburg
©2015

LEGALNOTICES:

Copyright Notice: All materials on the University of the Witwatersrand, Johannesburg Library website are protected by South African copyright law and may not be distributed, transmitted, displayed or otherwise published in any format, without the prior written permission of the copyright owner.

Disclaimer and Terms of Use: Provided that you maintain all copyright and other notices contained therein, you may download material (one machine readable copy and one print copy per page)for your personal and/or educational non-commercial use only.

The University of the Witwatersrand, Johannesburg, is not responsible for any errors or omissions and excludes any and all liability for any errors in or omissions from the information on the Library website.